HETEROLOGOUS EXPRESSION, CHARACTERIZATION, AND OPTIMIZATION OF PRODUCTION OF ALPHA-GALACTOSIDASE FROM *ASPERGILLUS FUMIGATUS* IN *ASPERGILLUS SOJAE*

A THESIS SUBMITTED TO
THE GRADUATE SCHOOL OF NATURAL AND APPLIED SCIENCES
OF
MIDDLE EAST TECHNICAL UNIVERSITY

BY

SÜMEYRA GÜRKÖK

IN PARTIAL FULFILLMENT OF THE REQUIREMENTS
FOR
THE DEGREE OF DOCTOR OF PHILOSOPHY
IN
BIOTECHNOLOGY

SEPTEMBER 2012

Approval of the thesis:

HETEROLOGOUS EXPRESSION, CHARACTERIZATION, AND OPTIMIZATION OF PRODUCTION OF ALPHA-GALACTOSIDASE FROM *ASPERGILLUS FUMIGATUS* IN *ASPERGILLUS SOJAE*

submitted by **SÜMEYRA GÜRKÖK** in partial fulfillment of the requirements for the degree of **Doctor of Philosophy in Department of Biotechnology, Middle East Technical University** by,

Prof. Dr. Canan Özgen _____
Dean, Graduate School of **Natural and Applied Sciences**

Prof. Dr. Nesrin Hasırcı _____
Head of Department, **Biotechnology**

Prof. Dr. Zümrüt Begüm Ögel _____
Supervisor, **Food Engineering Dept., METU**

Prof. Dr. Ufuk Bölükbaşı _____
Co-Supervisor, **Chemical Engineerng Dept., METU**

Examining Committee Members:

Prof. Dr. Sedat Dönmez _____
Food Engineering Dept., Ankara University

Prof. Dr. Zümrüt Begüm Ögel _____
Food Engineering Dept., METU

Assist. Prof. Dr. Deniz Çekmecelioğlu _____
Food Engineering Dept., METU

Assist. Prof. Dr. Can Özen _____
Biotechnology Dept., METU

Assist. Prof. Dr. Yeşim Soyer _____
Food Engineering Dept., METU

Date: 14.09.2012

I hereby declare that all information in this document has been obtained and presented in accordance with academic rules and ethical conduct. I also declare that, as required by these rules and conduct, I have fully cited and referenced all material and results that are not original to this work.

Name, Last Name: SÜMEYRA GÜRKÖK

Signature :

ABSTRACT

HETEROLOGOUS EXPRESSION, CHARACTERIZATION, AND OPTIMIZATION OF PRODUCTION OF ALPHA-GALACTOSIDASE FROM *ASPERGILLUS FUMIGATUS* IN *ASPERGILLUS SOJAE*

Gürkök, Sümeyra
Ph.D., Department of Biotechnology
Supervisor: Prof. Dr. Zümrüt B. Ögel
Co-supervisor: Prof. Dr. Ufuk Bölükbaşı

September 2012, 180 pages

α-Galactosidase is an exo-glycosidase that hydrolyses non-reducing, α-1,6-linked α-galactose units from oligosaccharides, galactomannans, and galactolipids. α-Galactosidase activity has biotechnological, industrial, and medical importance. α-Galactosidase from *A. fumigatus* IMI 385708, in particular, can catalyse unique hydrolysis and transgalactosylation reactions on polymeric substrates. In this study, α-galactosidase of the human pathogen *A. fumigatus* IMI 385708 was first produced in a GRAS organism, *Aspergillus sojae*. For this aim, α-galactosidase gene *(agl*B) of *A. fumigatus* IMI 385708 was ligated onto pAN52-4 vector (Acc. No: Z32699) and transformed into *Aspergillus sojae* ATCC11906, under the control of the constitutive glyceraldehyde-3-phosphate dehydrogenase promoter (*gpd*A) of *A. nidulans* and the signal sequence of glucoamylase gene (*gla*A) of *A. niger*. This allowed high level of α-galactosidase production on glucose instead of locust bean gum (2.45 U/mL), corresponding to a 3-fold increase

in volumetric production. Next, using response surface methodology, carbon and nitrogen sources and agitation speed were optimized (10.5% molasses (w/v); 1.3% NH_4NO_3 (w/v); 276 rpm). Compared to non-optimized cultivation, a further 4-fold increase in α-galactosidase production (10.4 U/mL) was achieved. Recombinant α-galactosidase was purified 18.7-fold using Anion Exchange and Hydrophobic Interaction Chromatography with an overall yield of 56% and 64.7 U/mg protein. The V_{max} and K_m values for the hydrolysis of *p*-nitrophenyl α-*D*-galactopyranoside were 78 U/mg protein and 0.45 mM, respectively. Optimum pH and temperature for α-galactosidase activity were between pH 4–6 and 50–60 °C, respectively. Among the tested chemical agents, Ag^{+}, Hg^{2+}, and Fe^{2+} drastically decreased the activity, while biotin, I^{+1}, Mn^{+2}, Pb^{+2}, Li^{+1}, and Mg^{+2} enhanced between 12–29%. To analyse the influence of osmotic stress as a means of further inducing α-galactosidase production, salt was added into the complete growth medium. In addition to enzyme production, fungal growth and morphology were analysed for both 'salt-adapted' and 'salt non-adapted' *A. sojae* Ta1 cells in the presence of KCl, $MgCl_2$, $MgSO_4$, NaCl, and Na_2SO_4 at 1 M and 2 M. Accordingly, 3-fold increase in α-galactosidase production was achieved by non-adapted cells in the presence of 1 M NaCl. Exposure of *A. sojae* Ta1 cells to salt resulted in predominantly mycelial form, rather than the pellet form observed under normal conditions. Finally, the transgalactosylation ability of α-galactosidase was studied. α-Galactosidase efficiently catalysed galactose transfer to different monosaccharides and disaccharides in the presence of *p*NPαGal as monitored by TLC, ESI-MS, and HPLC.

Keywords: α-Galactosidase, *Aspergillus fumigatus, Aspergillus sojae*, heterologous expression, *gpd*A promoter, response surface methodology, osmotic stress, enzyme purification and characterization, transgalactosylation

ÖZ

ASPERGILLUS FUMIGATUS ALFA-GALAKTOSİDAZININ *ASPERGILLUS SOJAE*'DE HETEROLOG ÜRETİMİ, KARAKTERİZASYONU VE ÜRETİMİNİN OPTİMİZASYONU

Gürkök, Sümeyra
Doktora, Biyoteknoloji Bölümü
Tez Yöneticisi: Prof. Dr. Zümrüt B. Ögel
Ortak Tez Yöneticisi: Prof. Dr. Ufuk Bölükbaşı

Eylül 2012, 180 sayfa

α-Galaktosidaz enzimi oligosakkaritlerden, galaktomannanlardan ve galaktolipidlerden, indirgeyici olmayan, α-1,6 bağlı galaktoz birimlerini hidroliz eden bir ekzo-glikosidazdır. α-Galaktosidaz aktivitesi biyoteknolojik, endüstriyel ve medikal öneme sahiptir. Özellikle, *A. fumigatus* IMI 385708'un α-galaktosidaz enzimi polimerik substratlar üzerinde farklı hidroliz ve transgalaktozilasyon reaksiyonlarını gerçekleştirebilmektedir. Bu çalışmada insan patojeni olan *A. fumigatus* IMI 385708'un α-galaktosidaz enzimi ilk olarak genel olarak güvenli kabul edilen bir organizmada, *Aspergillus sojae*'de, üretildi. Bu amaçla, *A. fumigatus* IMI 385708'un α-galaktosidaz geni (*agl*B) pAN52-4 (Acc. No: Z32699) vektörüne takılmış ve konstitütif *A. nidulans* gliseraldehit-3-fosfat dehidrojenaz geninin (*gpd*A) promotörü ve *A. niger* glukoamilaz geninin (*gla*A) sinyal sekansı kontrolünde *Aspergillus sojae* ATCC11906'ye transfer edilmiştir. Bu keçiboynuzu zamkı yerine glukozda 3 kat volumetric üretim artışına karşılık gelen yüksek

seviyede α-galaktosidaz üretimine (2.45 U/mL) izin vermiştir. Daha sonra yanıt yüzey yöntemi kullanılarak, YpSs büyüme ortamındaki rekombinant *A. sojae* Ta1 kültürünün karbon ve nitrojen kaynağı ile çalkalama hızı optimize edilmiştir [(%10,5 melas (w/v); %1,3 NH_4NO_3 (w/v); 276 rpm]. Optimize edilmeyen kültürle karşılaştırıldığında, optimum şartlar altında α-galaktosidaz üretiminde 4 kat daha artış sağlanmıştır (10.4 U/mL). Rekombinant α-galaktosidaz anyon değişim ve hidrofobik etkileşim kromatografileriyle % 56 toplam verim ve 64.7 U/mg protein spesifik aktivite ile 18.7 kat saflaştırılmıştır. *p*-Nitrophenyl α-*D*-galactopyranoside hidrolizi için V_{max} ve K_m değerleri sırasıyla 78 U/mg protein ve 0.45 mM olarak bulunmuştur. α-Galaktosidaz aktivitesi için en uygun pH ve sıcaklık aralıkları sırasıyla pH 4–6 ve 50–60 °C olarak bulunmuştur. Test edilen kimyasal maddeler arasından biotin, I^{+1}, Mn^{+2}, Pb^{+2}, Li^{+1} ve Mg^{+2} aktiviteyi % 12–29 artırırken, Ag^{+}, Hg^{2+} ve Fe^{2+} aktiviteyi oldukça düşürmüştür. Osmotik stres etkisinin α-galaktosidaz üretimini daha fazla artırmak amacıyla analizi için complete büyüme ortamına tuz eklenmiştir. Enzim üretimine ek olarak, fungusun büyüme ve morfolojisi tuza adapte olan ve olmayan *A. sojae* Ta1 hücrelerinde 1 M ve 2 M konsantrasyonda KCl, $MgCl_2$, $MgSO_4$, NaCl ve Na_2SO_4 varlığında incelenmiştir. Bu şekilde, 1 M NaCl varlığında adapte olmayan hücrelerle α-galaktosidaz üretiminde 3 kat artış sağlanmıştır. *A. sojae* Ta1 hücrelerinin tuza maruz kalması normal şartlarda gözlenen pelet formu yerine çoğunlukla misel formuyla sonuçlanmıştır. Son olarak, α-galaktosidazın transgalaktozilasyon yeteneği çalışılmıştır. TLC, ESI-MS ve HPLC analizlerine göre, α-galaktosidaz *p*-nitrophenyl α-*D*-galactopyranoside varlığında çeşitli monosakkarit ve disakkarite galaktoz transferini verimli bir şekilde katalizlemiştir.

Anahtar Kelimeler: α-galaktosidaz, *Aspergillus fumigatus, Aspergillus sojae*, heterolog ekspresyon, *gpd*A promotörü, tepki yüzey yöntemi, osmotik stres, enzim saflaştırma ve karakterizasyonu, transgalaktozilasyon

To my parents

ACKNOWLEDGMENTS

I would like to express my very special thanks to my supervisor, Prof. Dr. Zümrüt Begüm Ögel for her endless support, guidance, encouragement, and kindness throughout this study.

I wish to extend my thanks to my co-supervisor Prof. Dr. Ufuk Bölükbaşı for providing her laboratory facilities and for her valuable guidance.

I would like to express my thanks to Prof. Dr. Sedat Dönmez and Assist. Prof. Dr. Deniz Çekmecelioğlu for their valuable advises and criticism.

I would like to express sincere thanks to Prof. Dr. Sabine Flitsch for her great support, hospitality, kindness, and providing a great laboratory environment during my research at Manchester Interdisciplinary Biocentre.

We thank Dr. Punt from TNO, The Netherlands for *A. sojae* ATCC11906 ($pyrG^{-}$) strain and pAN52-4 expression vector.

I would like to thank METU Central Laboratory members, especially for HPLC analyses of the oligosaccharides.

I wish to thank my wise colleague Gökhan Duruksu, whose contribution to this study is deeply appreciated, and my other labmates, Abdulvali Valiyev, Alper-Betül Soyler, Ayla Öreroğlu, Banu Metin, Bengü Öztürk, Burçak Kocuklu, Ceren Aksoy, Gülden Avcı, Nansalmaa Amarsaikhan, Özlem Erçin, Tunca Doğan, and Yonca Yüzügüllü for their support and friendship throughout this study.

I wish also to thank my lab mates from MIB, Josef Voglmeir, Dominique Richardson, Jennifer Hopwood, Martin Weissenborn, Roberto Castangia, Robert Sardzik, and Will Allwood for their help, hospitality, and friendship.

I am also thankful to my friend, Gözde Kerman not only for her friendship but also for her endless support and precious encouragement.

Special thanks go to both of my lifelong friends, Burcu Tefon and Tuğba Özaktaş for being by my side through all the good times and the bad.

I would like to express my deepest thanks to a big lovely family; my dear, patient, and devoted parents, Şükran-Yüksel Gürkök, my heartening sisters, Jale Cortu, Şule Kazan, and beloved little sister, Müyesser Gürkök, my grandparents, Miyase-Ömer Gürkök and my sisterly aunt, Melek Gürkök, my monkeys, Özlem-Özgür Cortu, Elçin-Ceylin Kazan. You have been always there and believed in me and I have always felt your support and faith in me. I am so lucky to have each of you.

This work was supported by State Planning Organization of Turkey (BAP-08-11-DPT2002K120510).

TABLE OF CONTENTS

ABSTRACT iv

ÖZ vi

ACKNOWLEDGMENTS ix

TABLE OF CONTENTS xi

LIST OF TABLES xv

LIST OF FIGURES xvii

ABBREVIATIONS xxiv

CHAPTERS

1. INTRODUCTION 1
   1.1 Alpha-galactosidase 1
      1.1.1 Classification of glycosyl hydrolases 2
      1.1.2 Application areas of α-galactosidases 7
      1.1.3 Three dimensional (3-D) structure of α-galactosidase 12
      1.1.4 Properties of α-galactosidase of *A. fumigatus* IMI 385708 13
   1.2 The thermotolerant filamentous fungus *A. fumigatus* 15
   1.3 *A. sojae* as a cell factory for heterologous protein production 16
   1.4 Optimization of fermentation media and conditions 19
   1.5 Osmotic stress and fungi 21
   1.6 Transgalactosylation activity of *A. fumigatus* α-galactosidase 23
   1.7 Aim of the study 27

2. MATERIALS AND METHODS 28
2.1 Materials 28
2.1.1 Organisms and growth conditions 28
2.1.2 Chemicals, enzymes, and kits 29
2.1.3 Growth media, buffers, and solutions 29
2.1.4 Plasmids 30
2.1.5 Molecular size markers 30
2.2 Methods 30
2.2.1 Isolation of plasmid DNA 30
2.2.2 Recovering DNA from agarose gel 31
2.2.3 Purification of plasmid DNA for sequencing 32
2.2.4 The polymerase chain reaction (PCR) 33
2.2.5 Visualization and photography of nucleic acids 34
2.2.6 Transformation of *E. coli* XL1 Blue MRF′ 34
2.2.7 Restriction enzyme digestion of the DNA 35
2.2.8 Ligation 36
2.2.9 Identification of recombinant clones 37
2.2.10 Transformation of *A. sojae* 38
2.2.11 α-Galactosidase activity assay 41
2.2.12 Determination of fungal biomass 42
2.2.13 SDS-PAGE 42
2.2.14 Selection of the best carbon and nitrogen sources 45
2.2.15 Optimization by response surface methodology 46
2.2.16 Effect of culture volume on production 49
2.2.17 Purification of recombinant α-galactosidase 49
2.2.18 Determination of total protein concentration 50
2.2.19 N-Deglycosylation of the recombinant α-galactosidase 50
2.2.20 Enzyme kinetics of recombinant α-galactosidase 51
2.2.21 Effect of pH on recombinant α-galactosidase activity and stability 51
2.2.22 Effect of temperature on recombinant α-galactosidase activity and stability 51

2.2.23 Effects of additives on the recombinant α-galactosidase activity 52
2.2.24 Osmotic stress analysis 52
2.2.25 Analysis of transgalactosylation activity of recombinant α-galactosidase 54

3. RESULTS AND DISCUSSIONS 57
3.1 Overall experimental strategy of the study 57
3.2 Ligation of α-galactosidase gene (*agl*B) onto vector pAN52-4 and transformation into *E. coli* XL1 Blue MRF′ 59
3.3 Transformation into *A. sojae* and screening 62
3.3.1 Protoplast transformation and selection of transformants 62
3.3.2 Screening of α-galactosidase activity and comparison 64
3.3.3 Analysis of protein profiles 65
3.4 Optimization of heterologous α-galactosidase production 68
3.4.1 Selection of best carbon and nitrogen sources 68
3.4.2 Box-Behnken design and response surface methodology 69
3.5 Effect of culture volume on production 80
3.6 Purification and N-Deglycosylation of recombinant α-galactosidase 82
3.7 Kinetic analysis of recombinant α-galactosidase 86
3.8 Effect of pH on recombinant α-galactosidase activity and stability ... 87
3.9 Effect of temperature on recombinant α-galactosidase activity and stability 89
3.10 Effect of additives on recombinant α-galactosidase activity and stability 91
3.11 Effect of osmotic stress 92
3.11.1 Effect of salt stress on fungal growth 93
3.11.2. Effect of salt stress on α-galactosidase production by non-adapted *A. sojae* Ta1 95
3.11.3 Effect of salt stress on α-galactosidase production by salt-adapted *A. sojae* Ta1 98
3.11.4 Effect of osmotic stress on fungal morphology..... 102
3.12 Transgalactosylation activity of recombinant α-galactosidase 106

3.12.1 Detection of transgalactosylation products..... 106
3.12.2 Quantitative analysis of transgalactosylation products..... 116

4. CONCLUSIONS..... 123

5. RECOMMENDATIONS..... 125

REFERENCES 126

APPENDICES..... 144
A. CHEMICALS, ENZYMES, AND THEIR SUPPLIERS..... 144
B. PREPARATION OF GROWTH MEDIA, BUFFERS, AND SOLUTIONS 147
C. PLASMIDS..... 158
D. MARKERS 160
E. SEQUENCES OF THE PRIMERS 163
F. NUCLEOTIDE AND AMINO ACID SEQUENCE 165
G. *p*-NITROPHENOL STANDARD CURVE 169
H. COLUMN CHARACTERISTICS..... 171
I. LOWRY PROTEIN DETERMINATION..... 173

CURRICULUM VITAE..... 175

LIST OF TABLES

TABLES

Table 1.1 Kinetic parameters of *A. fumigatus IMI 385708* α-galactosidase for three substrates (Puchart *et al*., 2000) 15

Table 2.1 PCR cycles 33

Table 2.2 Separating gel preparation 43

Table 2.3 Stacking gel preparation 43

Table 2.4 Coded and uncoded variables of independent factors in RSM ... 46

Table 2.5 Experimental design for optimization of α-galactosidase and biomass production using response surface methodology 48

Table 2.6 Donor and acceptor substrates used in transgalactosylation reactions 56

Table 3.1 Estimated regression coefficients of multiple determinations (R^2) for α-galactosidase production 71

Table 3.2 Estimated regression coefficients of multiple determinations (R^2) for biomass production 72

Table 3.3 Analysis of variances for α-galactosidase production using coded values 74

Table 3.4 Analysis of variances for biomass generation using coded values 74

Table 3.5 α-Galactosidase production by different strains after optimization 80

Table 3.6 Summary of the purification of recombinant α-galactosidase from *A. sojae* Ta1 by anion exchange (AEC) and hydrophobic interaction chromatography (HIC).....84

Table 3.7 Linkages and functions of natural α-galactosides in animals (Yamashita *et al*., 2005) 115

Table 3.8 Yields of galactosylation products analysed by HPLC after 1-hour incubation of 0.5 U/mL recombinant α-galactosidase with 0.25 M *p*NPαGal and 1 M acceptor sugar at 50 °C 121

LIST OF FIGURES

FIGURES

Figure 1.1 The structural relationships of raffinose family oligosaccharides.1

Figure 1.2 Schematic representation of galactomannan 2

Figure 1.3 Mode of action of glycosyl hydrolases (www.cazypedia.org/) 2

Figure 1.4 Catalytic mechanisms of α-glycosidase; (a) retaining and (b) inverting (http://www.cazypedia.org/) 5

Figure 1.5 Guar gum processing by three hydrolytic enzymes; α-galactosidase, β-mannanase, and β-mannosidase (Dias *et al*., 2004).....9

Figure 1.6 Alteration of blood group B to blood group 0 by α-galactosidase (Guce, 2010) 10

Figure 1.7 Elimination of terminal galactose from globotriaosylceramide by α-galactosidase (Guce, 2010) 11

Figure 1.8 The 3-D crystal structure of α-galactosidase from *T. reesei*. β-strands (arrows), α-helices (coils), catalytic residues (Asp132 and Asp226), two Trp residues responsible for hydrophobic interactions with the substrate, and four N-glycosylation sites (sticks) are shown (Golubev *et al*., 2004). ...13

Figure 1.9 *A. fumigatus* genome view showing putative α-galactosidases (http://www.ncbi.nlm.nih.gov/) 14

Figure 1.10 *A. fumigatus* IMI 385708; (a) macroscopic (Photo by Dr. David Midgley) and (b) under the light microscope (4x) 16

Figure 1.11 *A. sojae* (a) grown on minimal medium agar plate after transformation and (b) its conidia and conidiospores under the light microscope (4x) 17

Figure 1.12 The auto-condensation reaction catalysed by glycosyl hydrolases (Spangenberg *et al*., 2000) 25

Figure 1.13 The condensation reaction catalysed by glycosyl hydrolases (Spangenberg *et al*., 2000) 25

Figure 3.1 Flow chart of the experimental strategy.....58

Figure 3.2 Restriction digestion of recombinant plasmid (pANaglB) with Hind III. Lane 1 and 3: isolated pANaglB; lane 2 and 4: Hind III-cut pANaglB; lane M: Lambda DNA/EcoRI + HindIII marker (Appendix D).....60

Figure 3.3 Schematic representation of recombinant plasmid, pANaglB for the expression of *agl*B of *A. fumigatus*. Promoter sequence of *A. nidulans gpd*A gene, major transcription start site, *poly A* tail, HindIII cut site used to insert the gene, terminator sequence of *A. nidulans trp*C gene, and signal and pro sequences of *A. niger gla*A gene are indicated.....60

Figure 3.4 A−D are 4 different recombinant plasmids. Each lane 1, the result of PCR with pB1 and pA2 primers yielding 1622 bp PCR product; Each lane 2, the result of PCR with pB1 and pV1 primers yielding 5748 bp PCR product; Each lane 3, the result of PCR with pA2 and pV1 primers yielding no PCR product; Lane M, Molecular size marker, λ DNA/EcoRI + HindIII (Appendix D).....62

Figure 3.5 Protoplast formation from the mycelium of *A. sojae* ATCC11906 (*pyr*G⁻) resuspended in the lytic solution (A−F). Samples were taken at 30 minutes intervals. 63

Figure 3.6 Comparison of α-galactosidase secretion by *A. fumigatus* IMI 385708 grown on medium containing 0.5% LBG, *A. sojae* ATCC11906 (control), and *A. sojae* Ta1 grown on YpSs medium containing 2% glucose 65

Figure 3.7 SDS-PAGE of culture supernatants. Lane 1, *A. sojae* ATCC11906 (*pyr*G⁻); lanes 2 and 3, *A. sojae* Ta1; lane 4, *A. fumigatus*; lane M, PageRuler™ unstained protein ladder (Appendix D.2.1) 66

Figure 3.8 Effect of carbon sources (2%) on α-galactosidase production by *A. sojae* Ta1 grown in 100 mL YpSs medium at 30 °C and 155 rpm. 68

Figure 3.9 Effect of nitrogen sources (0.4%) on α-galactosidase production by *A. sojae* Ta1 grown in 100 mL YpSs medium at 30 °C and 155 rpm.....69

Figure 3.10 Response surface plots showing the effect of (a) Molasses and NH_4NO_3, (b) Molasses and Agitation speed, and (c) NH_4NO_3 and Agitation speed on α-galactosidase production 75

Figure 3.11 Contour plots showing the effect of (a) Molasses and NH_4NO_3, (b) Molasses and Agitation speed, and (c) NH_4NO_3 and Agitation speed on α-galactosidase production 75

Figure 3.12 Response surface plots showing the effect of (a) Molasses and NH_4NO_3, (b) Molasses and Agitation speed, and (c) NH_4NO_3 and Agitation speed on biomass generation 76

Figure 3.13 Contour plots showing the effect of (a) Molasses and NH_4NO_3, (b) Molasses and Agitation speed, and (c) NH_4NO_3 and Agitation speed on biomass generation.....76

Figure 3.14 Comparison of the highest extracellular α-galactosidase activities of *A. fumigatus* IMI 385708 grown on 0.5% LBG, *A. sojae* Ta1 grown under unoptimized basal culture conditions (2% glucose, 0.4% yeast extract, 155 rpm), and *A. sojae* Ta1 grown under optimized culture conditions (10.5% molasses, 1.3% NH_4NO_3, 276 rpm) on the third day of the cultivation in modified YpSs medium.....79

Figure 3.15 Effect of culture volume on recombinant α-galactosidase production by *A. sojae* Ta1 under optimized conditions (10.5% molasses, 1.3% NH_4NO_3, and 276 rpm) 81

Figure 3.16 SDS-PAGE of the recombinant α-galactosidase purification steps after staining with Coomassie Brilliant Blue G-250. Lane M: PageRuler™ prestained protein ladder plus (Appendix D.3); lane C: culture supernatant, lane 1: recombinant α-galactosidase purified by AEC; lane2: recombinant α-galactosidase purified by HIC.....83

Figure 3.17 N-deglycosylation of recombinant α-galactosidase; lane 1: purified recombinant α-galactosidase, lane 2: purified recombinant α-galactosidase after N-glycanase treatment. 85

Figure 3.18 Michaelis-Menten curve of recombinant α-galactosidase.....86

Figure 3.19 Lineweaver Burk plot of recombinant α-galactosidase activity 87

Figure 3.20 pH-dependence of recombinant α-galactosidase activity 88

Figure 3.21 pH-dependence of recombinant α-galactosidase stability 88

Figure 3.22 Temperature-dependence of recombinant α-galactosidase activity 89

Figure 3.23 Temperature-dependence of recombinant α-galactosidase stability 90

Figure 3.24 Effects of additives on recombinant α-galactosidase activity ..91

Figure 3.25 Effect of osmotic stress on the growth of *A. sojae* Ta1 in salt non-adapted cultures grown at 1 M (green) and at 2 M (blue), and salt-adapted cultures grown at 1 M (red), at the end of 8 days of cultivation at 30 °C in 2% glucose containing complete medium at 200 rpm. Error bars represent the standard deviations from the mean of two independent experiments. 94

Figure 3.26 α-Galactosidase production by non-adapted *A. sojae* Ta1 in the presence of 1 M and 2 M NaCl. Error bars represent the standard deviations from the mean of two independent experiments. 96

Figure 3.27 α-Galactosidase production by non-adapted *A. sojae* Ta1 in the presence of 1 M and 2 M KCl. Error bars represent the standard deviations from the mean of two independent experiments. 96

Figure 3.28 α-Galactosidase production by non-adapted *A. sojae* Ta1 in the presence of 1 M and 2 M $MgSO_4$. Error bars represent the standard deviations from the mean of two independent experiments. 97

Figure 3.29 α-Galactosidase production by non-adapted *A. sojae* Ta1 in the presence of 1 M and 2 M Na_2SO_4. Error bars represent the standard deviations from the mean of two independent experiments. 97

Figure 3.30 α-Galactosidase production by salt-adapted *A. sojae* Ta1 in the presence of 1 M KCl, $MgCl_2$, $MgSO_4$, NaCl, and Na_2SO_4. Error bars represent the standard deviations from the mean of two independent experiments. 99

Figure 3.31 Biomass-based α-galactosidase production by *A. sojae* Ta1. Salt non-adapted cultures grown at 1 M (green) and at 2 M (blue), and salt-adapted cultures grown at 1 M (red) of each salt in 2% glucose containing complete medium at 30 °C at 200 rpm. Error bars represent the standard deviations from the mean of two independent experiments. 100

Figure 3.32 Effects of osmotic stress at 1 M and 2 M concentrations on non-adapted fungal macro (X) and micro-morphology (4X and 10X).....103

Figure 3.33 Effects of osmotic stress at 1 M concentration on salt-adapted fungal macro (X) and micro-morphology (4X and 10X).....104

Figure 3.34 TLC analysis of 1-hour transgalactosylation reaction at 50 °C. Reaction mixtures were composed of 0.5 U/mL recombinant α-galactosidase, 0.25 M *p*NPαGal (*p*NPG), and 1 M of each acceptor sugar. R: reaction mixture; C: control acceptor sugar 107

Figure 3.35 ESI-MS analysis of transgalactosylation mixture of recombinant α-galactosidase (0.5 U/mL) with galactose (1 M) as acceptor and *p*NPαGal (0.25 M) as donor at 50 °C for 1 hour.....108

Figure 3.36 Products of transglycosylation reaction catalysed by recombinant α-galactosidase in the presence of α-*D*-galactose as acceptor. Drawn by ChemBioOffice Ultra 2010 Trial Version. 109

Figure 3.37 ESI-MS analysis of transgalactosylation mixture of recombinant α-galactosidase (0.5 U/mL) with mannose (1 M) as acceptor and *p*NPαGal (0.25 M) as donor at 50 °C for 1 hour.....110

Figure 3.38 ESI-MS analysis of transgalactosylation mixture of recombinant α-galactosidase (0.5 U/mL) with glucose (1 M) as acceptor and *p*NPαGal (0.25 M) as donor at 50 °C for 1 hour.....111

Figure 3.39 ESI-MS analysis of transgalactosylation mixture of recombinant α-galactosidase (0.5 U/mL) with cellobiose (1 M) as acceptor and *p*NPαGal (0.25 M) as donor at 50 °C for 1 hour.....112

Figure 3.40 ESI-MS analysis of transgalactosylation mixture of recombinant α-galactosidase (0.5 U/mL) with lactose (1 M) as acceptor and *p*NPαGal (0.25 M) as donor at 50 °C for 1 hour.....113

Figure 3.41 ESI-MS analysis of transgalactosylation mixture of recombinant α-galactosidase (0.5 U/mL) with maltose (1 M) as acceptor and *p*NPαGal (0.25 M) as donor at 50 °C for 1 hour.....113

Figure 3.42 ESI-MS analysis of transgalactosylation mixture of recombinant α-galactosidase (0.5 U/mL) with sucrose (1 M) as acceptor and *p*NPαGal (0.25 M) as donor at 50 °C for 1 hour.....114

Figure 3.43 HPLC chromatogram of galactose standard against the transgalactosylation reaction mixture of recombinant α-galactosidase (0.5 U/mL) with galactose (1 M) and *p*NPαGal (0.25 M) at 50 °C for 1 hour 117

Figure 3.44 HPLC chromatogram of glucose standard against the transgalactosylation reaction mixture of recombinant α-galactosidase (0.5 U/mL) with glucose (1 M) and *p*NPαGal (0.25 M) at 50 °C for 1 hour 117

Figure 3.45 HPLC chromatogram of mannose standard against the transgalactosylation reaction mixture of recombinant α-galactosidase (0.5 U/mL) with mannose (1 M) and *p*NPαGal (0.25 M) at 50 °C for 1 hour.....118

Figure 3.46 HPLC chromatogram of cellobiose standard against the transgalactosylation reaction mixture of recombinant α-galactosidase (0.5 U/mL) with cellobiose (1 M) and *p*NPαGal (0.25 M) at 50 °C for 1 hour....118

Figure 3.47 HPLC chromatogram of lactose standard against the transgalactosylation reaction mixture of recombinant α-galactosidase (0.5 U/mL) with lactose (1 M) and *p*NPαGal (0.25 M) at 50 °C for 1 hour 119

Figure 3.48 HPLC chromatogram of maltose standard against the transgalactosylation reaction mixture of recombinant α-galactosidase (0.5 U/mL) with maltose (1 M) and *p*NPαGal (0.25 M) at 50 °C for 1 hour 119

Figure 3.49 HPLC chromatogram of sucrose standard against the transgalactosylation reaction mixture of recombinant α-galactosidase (0.5 U/mL) with sucrose (1 M) and *p*NPαGal (0.25 M) at 50 °C for 1 hour 120

Figure C.1. Cloning vector pUC19; (a) map and (b) multiple cloning site (http://www.fermentas.com) 158

Figure C.2 Map of expression vector pAN52-4 (Acc. No: Z32699). Enzymes with unique restriction sites are shown in red..... 159

Figure D.1 Lambda DNA/EcoRI + HindIII Marker (www.fermentas.com) .160

Figure D.2 PageRuler™ unstained protein ladder (www.fermentas.com) 161

Figure D.3 PageRuler™ Plus prestained protein ladder (www.fermentas.com) 162

Figure G.1 Standard curve of *p*-nitrophenol. The equation y=15.967x + 0.0521 and the R^2= 0.9925 were obtained..... 170

Figure I.1 BSA standard curve used in Lowry Method for the determination of total protein concentration after the purification of recombinant α-galactosidase 174

ABBREVIATIONS

AEC: Anion Exchange Chromatography

ANOVA: Analysis Of Variance

ATCC: American Type Culture Collection

ATP: Adenosine Triphosphate

BBD: Box Behnken Design

BSA: Bovine Serum Albumin

CC: Central Composite

DNA: Deoxyribonucleic acid

EC: Enzyme Commission

ESI-TOF MS: Electro Spray Ionization-Time Of Flight Mass Spectrometry

FPLC: Fast Protein Liquid Chromatography

GG: Guar Gum

GH: Glycosyl Hydrolase

GOS: Galactooligosaccharide

GPD: Glyceraldehyde-3-Phosphate Dehydrogenase

GRAS: Generally Regarded As Safe

HIC: Hydrophobic Interaction Chromatography

HOG: High Osmolarity Glycerol

HPLC: High Performance Liquid Chromatography

IMI: International Mycological Institute

IPTG: Isopropyl-Beta-*D*-Thiogalactoside

kDa: Kilo Dalton

K_m: Michaelis-Menten Constant

LBG: Locust Bean Gum

LB: Luria-Bertani

MAP: Mitogen-Activated Protein

NTP: Nucleotide Triphosphate

OD: Optical Density

*p*NPαGal: Para (4) nitrophenyl-α-*D*-galactopyranoside

PCR: Polymerase Chain Reaction

RSM: Response Surface Methodology

Rpm: Revolutions per minute

SDS-PAGE: Sodium Dodecyl Sulfate Polyacrylamide Gel Electrophoresis

TLC: Thin Layer Chromatography

TNO: Nederlands Instituut voor Toegepaste Geowetenschappen

U: Unit

V_{max}: Maximum Velocity

X-gal: 5-bromo-4-chloro-3-indolyl-beta-*D*-galactopyranoside

CHAPTER 1

INTRODUCTION

1.1 Alpha-galactosidase

α-Galactosidase is a glycosyl hydrolase and catalyses the release of terminal, non-reducing α-1,6-linked *D*-galactosyl residues from a wide range of substrates including raffinose family oligosaccharides (RFOs) (Figure 1.1).

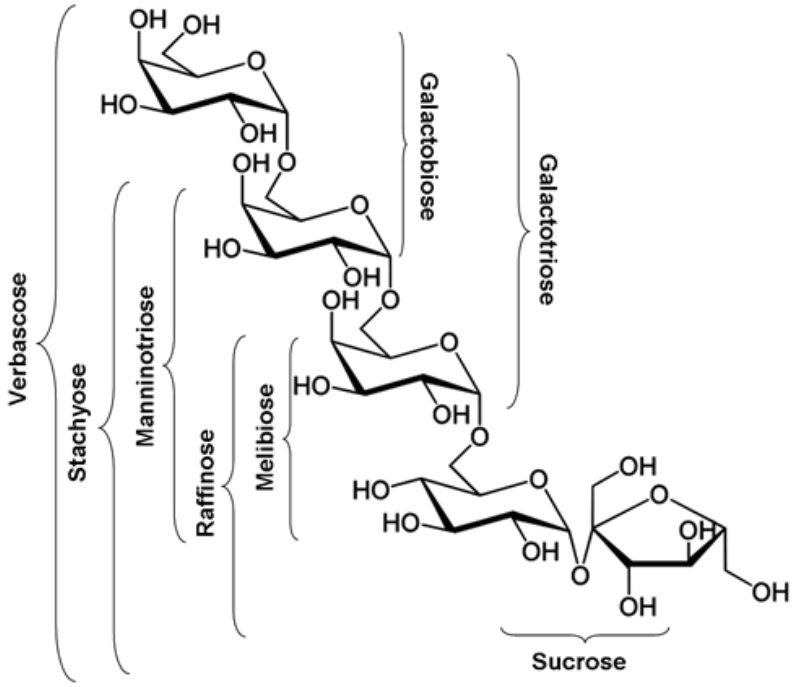

Figure 1.1 The structural relationships of raffinose family oligosaccharides

RFOs include melibiose (α-galactosyl-1,6-glucose), raffinose (α-galactosyl-1,6-sucrose), stachyose (α-galactosyl-1,6-raffinose), verbascose (α-galactosyl-1,6-stachyose), and polysaccharides of galactomannan, locust bean gum, and guar gum (Figure 1.2). α-Galactosidase also acts on galactose containing glycoconjugates, glycoproteins, and glycosphingolipids (Dey *et al*., 1972).

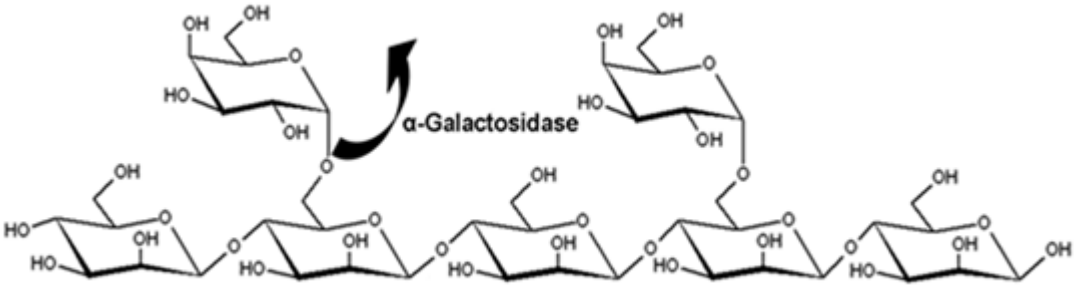

Figure 1.2 Schematic representation of galactomannan

1.1.1 Classification of glycosyl hydrolases

1.1.1.1 Mode of action of glycosyl hydrolases

Exo- and endo- refers to the ability of a glycoside hydrolase to cleave a substrate at the end or within the chain (Figure 1.3). Exo-acting enzymes most frequently act on the non-reducing end.

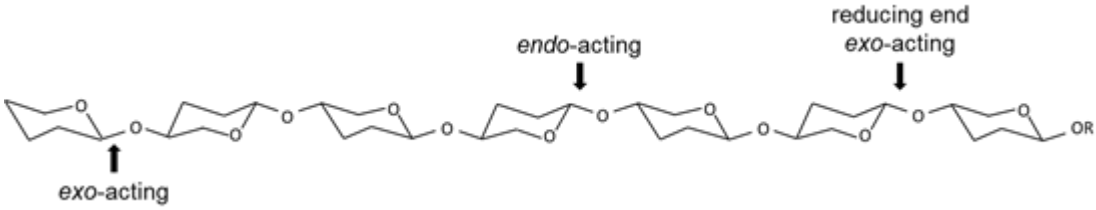

Figure 1.3 Mode of action of glycosyl hydrolases (www.cazypedia.org/)

As α-galactosidase catalyses the release of terminal, non-reducing α-1,6-galactose residues from its substrates, it is an exo-acting glycoside hydrolase.

1.1.1.2 Substrate specificity of α-galactosidase

α-Galactosidase mainly possesses hydrolase activity and cleaves the glycosidic bonds between two or more carbohydrates or between a carbohydrate and a non-carbohydrate moiety.

Glycosyl hydrolases can be classified according to their substrate specificities. This classification is based on the recommendations of the International Union of Biochemistry and Molecular Biology (IUBMB) (IUBMB:Enzyme Nomenclature Recommendations, San Diego, Academic Press; 1992) and is expressed in the EC (Enzyme Commission) numbers. EC 3.2.1 is used for *O*-glycoside hydrolases and the code EC 3.2.1.22 is given for α-galactosidase. The last number defines the substrate specificity and occasionally, molecular mechanism or the linkage type of the enzyme. Enzymes acting on several substrates cannot be classified properly by this classification.

α-Galactosidases are also divided into two groups based on their substrate specificities (Dey *et al*., 1978). α-Galactosidases in the first group generally act on artificial substrates like aryl α-galactosides and act only on oligosaccharides with low degree of polymerization such as melibiose, raffinose, stachyose (Figure 1.1), and short fragments of galacto(gluco)mannans (Figure 1.2). α-Galactosidases in the second group are active on mainly polymeric substrates such as, locust bean gum and guar gum (Figure 1.2). They can also act on short oligosaccharides as well as artificial α-galactosides as in the case of the enzymes in the first group.

1.1.1.3 Mechanism of action

Glycoside hydrolases release products with an inversion or overall retention of the anomeric carbon via either single or double displacement mechanisms, respectively (Figure 1.4). In both of these mechanisms, hydrolysis of the glycosidic bond is performed by two critical catalytic residues, a proton donor and a nucleophile/base. (Koshland, 1953; Sinnott, 1990).

Retaining enzymes use one residue as a nucleophile and the other as a general acid/base catalyst (Koshland, 1953). The nucleophilic catalyst attacks the anomeric carbon of the sugar substrate, hydrolyse the glycosidic bond of the bound sugar generating a covalent glycosyl-enzyme intermediate, while the general acid/base catalyst protonates the glycosidic oxygen with bond cleavage in the glycosylation step and deprotonates the incoming water nucleophile in the deglycosylation step (Figure 1.4.a). On the other hand, one residue acts as a general acid and the other acts as a general base catalyst in inverting enzymes (McCarter and Withers, 1994). The acid catalyst donates a proton to the departure aglycon, and the base catalyst simultaneously deprotonates the incoming water molecule, which attacks the anomeric carbon (Figure 1.4.b). Unlike the retaining enzymes, the inverting enzymes do not involve a glycosyl-enzyme intermediate, which is quite important for transglycosylation.

Based on the release of α-galactopyranose as the primary product of hydrolysis of both 4-nitrophenyl α-galactopyranoside (*para*-nitrophenyl-α-*D*-galactopyranoside: *p*NPαGal) artificial substrate and galactosylmannotriose, naturally occurring substrate, it is concluded that *A. fumigatus* α-galactosidase is a retaining glycosyl hydrolase (Puchart *et al*., 2000).

a)

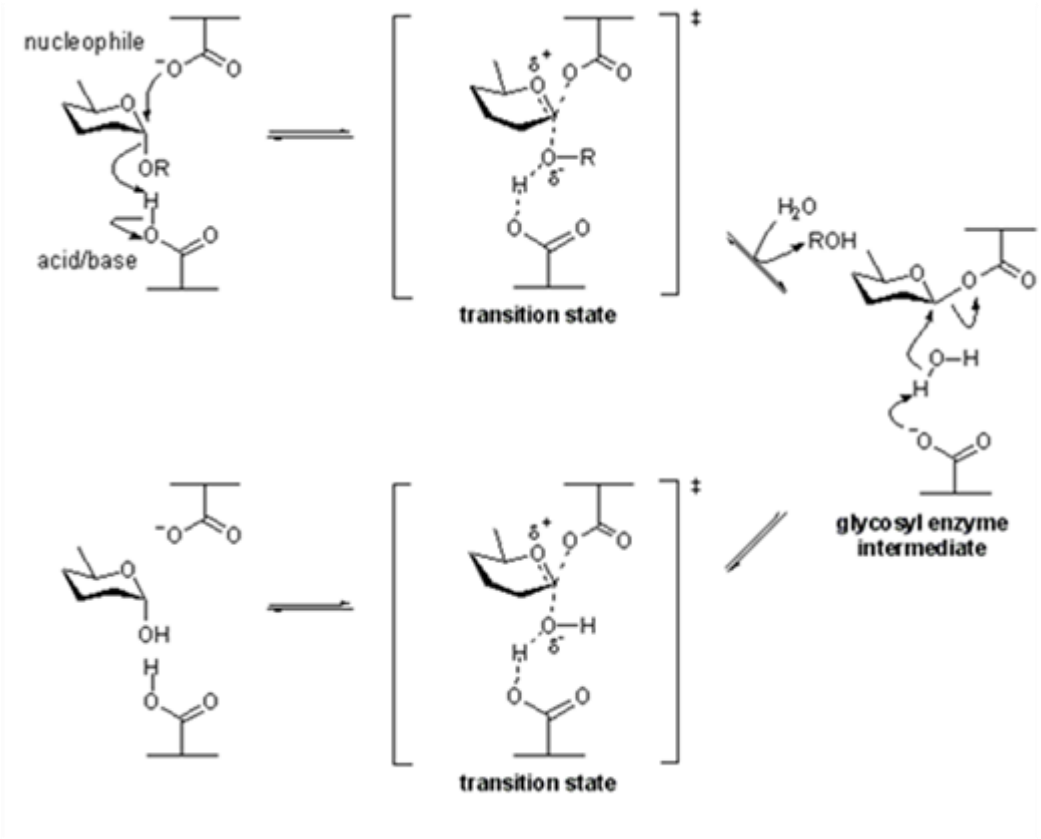

b)

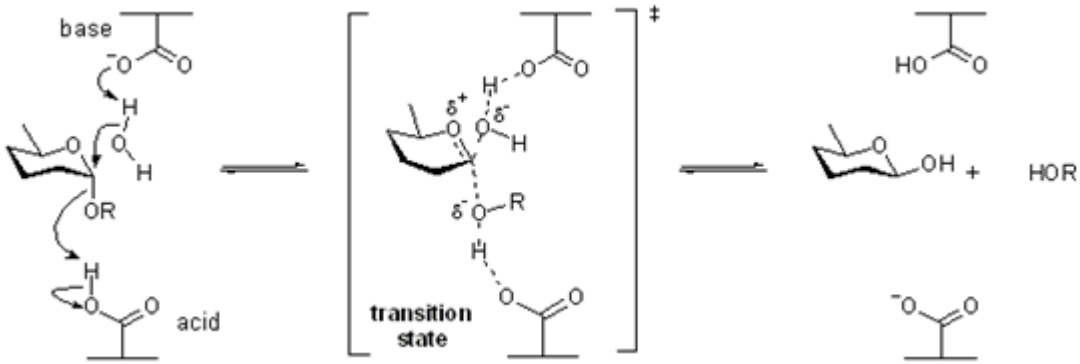

Figure 1.4 Catalytic mechanisms of α-glycosidase; (a) retaining and (b) inverting (http://www.cazypedia.org/)

Henrissat *et al*. (1991) proposed a classification system according to the amino acid sequence similarities of glycoside hydrolases in 1991. In this system, enzymes possessing different substrate specificities may be found in the same family, indicating an evolutionary divergence to acquire new specificities. On the other hand, enzymes hydrolysing the same substrate may be found in different families. As the relationship between sequence and folding similarities is obvious, such a classification shows the structural features of these enzymes better than their only substrate specificity, helps to detect the evolutionary relationships between these enzymes, gives information to derive mechanistic features (Henrissat and Bairoch, 1993), and reflects the difficulty of providing relationships between family membership and substrate specificity.

Based on amino acid sequence similarity, the glycoside hydrolases have been classified into more than 100 families (Henrissat *et al*., 1991). As the folding of proteins is better conserved than their sequences, some of the families can be divided in “clans”. The list of glycosyl hydrolase families is permanently available through the Carbohydrate Active Enzyme database (http://www.cazy.org).

Four of these glycosyl hydrolase families (GH 4, GH 27, GH 36, and GH 57) have the enzymes with α-galactosidase activity. α-Galactosidase activity has been characterized only for few enzymes of GH 4 family (from *Bacillus halodurans, B. subtilis, Citrobacter freundii, Enterococcus faecium, Escherichia coli, Salmonella typhimurium, Sinorhizobium meliloti*) and two enzymes of GH 57 family (from *Pyrococcus furiosus* and *Thermococcus alcaliphilu*s) (http://www.cazy.org).

The majority of the characterized α-galactosidases belongs to GH 27 and GH 36 families and comprises the clan-D superfamily. With a few exceptional members, bacterial α-galactosidases are generally classified in the family 36.

The known eukaryotic enzymes possess a significant degree of amino acid sequence similarity and have been classified in GH 27 family of glycosyl hydrolases (Henrissat *et al*., 1991). The exceptions are the fungal α-galactosidases, AGLII from *Trichoderma reesei* (Margolles *et al*., 1996) and *Agl*B from *A. niger* (De Vries *et al*., 1999), which resemble bacterial counterparts of GH 36 family. These enzymes show a low level of amino acid sequence homology with α-galactosidases of GH 36 family, and they have a lower molecular mass, with a subunit size of ~62 kDa versus ~80 kDa for the family 36 representatives. The eukaryotic α-galactosidases of GH 27 family with 50 kDa average subunit molecular mass are mostly smaller than the bacterial α-galactosidases of family 36.

Only a limited amino acid sequence similarity takes place between the α-galactosidases of the GH 27 and GH 36 families. The shared consensus pattern, [LIVMFY]-x(2)-[LIVMFY]-x-[LIVM]-D-[DS]-X-[WY], is within the central region of the bacterial α-galactosidases (GH 36) and near the amino-terminal end of eukaryotic α-galactosidases (GH 27) (Fridjonsson, *et al*., 1999). The presence of this consensus sequence, in both GH 27 and GH 36 families, suggests a similar reaction mechanism or a substrate-binding site for them.

Based on the amino acid sequence of α-galactosidase enzyme encoded by α-galactosidase B (*agl*B) gene of *A. fumigatus* IMI 385708, it is classified in GH 27 family and clan D. The DNA and amino acid sequences are available with the Genebank Accession Number FJ843023.1 and Protein ID ACO72591.1, respectively (Appendix F).

1.1.2 Application areas of α-galactosidases

Carbohydrates in the form of oligosaccharide and polysaccharide possess varied biological roles in nature, such as food storage and utilization, pathogen recognition and invasion, structure and highly selective cellular

signalling events. Therefore, glycoside hydrolases are indispensable for many vital processes in life: hydrolysis of structural or storage polysaccharides, defence against pathogens, penetration of certain pathogens into cells, turnover of cell surface carbohydrates, etc. (Henrissat *et al*., 1995).

α-Galactosidases have a number of biotechnological, medical, and industrial applications. The most important application of α-galactosidases is presently in the sugar-making industry (Kobayashi *et al*., 1972). Small quantities of raffinose and/or stachyose negatively affect crystallization of sucrose. Thus, enzymatic hydrolysis increases the yield of product by eliminating and converting raffinose and stachyose to sucrose. As these enzyme properties reduce expenses for cooling and re-heating, it is important that the mode of action and stability of α-galactosidases be covered with industrial demands.

α-Galactosidases have potential use in the processing of food products from soybean. Soybean is an excellent source of protein, dietary fibres, and micronutrients. However, the increase in human consumption of soy-derived products has been limited by the presence of non-digestible α-galactosides, mostly raffinose and stachyose, in soybeans. α-Galactosides are carbohydrate reserves in many plant tissues and particularly in seeds. They include one or several galactose units, linked together or to the glucose moiety of sucrose through α-1,6 linkages (Figure1.1).

As humans and monogastric animals are deficient in pancreatic α-galactosidase enzyme, α-galactosides cannot be digested in the duodenum. They pass into the large intestine where gas-producing intestinal bacteria, such as *Clostridium* spp. and *Bacteroides* spp. digest them by yielding considerable amounts of CH_4, CO_2, and H_2. The excessive accumulation of these flatulent rectal gasses leads to gastrointestinal distress, such as abdominal pain, nausea, diarrhoea, and increased peristalsis. To defeat this problem by removing the α-galactosides from soybeans and to enhance the

consumption of these otherwise highly nutritional food products, many approaches have been made. As an alternative to laborious physical methods, the use of α-galactosidase as food additive for the removal of α-galactosides from soybean and other legume is widely used (Cruz *et al*., 1981; Gote *et al*., 2004).

Another potential use of α-galactosidase is seen in pulp and paper industry, where galactosidases can promote the bleaching effect of endo-β-1,4-mannanases on softwood kraft pulp (Ratto *et al*., 1993).

Locust bean gum (LBG) contains 22−24% galactose moiety and can form gels both in the native stage and together with other polysaccharides such as agar, carrageenan, and xanthan. On the other side, guar gum (GG) has 38−40% galactose content and has poorer gelling properties than LBG. Alteration of GG, to more efficient gelling agent LBG-like polysaccharides can be accomplished by partially removing the galactoside units from guar polysaccharide by taking advantage of α-galactosidase (Bulpin *et al*., 1990) (Figure 1.5).

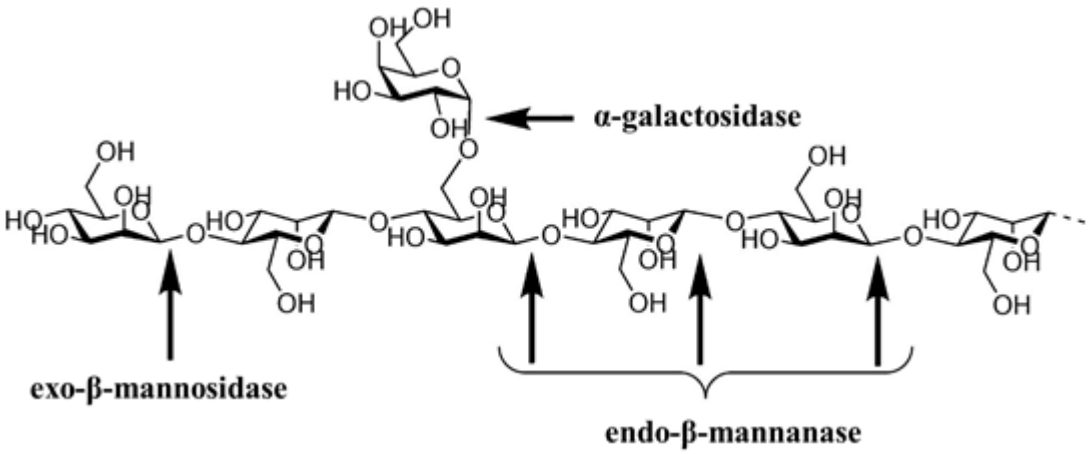

Figure 1.5 Guar gum processing by three hydrolytic enzymes; α-galactosidase, β-mannanase, and β-mannosidase (Dias *et al*., 2004)

Presently, an increased demand in α-galactosidases is seen in human medicine. The ABH blood group specificity is determined by the nature and linkage of monosaccharides at the ends of the oligosaccharide chains. The oligosaccharide chains are linked to peptide (glycoprotein) or lipid (glycosphingolipid) backbones, which are attached to the cell membrane. The immunodeterminant monosaccharide in blood group A is a terminal α-1,3 linked N-acetylgalactosamine, while the corresponding monosaccharide of blood group B is an α-1,3 linked galactose. Blood group 0 cells lack either of these monosaccharides at the end of carbohydrate chains, which instead are ended with α-1,2 linked fucose residues and called the H antigen (Watkins *et al*., 1980). Several α-galactosidases are able to recognize the terminal α-1,3 linked galactose unit of the human blood group B antigen and catalyse the alteration of it to the universal donor, blood group 0 (Olsson *et al*., 2004) (Figure 1.6).

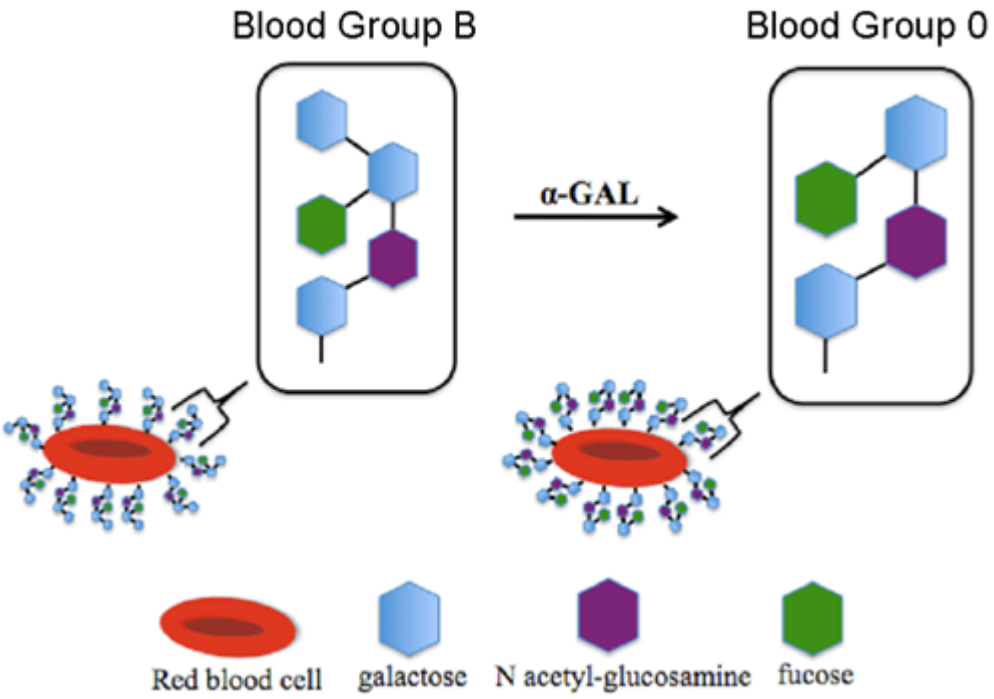

Figure 1.6 Alteration of blood group B to blood group 0 by α-galactosidase (Guce, 2010)

Another increased interest in the use of α-galactosidase in human medicine is to treat Fabry Disease. Fabry Disease is an X-chromosome-linked recessive lysosomal storage disorder caused by genetic deficiency of the lysosomal α-galactosidase A, resulting in progressive systemic accumulation of metabolic intermediates, i.e., glycosphingolipids, particularly globotriaosylceramide (ceramide trihexoside) (Desnick *et al*., 2001). α-Galactosidases able to cleave terminal α-galactosyl unit from globotriaosylceramide and convert it to lactosylceramide, might be employed for the treatment of Fabry Disease by recombinant α-Gal A replacement therapy (Figure 1.7). Recently, safety and effectiveness of enzyme replacement therapy for Fabry Disease have been reported (Schiffmann *et al*., 2001, Eng *et al*., 2001).

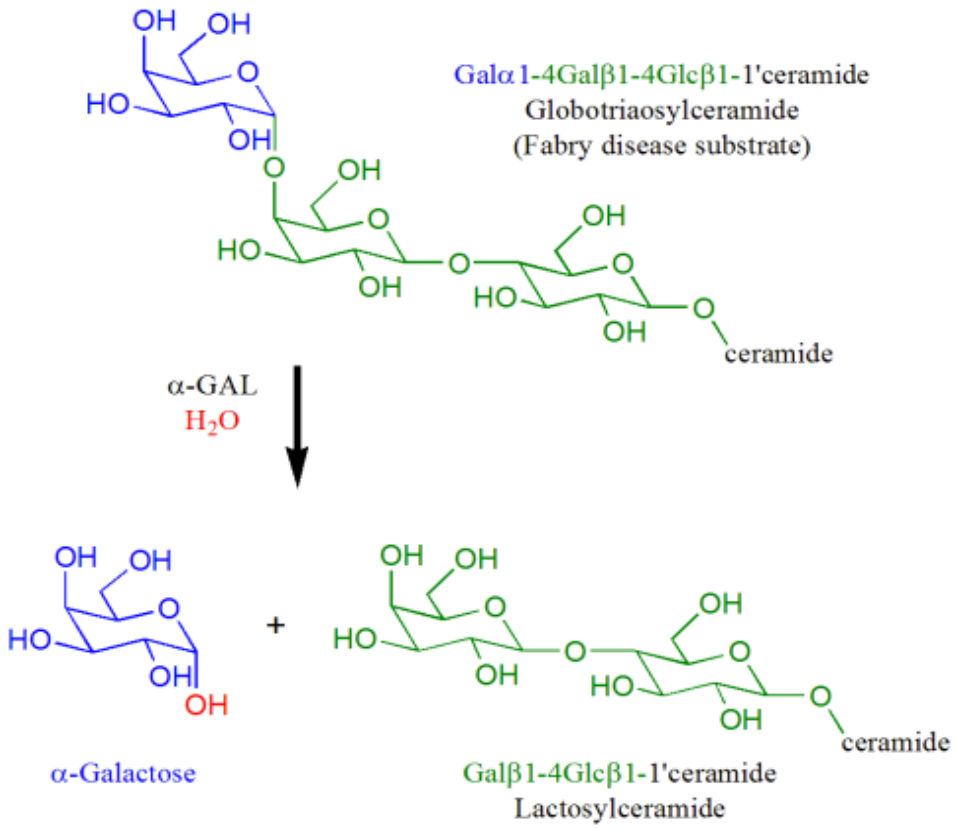

Figure 1.7 Elimination of terminal galactose from globotriaosylceramide by α-galactosidase (Guce, 2010)

Currently, glycosyl hydrolases have gained interest as a powerful tool for convenient oligosaccharide synthesis through transglycosylation or reverse hydrolysis reactions (Kren *et al*., 1997). A few α-galactosidases have been shown to synthesize α-galactooligosaccharides at high substrate concentrations by catalysing the transfer of a galactosyl moiety to an acceptor molecule other than water with α-(1,3), α-(1,4), or α-(1,6) regioselectivity (Hashimoto *et al*., 1995, Spangenberg *et al*., 2000).

1.1.3 Three dimensional (3-D) structure of α-galactosidase

Among the crystallized glycoside hydrolase family 27 members, the highest similarity to *A. fumigatus* α-galactosidase is belong to *Trichoderma reesei (Hypocrea jecorina*) α-galactosidase with 57% homology, based on the multiple sequence alignment.

Crystallographic model structure showing the overall fold and the active site of *T. reesei* α-galactosidase is shown in Figure 1.8. The protein structure possesses two domains, an N-terminal catalytic domain of the $(\beta/\alpha)_8$ barrel topology and a small C-terminal domain arranged by an antiparallel α-structure. The model includes 19 α-helices (29%) and 16 β-strands (19%). Four N-binding sugar chains were determined in the catalytic domain of the structure (Golubev *et al*., 2004).

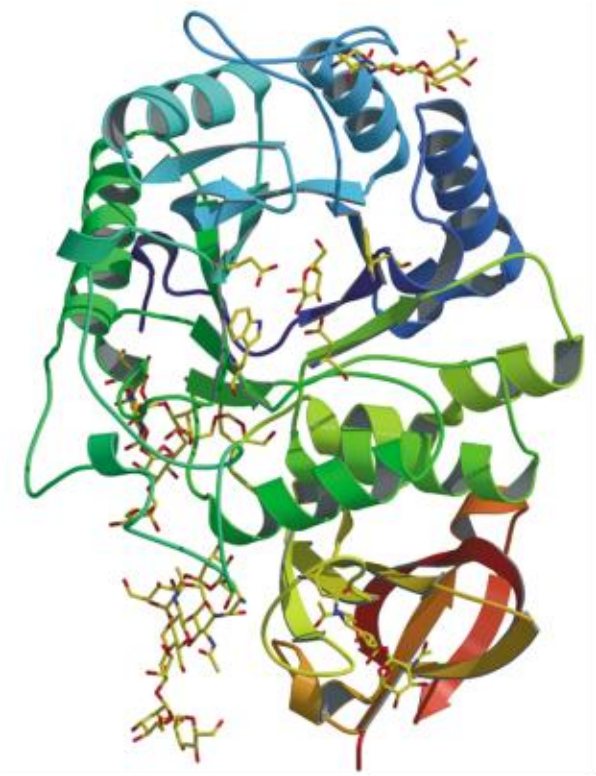

Figure 1.8 The 3-D crystal structure of α-galactosidase from *T. reesei*. β-strands (arrows), α-helices (coils), catalytic residues (Asp132 and Asp226), two Trp residues responsible for hydrophobic interactions with the substrate, and four N-glycosylation sites (sticks) are shown (Golubev *et al*., 2004).

1.1.4 Properties of α-galactosidase of *A. fumigatus* IMI 385708

The α-galactosidase gene of interest is located on the chromosome 5 of *A. fumigatus* genome (Figure 1.9). Its nucleotide and protein sequences are given in Appendix F. *A. fumigatus* α-galactosidase comprises 5 introns. Its calculated molecular weight is 47 kDa and isoelectric point is 4.93.

Puchart *et al.* (2000) observed that *A. fumigatus* IMI 385708, grown on 2% LBG produced high levels of extracellular α-galactosidase. The maximum α-galactosidase activity reached about 0.8 U/mL in a typical experiment was obtained after 72−75 hours. They isolated and characterized the extracellular α-galactosidase , which was found to have a molecular weight

of 57 kDa and an isoelectric point of 5.2. Optimum pH of the enzyme was pH 4.5−5.0 and the temperature optimum was found as 65−70 °C.

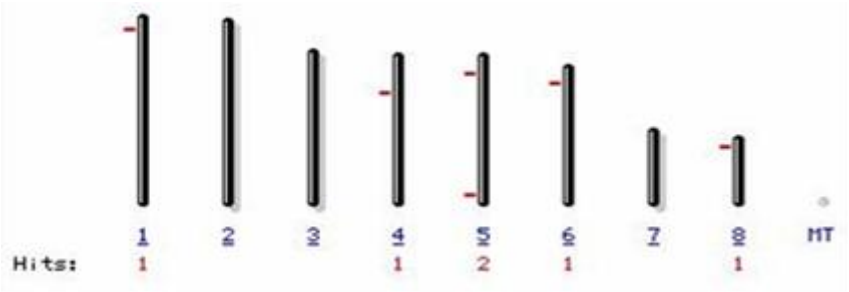

Chr	Match	Map element	Type	Maps
1	alpha-galactosidase	Afu1g01200	GENE	Genes seq
4	alpha-galactosidase	Afu4g03580	GENE	Genes seq
5	all matches			
*	alpha-galactosidase	Afu5g13830	GENE	Genes seq
	alpha-galactosidase	Afu5g02130	GENE	Genes seq
6	alpha-galactosidase	Afu6g02560	GENE	Genes seq
8	alpha-galactosidase C	Afu8g01130	GENE	Genes seq

Figure 1.9 *A. fumigatus* genome view showing putative α-galactosidases (http://www.ncbi.nlm.nih.gov/)

The aryl glycoside proved to be the best substrate for α-galactosidase of *A. fumigatus* IMI 385708 with the highest V_{max} and the lowest K_m values shown in Table 1.1 (Puchart *et al*., 2000).

The *A. fumigatus* IMI 385708 α-galactosidase also performs the efficient transgalactosylation of a variety of monosaccharides, disaccharides and oligosaccharides such as, maltooligosaccharides, cellooligosaccharides and mannooligosaccharides (Puchart and Biely, 2005).

Table 1.1 Kinetic parameters of *A. fumigatus IMI 385708* α-galactosidase for three substrates (Puchart *et al*., 2000)

Substrate	**K_m (mM)**	**V_{max} (U/mg)**	**K_{cat} (s^{-1})**	**K_{cat}/K_m ($mM^{-1}s^{-1}$)**
*p*NPαGal	0.5	52.4	49.8	97.8
Melibiose	2.4	2.4	2.3	0.9
Raffinose	11.3	34.1	32.4	2.9

1.2 The thermotolerant filamentous fungus *A. fumigatus*

A. fumigatus shown in Figure 1.10 is a saprophytic, haploid fungus that does not show a natural sexual cycle. *A. fumigatus* is a thermotolerant fungus and its natural niche is decaying organic material; consequently, it is one of the most common inhabitants of compost (Latgé, 1999).

A. fumigatus is the most common human and animal pathogen among the 182 recognized species of *Aspergillus* (Pitt *et al.*, 2000). Spores of *Aspergillus* are ubiquitous in the air but do not normally cause illness. However, individuals with a weakened immune system are affected by opportunistic *Aspergillus* (Martinez *et al.*, 2000). Infection is usually related with the pulmonary system, although ear, eye, and sinus cavities can also be affected. It is also a principal cause of aspergillosis and inhalation can cause mycosis, allergic asthma, hypersensitivity pneumonitis, aspergilloma (Denning, 1998; Smith, 1989). During the last decade *A. fumigatus* has become the most common agent of airborne pathogenic fungal infections (Latgé, 1999) and of invasive infections in humans (Brookman and Denning, 2000).

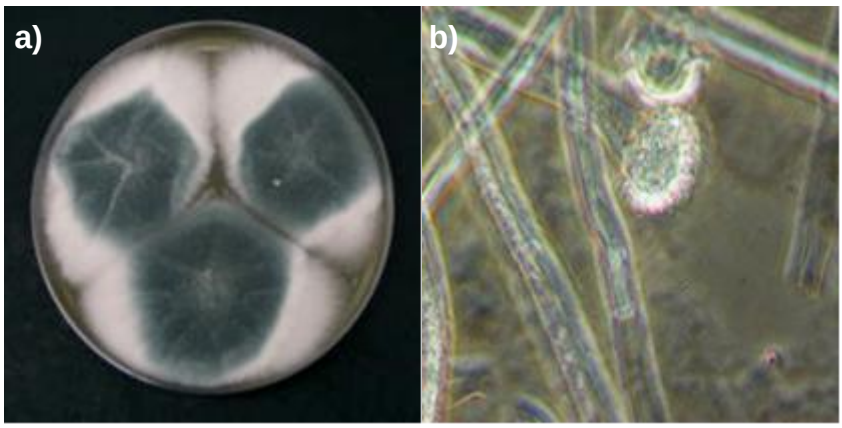

Figure 1.10 *A. fumigatus* IMI 385708; (a) macroscopic (Photo by Dr. David Midgley) and (b) under the light microscope (4x)

The *A. fumigatus* genome is estimated to be 30 Mb, organized in 8 chromosomes (Brookman *et al*., 2000). The sequencing and analysis of the *A. fumigatus* genome contributed to the understanding of the biology of this important human and animal pathogen and the identification of the molecular pathology of aspergillosis.

1.3 *A. sojae* as a cell factory for heterologous protein production

Various proteins have been produced, isolated, and characterized from filamentous fungi. Recently, they are employed as cell factories for heterologous protein production (Archer, 2000).

One of the advantages of using fungi in comparison to bacteria is their ability to produce eukaryotic proteins, which need post-translational modifications like glycosylation and disulphide bridge formation (Maras *et al.,* 1999). Only few fungal species are currently employed as hosts for protein production (Punt *et al.,* 2002). Among these, *Aspergillus* species play a dominant role as they are represented among the strains used for traditional food production process. Several food products produced by *Aspergillus* strains had already gained a Generally Recognized As Safe

(GRAS) status from the regulatory authorities and these fungi are accepted as safe and reliable expression platform. New fungal species are identified to meet commercial interests to use them as expression hosts for heterologous protein production (Punt *et al*., 2002). A new expression system, *A. sojae* was identified because of this commercial need (Figure 1.11).

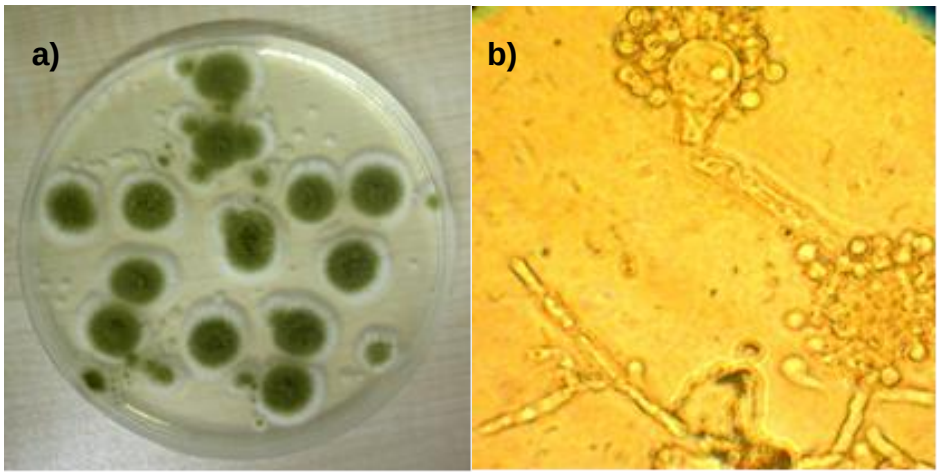

Figure 1.11 *A. sojae* (a) grown on minimal medium agar plate after transformation and (b) its conidia and conidiospores under the light microscope (4x)

A. sojae, believed to be a domesticated strain of *A. parasiticus*, has all of the aflatoxin biosynthetic genes but does not produce aflatoxin and considered as GRAS for producing fermented foods (Chang, 2003). The reason behind the non-aflatoxigenicity of *A. sojae* comes from a nucleotide change in *aflR* gene, which is responsible for transcriptional activation of more than 20-clustered aflatoxin biosynthetic genes (Payne and Brown, 1998). This nucleotide change truncates the last 62 amino acids of the protein (Watson *et al*., 1999) and pretermination obviously make *A. sojae* non-aflatoxigenic (Matsushima *et al*., 2001; Takahashi *et al*., 2002).

The non-aflotoxigenic species have been widely employed for food fermentation or enzyme production. Like *A. oryzae*, *A. sojae* is an important species for industry and widely employed in food fermentation, such as soy sauce and bean paste production (Chang, 2003).

A new expression host from *A. sojae* ATCC strain was improved by Margreet Heerikhuisen, Cees van den Hondel and Peter Punt from TNO Nutrition and Food Research, Department of Microbiology (Zeist, The Netherlands). In their study, *A. sojae* ATCC11906 strain with the lowest proteolytic activity was chosen for further research. NaCl method showing higher protoplasting efficiency for *A. sojae* ATCC11906 strains was selected for transformation experiments (Punt *et al*., 1991).

pyrG auxotrophic marker system was improved for *A. sojae* as selection marker. Auxotrophic mutant of *A. sojae*, unable to synthesize uridine was employed. During fungal transformation, *p*AMDSPYRG co-transformation vector, possessing *amd*S and *pyrG* genes was used. By co-transformation of pAMDSPYRG the true transformants would be able to grow in the minimal medium while untransformed *pyr*G^{-} mutants would not grow in the absence of uridine from the selective medium as they were blocked in pyrimidine biosynthesis because they lack orotidine-5′-phosphate-decarboxylase. In their study, they could transform *A. sojae* and obtained high levels of the fungal phytase and glucoamylase using *pFytF3* and *pGLA6S* plasmids, which included *A. nidulans gpd*A glyceraldehyde-3-phosphate dehydrogenase (GPD) promoter and *trpC* terminator regions (Punt *et al*., 1991).

1.4 Optimization of fermentation media and conditions

To meet industrial expectations it is essential to improve the efficiency of the bioprocess by increasing the yield while decreasing the cost of the production. Fermentative processes are highly affected by medium composition and cultivation conditions. Carbon and nitrogen sources of the culture medium can be regarded as the major media component. In order to achieve cost-effective production, cheap sources should be selected.

Sugar beet molasses is a by-product obtained after the final crystallization process in sugar industry. Molasses contains trace elements such as, magnesium, potassium, sodium, calcium, iron, and copper in addition to the sucrose as the major carbohydrate (El-Abyad *et al*., 1992). The use of molasses as a cost effective carbon source for fermentation processes is common in literature. The optimum amount of molasses varies with the process. 15% cane molasses (w/v) for citric acid production by *A. niger* (Ikram-ul *et al*., 2004), 18% beet molasses (w/v) for cephalosporin C production by *Acremonium chrysogenum* (Lotfy, 2007), 8% cane molasses (w/v) for cell-bound phytase production by *Pichia anomala* (Kaur *et al*., 2005) were determined as the optimal molasses concentrations. Molasses is also utilized as a substrate for commercial yeast production and has been used for construction of α-galactosidase-producing Baker's yeast strain (Liljestrom-Suomınen *et al*., 1987). However, to our knowledge, sugar beet molasses has not been used for α-galactosidase production by fungi so far.

In spite of the common utilization of organic nitrogen sources (e.g. yeast extract, peptone, tryptone, casein), cheap inorganic salts (e.g. NH_4NO_3, $NaNO_3$, KNO_3 Na_2SO_4) are also promising media components for fermentation processes (Xu *et al*., 2006).

Agitation speed of the cultivation is also quite important for the morphology and the productivity of the fungal cultivations. In agitated submerged

cultures, filamentous fungi generally grow either in the form of freely dispersed filaments (hyphae) or in compact spherical mycelial pellets. Besides, some other intermediary growth forms like fluffy mycelia (diffuse mycelia), clumpy mycelia (aggregated mycelia), looser and more hairy pellets, can also be recognized (Thomas and Paul, 1996). Fungal morphology strongly affects the overall cell performance. In general, increasing the agitation speed changes the fungal morphology from pelleted form to filamentous form and increases the protein productivity. In pelleted form are mass transfer limitations leading to significant concentration gradients of oxygen and nutrients from the culture fluid to the inner part of the pellet. Finally, autolytic processes take place within the inner core of the large fungal pellets. On the other hand, extremely high agitation rate causes shear stress resulting in lower biomass yields and increased respiration and acid formation (Grimm *et al*., 2005, El-Enshasy *et al*., 2006).

The optimization of fermentation conditions has long been used in enhancing the yield of many bioprocesses due to its effect on the economy and feasibility of the process. Optimization by the traditional ‘one-factor at a time’ technique was frequently used in biotechnology; however, this classical optimization method involves varying a single factor while keeping the others constant, and so on. Thus, it is time-consuming and assumes that the various fermentation parameters do not interact and the process response is a direct function of the single varied parameter. Unlike this approach, statistical optimization methods (e.g. full factorial design, response surface, etc.) take into account the interactions of variables in generating the optimum process response (Haaland, 1989).

Full factorial design provides extensive information but involves unfeasible complexity resulting from high number of experiments. Response surface methodology (RSM) decreases time and cost by providing fewer numbers of experiments compared to full factorial design. It was widely used in the optimization of fermentation process, e.g. media components on enzyme

production, production of other metabolites (Zhang, *et al*., 1996), and biomass production (Lhomme and Roux, 1991) optimization.

Box-Behnken (BB) and Central Composite (CC) response surface design types are available. Unlike CC design, BB designs are generally recommended when performing non-sequential experiments, that is, when planning to perform the experiment once. BB designs do not have axial points but CC has, thus, in BB design all design points will fall within the safe operating zone (Box and Behnken, 1960). In other words, BB design ensures that, all factors are never set at their high levels simultaneously.

1.5 Osmotic stress and fungi

As free-living filamentous fungi are ubiquitous in nature and inhabit variable ecological niches, they need to adapt to environmental alterations quickly and continuously by adjusting their physiology in order to survive. Fungi have complex signal transduction pathways allowing their adaptation appropriately to changes in external factors. These factors may be biotic or abiotic stresses involving changes in temperature, pH, nutrient availability, oxidative stress, and osmotic stress. Among these factors, osmotic stress will be focused on in this thesis.

Many studies concerning the molecular regulation of cellular responses to osmotic stress were conducted for the yeast *Saccharomyces cerevisiae* and these are reviewed recently (Hohmann *et al*., 2007). The high osmolarity glycerol (HOG) pathway regulated by MAP (mitogen-activated protein)-kinase signalling pathway in osmotic stress response were identified (Hohmann, 2002). A recent review of annotated stress proteins by Miskei *et al*. (2009) identified a number of genes in different *Aspergillus* species (*A. clavatus*, *A. flavus*, *A. fumigatus*, *A. niger*, *A. nidulans, A. oryzae*, *A. terreus*, and *N. fisheri*) that are orthologous to those encoding components of the *S. cerevisiae* HOG pathway (Hohmann, 2002).

Activation of the HOG pathway depends on the increase in osmotic pressure and activated MAPKs phosphorylate a number of transcriptional factors required for osmotic stress response, for example, glycerol biosynthesis genes such as the genes encoding a glycerol-3-phosphate dehydrogenase and glycerol-3-phosphatase (Albertyn *et al*., 1994; Norbeck *et al*., 1996). HOG pathway is necessary for the activation and increase of the RNA polymerase II complex and mRNA, behaving as a transcriptional elongation factor specific for genes induced upon osmotic stress (Mas *et al*., 2009; De Nadal *et al*., 2004).

In both yeasts and filamentous fungi, osmotic stress responses result in the biosynthesis and accumulation of compatible molecules such as polyols, proline, trehalose and glycerol to resist the osmotic pressure and prevent loss of water (Fillinger *et al*., 2001; de Vries *et al*., 2003).

Glyceraldehyde-3-phosphate dehydrogenase (GPD) is an important enzyme in carbon metabolism and catalyses the oxidation of glyceraldehyde-3-phosphate to 1,3-bisphosphate glyceric acid. Increased GPD expression in osmo-adapted A. *nidulans* cells was previously shown (Redkar *et al*., 1998; Kim *et al*., 2007). The induction of gpdA expression in salt-adapted culture was surprising because Redkar *et al*., (1995) have previously shown that *A. nidulans* accumulated glycerol as a compatible solute in salt-adapted cultures. Increased expression of GPD mobilizes carbon away from glycerol and into the pathway leading to glycolysis and ATP formation. Cellular regulation in salinity conditions requires extra energy for growth and expression of several stress related genes involved in mitochondrial ATP formation is known to be induced in salt-adapted cultures (Redkar *et al*., 1996a). Thus, GPD regulates stress response and ATP formation during growth under osmotic stress conditions. Although *gpd*A is constitutively expressed (Punt *et al*., 1990), Redkar *et al*. (1998) showed increased transcription level of the gene in NaCl-adapted cultures. These observations imply that the *gpd*A promoter is responsive to osmotic signals, and can be

induced in order to enhance the expression levels of heterologous genes under its control. Therefore, the advantage of fungal expression system pAN52-4 could be taken to further enhance heterologous α-galactosidase production by *A. sojae* Ta1, using the facility of *gpd*A promoter induction by osmotic stresses.

Based on the results of previous reports (Redkar *et al*., 1998), in this study, salt stress was employed as a means of further increasing heterologous α-galactosidase production in *A. sojae*. Cultures were either salt-adapted by a gradual increase in medium salt concentration or they were suddenly exposed to salt stress (non-adapted cells) in the presence of different salts and at different concentrations. The influence of osmotic signals on fungal growth and morphology was also analysed, due to their importance for large-scale applications.

1.6 Transgalactosylation activity of *A. fumigatus* α-galactosidase

Galactooligosaccharides (GOS), which are not digested by human gastrointestinal tract due to the lack of α-galactosidase enzyme, are one of the most important groups of prebiotic oligosaccharides. These undigested oligosaccharides are selectively fermented by gastrointestinal microbiota and beneficially affect the human health by promoting the growth of the beneficial bacteria like Bifidobacterium and Lactobacilli.

Although there are some GOS prebiotics on the market currently, there is still great interest in the production and improvement of new prebiotic candidates.

The synthesis of galactooligosaccharides via enzymatic ways has advantages over the chemical approaches, which are usually laborious and expensive due to the protection and de-protection steps. Glycosyl transferases and glycosidases are employed to glycosylate carbohydrate

substrates. Glycosyl transferases catalyse the transfer of the glycosyl residue to the acceptor efficiently and selectively, however, they require for a complex glycosyl donor and they are not available as the glycosidases. In contrast, the glycosidases, which are readily available, use simpler glycosyl donors. Moreover, glycosidases are preferred due to their low cost, high stereoselectivity and stability. Their main disadvantage is that regioselectivity may not be observed in all cases (Crout and Vic, 1998).

Some of the glycosidases have been found to possess transglycosylation activities in addition to hydrolytic activity (Eneyskaya *et al*., 1993; Spangenberg *et al*., 2000) especially at a high concentration of substrate.

In transglycosylation, the glycosyl part of the substrate is transferred to hydroxyl-containing compounds other than water. The transglycosylation reaction occurs between an activated monosaccharide, the donor (*p*-nitrophenylglycoside) and an acceptor. The acceptor is a molecule having at least one hydroxyl group and may be an aliphatic alcohol, a hydroxyaminoacid (serine, threonine, and peptide derivatives), or a saccharide. Transglycosylation reaction remains in competition with the hydrolysis of the donor and of the transglycosylated products. Therefore, excess amount of the acceptor relative to the donor is commonly used. However, when the acceptor is a rare and/or an expensive molecule, the donor is used in excess over the acceptor (Hashimoto *et al*., 1995; Spangenberg *et al*., 2000).

The donors to be used in transglycosylation reactions should be more reactive than the products, react fast to reduce the possible product hydrolysis, and bind tightly (low K_m) to prevent product inhibition (Osborn, 2003). Prevalently, *p*-nitrophenyl glycosides are used as donor because they are highly reactive and are efficiently recognized by glycosidases. They enable fast transfer of glycosyl units in short time and therefore prevent or reduce the hydrolysis of the product.

The donor can also act as an acceptor and the result is a competition between two transglycosylation reactions: the auto condensation (Figure 1.12) and the condensation with the acceptor (Figure 1.13).

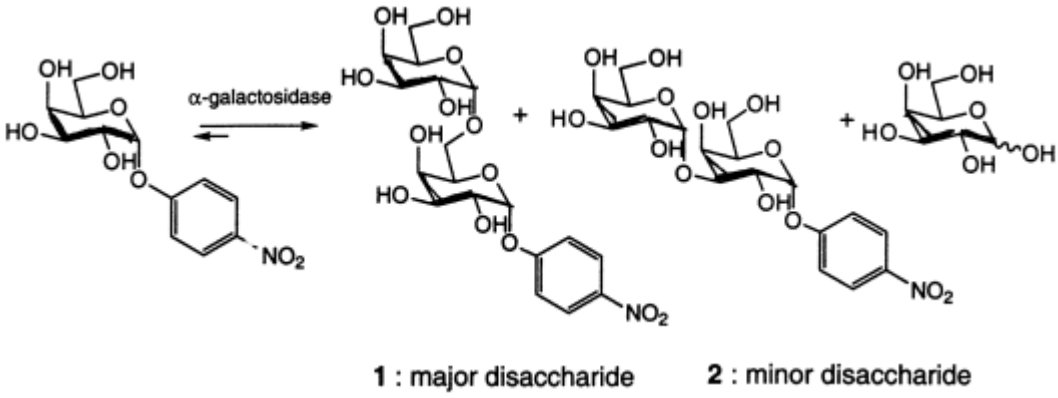

Figure 1.12 The auto-condensation reaction catalysed by glycosyl hydrolases (Spangenberg *et al*., 2000)

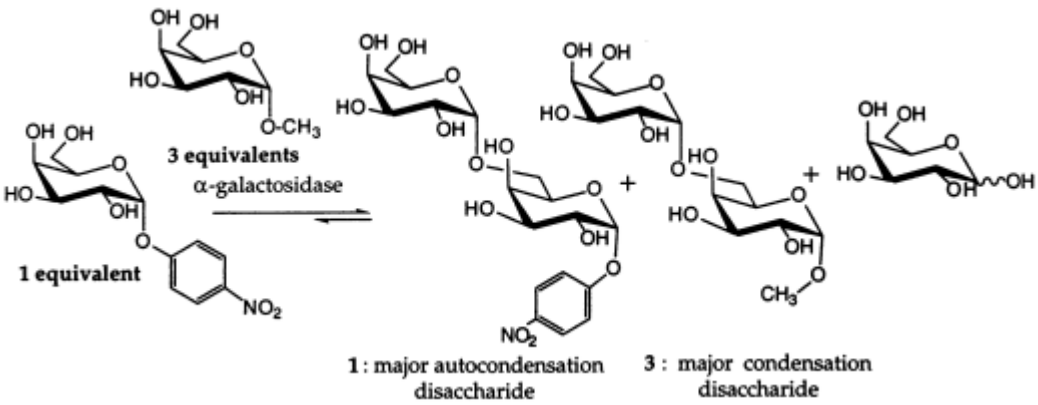

Figure 1.13 The condensation reaction catalysed by glycosyl hydrolases (Spangenberg *et al*., 2000)

The transferase properties of α-galactosidases have been studied extensively with respect to the effect of various parameters, such as galactosyl donor and acceptor specificity, acceptor concentration, pH, temperature, and the source of enzyme (Dey and Pridham, 1972).

A. fumigatus α-galactosidase was previously shown to catalyse transgalactosylation reaction to a variety of monosaccharides, disaccharides and oligosaccharides including the maltooligosaccharides, cellooligosaccharides, and mannooligosaccharides (Puchart and Biely, 2005). Regarding the yields of galactosyl transfer products, the best galactosyl acceptor was β-(1,4) mannooligosaccharides. In contrast to acceptor regiospecificity of other glycosidases, *A. fumigatus* α-galactosidase was able to transfer the galactosyl moiety to reducing-end terminal or internal sugar units of oligosaccharide acceptors (Puchart and Biely, 2005). However, the efficiency was very low with monosaccharide and disaccharide acceptors. *A. fumigatus* α-galactosidase having novel glycosylation activity by transferring the galactosyl units to internal sugar units of acceptor molecules is worth to be studied in more detail for mono- and disaccharide transgalactosylation. In this thesis, different monosaccharides and disaccharides were tested as acceptor in α-galactosidase mediated transgalactosylation and the results were analysed by TLC, ESI-MS, and HPLC.

1.7 Aim of the study

A. fumigatus IMI 385708 is a thermotolerant fungus efficiently producing extracellular α-galactosidase. The enzyme was proved to have significant catalytic properties (Puchart *et al*., 2000) and potential application areas in a number of industries. Furthermore, most of the enzymes of *A. fumigatus* appear to be thermostable due to the thermotolerant nature of the fungus. The thermostability of enzymes is also desired in many industrial applications. However being a human pathogen, *A. fumigatus* cannot be used in industrial applications.

In their previous studies, Yalçındağ (2002) and Söyler (2004) performed cDNA library construction of *A. fumigatus*, isolation of α-galactosidase gene (*agl*B), and cloning into *E. coli* XL1 Blue MRF′ on vector pUC 19. In this study, the primary aim was to clone and express the α-galactosidase gene in a GRAS organism namely *A. sojae* ATTCC11906. After the protoplast transformation of *A. sojae* with recombinant expression vector, pAN52-4 containing α-galactosidase gene, heterologous expression was aimed. This aim was followed by optimization of culture conditions for the heterologous production and analysing the influence of osmotic stress on the production of α-galactosidase. The next aim was to purify recombinant enzyme and subject it to kinetic analysis and characterization. In the final stage of the study, the purified recombinant α-galactosidase enzyme was aimed to apply in transgalactosylation reactions of various mono- and disaccharides.

CHAPTER 2

MATERIALS AND METHODS

2.1 Materials

2.1.1 Organisms and growth conditions

The thermotolerant filamentous fungus, *A. fumigatus* strain IMI 385708 (International Mycological Institute, Kew, Surrey, UK), which was formerly known as *Thermomyces lanuginosus* IMI 158749 (Puchart *et al*., 2000) was kindly provided by Dr. Peter Biely from the Slovak Academy of Sciences, Institute of Chemistry. Stock cultures of *A. fumigatus* were grown on YpSs agar slants containing starch as the only carbon source (Appendix B) at 45 °C until sporulation and then stored at 4 °C. For the induction of α-galactosidase gene, *A. fumigatus* was grown in induction medium containing 0.5% LBG at 45 °C and 155 rpm.

A. sojae ATCC11906 (*pyr*G^{-}) strain was kindly supplied by Dr. Peter Punt (TNO Nutrition and Food Research, Department of Microbiology, The Netherlands). Stock cultures of *A. sojae* ATCC11906 (*pyr*G^{-}) were grown on glucose containing modified YpSs agar with uridine and uracil supplementation (Appendix B).

Modified YpSs broth without uridine and uracil supplementation was used as the basal medium for the enzyme production by recombinant *A. sojae* (*A.*

sojae Ta1). Complete broth medium (Appendix B) without uridine and uracil supplementation was used for transformation of *A. sojae* ATCC11906 (*pyr*G^{-}) and osmotic stress treatment of *A. sojae* Ta1.

Unless specified, all the cultivations were carried out in 250 mL Erlenmeyer flasks with 100 mL working volume and the cultures were incubated at 30 °C for *A. sojae* and 45 °C for *A. fumigatus* in a shaker incubator at 155 rpm.

Fungal spores ($1x10^6$) from the stock cultures stored at 4 °C were inoculated into liquid pre-culture media, which was transferred into the main culture media after overnight incubation at required temperature and agitation speed. The volume of the pre-culture was 2% of the main culture volume.

Escherichia coli XL1 Blue MRF′ was purchased from Stratagene (La Jolla, USA). Stock cultures were grown on LB (Luria-Bertani)-broth (Appendix B at 37 °C, 155 rpm, and stored at 4 °C on LB-agar containing 25 mg/mL tetracycline.

2.1.2 Chemicals, enzymes, and kits

The list of chemicals, enzymes, and kits, used throughout the study, and their suppliers are given in Appendix A.

2.1.3 Growth media, buffers, and solutions

The preparation of growth media, buffers, and solutions used throughout the study are given in Appendix B.

2.1.4 Plasmids

Plasmids used throughout the study are given in Appendix C.

2.1.5 Molecular size markers

DNA and protein molecular size markers used throughout the study are given in Appendix D.

2.2 Methods

2.2.1 Isolation of plasmid DNA

The plasmids were purified according to the instructions given in the Plasmid Mini Kit (Qiagen®).

E. coli XL1 Blue MRF′ cells having plasmid were cultivated in 3−5 mL LB-broth containing 50 µg/mL ampicillin. The cells were centrifuged at 6000 rpm for 8 minutes and the supernatant was discarded. The bacterial pellet was resuspended in 300 µL of buffer P1 (resuspension buffer) (Appendix B). Then, 300 µL of buffer P2 (lysis buffer) (Appendix B) was added and mixed gently for 7−8 times, incubated at room temperature for exactly 5 minutes. After adding 300 µL of buffer P3 (neutralization buffer) (Appendix B), the tube was gently mixed for 7−8 times and incubated on ice for 5 minutes. The mixture was centrifuged at 13000 rpm for 10 minutes. The supernatant was removed and passed through the column which was previously equilibrated earlier with 1 mL QBT buffer (equilibration buffer) (Appendix B), allowed it to enter the resin by gravity flow. The column was washed 4 times with 1 mL QC buffer (wash buffer) (Appendix B). After the elution of plasmid DNA with 800 µL QF buffer (elution buffer) (Appendix B), plasmid DNA was precipitated with 700 µL of isopropanol at room temperature. Then, the mixture was centrifuged immediately at 13000 rpm for 30 minutes and the

supernatant was decanted carefully. The plasmid DNA was washed with 1 mL of 70% ethanol and centrifuged at 13000 rpm for 5 minutes. The supernatant was decanted, the pellet was air-dried for 5 minutes and dissolved in a 15 µL of double distilled water.

2.2.2 Recovering DNA from agarose gel

DNA Extraction Kit (Fermentas®) was used for recovering DNA from agarose gels. DNA containing sample was loaded on agarose gel and the gel was run to separate DNA bands. The gel slice containing the desired DNA band was then excised and transferred into a 1.5 mL microcentrifuge tube. The approximate volume of the gel slice was determined and 3 volumes of extraction binding solution (Appendix B) were added to the tube. The tube was incubated for 5 minutes at 55 °C to dissolve agarose. Per 1 µL of DNA, 2 µL of silica powder was added and incubated for 5 minutes at 55 °C. The tube was vortexed every 2 minutes to keep silica powder in suspension. The silica powder/DNA complex was centrifuged for 5 seconds at maximum speed to form a pellet and the supernatant was removed. Ice-cold 500 µL of extraction wash buffer (Appendix B) was added, vortexed, and centrifuged for 5 seconds. The supernatant was discarded. This procedure was repeated three times. After the supernatant from the last wash was removed, the tube was centrifuged again to remove the remaining liquid. The pellet was air-dried for 10−15 minutes and 10−15 µL sterile deionized water was added to dissolve DNA. The tube was centrifuged and the supernatant was removed into a new tube avoiding mixing with the pellet. The procedure was repeated once more for the removal of small amounts of remaining silica powder.

2.2.3 Purification of plasmid DNA for sequencing

Plasmid Mini Kit (Qiagen®) was used for purification of plasmids for sequencing. First QIAGEN-tip was placed into a tip holder. 1 mL Buffer QBT (Appendix B) was allowed to flow through the tip by reduction in surface tension due to the presence of detergent in the equilibration buffer. QIAGEN-tip was allowed to drain completely. The plasmid solution was loaded onto the QIAGEN-tip promptly. 4 x 1 mL Buffer QC (Appendix B) was allowed to move through the QIAGEN-tip by gravity flow. The first 2 mL was sufficient to remove all contaminants in the majority of plasmid DNA preparations. The second 2 mL ensured complete removal of contaminants. DNA was eluted with 0.8 mL Buffer QF (Appendix B). Plasmid DNA is collected in a 1.5 mL microcentrifuge tube. DNA was precipitated with 0.7 volumes of isopropanol at room temperature. The tube was centrifuged at lower than 10000 rpm for 30 minutes and the supernatant was decanted. DNA was washed with 1 mL of 70% ethanol, air dried for 5 minutes, and then dissolved in 20 µL sterile double distilled water.

Recombinant plasmid was sequenced by Refgen (Ankara). The primers used for sequence analysis of the recombinant plasmid were designed by Oligo Analyzer Programme (www.idtdna.com/analyzer/Applications/ OligoAnalyzer/) and provided in Appendix E.

2.2.4 The polymerase chain reaction (PCR)

A 50 µL of reaction mixture contained

- sterile double distilled water to give a final volume of 50 µL
- 10X reaction buffer to give a final concentration of 1X
- 200 µM dNTP mix
- 1 unit Taq DNA polymerase
- 100 *p*mol from each degenerate primer or 25 *p*mol from each specific primer
- 0.25 µg genomic DNA
- 30 µL mineral oil was added to prevent evaporation.

Amplifications were performed according to the cycles in Table 2.1.

Table 2.1 PCR cycles

1. Initial Denaturation	95 °C, 3 minutes	
2. Amplification	95 °C, 1 minute	X 35 cycles
	$T_{a,}$ 1 minute	
	72 °C, 1 minute/kb	
3. Final Extension	72 °C, 1 minute	

Where T_a is the annealing temperature, ranging from 48 °C to 58 °C, according to the degeneracy and melting temperature of the primers.

2.2.5 Visualization and photography of nucleic acids

0.8% agarose gel (Appendix B) was used for the visualization and analysis of genomic DNA and PCR products. The gel was melted and cooled to 50−60 °C. After the addition of 0.5 µg/mL ethidium bromide, the gel was poured into a mould and allowed to solidify, then placed into the tank of horizontal electrophoresis apparatus covered with 1X TAE buffer (Appendix B). The samples to be visualized were mixed with a loading dye at a ratio of 5:1 and gently loaded to the wells. Lambda DNA / EcoRI + HindIII marker was used as the size marker (Appendix D, Figure D.1). Electrophoresis was carried out at 70 volt for 60 minutes. Finally, the gel was visualized on a UV transilluminator and photographed by a digital camera (Nikon Coolpix 4500).

The photographs were taken black and white with auto focus. The aperture being 5.2 and exposure varying as 1, 2 and 4 seconds according to the brightness.

2.2.6 Transformation of *E. coli* XL1 Blue MRF′

2.2.6.1 Preparation of *E. coli* competent cells

E. coli XL1 Blue MRF′ cells were cultivated in 5 mL LB medium (Appendix B) overnight at 37 °C, 200 rpm. 100 mL of LB medium was inoculated with 1 mL of an overnight culture of *E. coli* XL1 Blue MRF′ cells and incubated at 37 °C until the OD_{550} reached 0.4−0.5.

The culture was dispensed into two falcon tubes. The tubes were chilled on ice for 10 minutes and centrifuged at 6000 rpm for 5 minutes at 4 °C. The supernatant was discarded and the cells were resuspended in 25 mL ice-cold 50 mM $CaCl_2$ and 10 mM Tris-HCl (pH 8.0) solution, and the tubes were kept on ice for 15 minutes and centrifuged at 6000 rpm for 5 minutes

at 4 °C. Again, the supernatant was discarded, the cells were resuspended in 3.5 mL ice-cold 50 mM $CaCl_2$ and 10 mM Tris-HCl (pH 8.0) solution, and 700 µL of 100% sterile glycerol was added to reach the final concentration of 20%. Finally, 300 µL aliquots were dispensed into microcentrifuge tubes and stored at −80 °C until use.

2.2.6.2 Transformation of competent cells

1−10 µL plasmid (1 µg) was mixed with sterile double distilled water to a final volume of 50 µL. Diluted plasmid was mixed with 300 µL competent cells and kept on ice for 30 minutes. The mixture was transferred into a water bath at 42 °C for 2 minutes and then kept on ice for 2 minutes again. 1 mL LB medium preheated to 42 °C was added and the mixture was incubated in a water bath at 37 °C for an hour. 100−150 µL aliquots were spread on LB agar plates containing 50 µg/µL ampicillin and incubated overnight at 37 °C.

2.2.7 Restriction enzyme digestion of the DNA

In restriction enzyme digestion, 0.1−1 µg DNA and 1−30 unit restriction enzyme were used. Appropriate 10X restriction enzyme buffer to give a final concentration of 1X was used and the final volume of 10−30 µL was adjusted with sterile double distilled water. The reaction mixture was incubated at 37 °C overnight. PCR products were cleaned by Fermentas DNA Extraction Kit or Phenol:choloform:isoamylalcohol (25:24:1) extraction before digestion. After phenol:choloform:isoamylalcohol extraction, DNA was concentrated by isopropanol precipitation to remove interfering oligonucleotides and dNTPs before restriction digest for ligation.

2.2.8 Ligation

5 µg plasmid DNA was digested with appropriate restriction enzyme(s) as explained in Section 2.2.7. The plasmid was then dephosphorylated with alkaline phosphatase. The alkaline phosphatase treatment was directly performed after the cleavage by restriction endonuclease, in the same reaction mixture. The reaction mixture for the dephosphorylation of plasmid DNA was prepared as follows;

- sterile double distilled water to give a final volume of 50 µL
- appropriate 10X restriction enzyme buffer to give a final concentration of 1X
- DNA solution of 1−20 *p*mol DNA termini
- 0.5−2 units calf intestine alkaline phosphatase

The reaction mixture was left at 37 °C for minimum 2 hours up to overnight. Then equal volume of phenol:chloroform:isoamylalcohol (25:24:1) was added. The mixture was centrifuged at 13 000 rpm for 10 minutes and the upper phase was put into a new tube. DNA was precipitated with 0.1 volume of 3 M sodium acetate, pH 5.2 (Appendix B), and 2.5 volume of cold absolute ethanol. The mixture was incubated overnight at −20 °C. Then the tubes were centrifuged at 13000 rpm for 10 minutes at 4 °C. The supernatant was discarded and the pellet was washed with 100 µL of 70% ethanol (Appendix B). The tubes were centrifuged at 13000 rpm for 3 minutes and the supernatant was discarded. The pellet was air-dried for 20 minutes.

The PCR fragments (insert) to be ligated were also digested with the same restriction endonuclease, which were used for the digestion of the plasmid. Phenol:chloroform:isoamylalcohol extraction was also applied to the insert.

In a microfuge tube the following ligation mixture was set up;

- sterile double distilled water to give a final volume of 20 µL
- 10X ligation buffer to give a final concentration of 1X
- 1 mM ATP
- 1 unit T_4 DNA ligase
- 0.1 µg plasmid
- µg insert is calculated according to the following equation; molar ratio of insert to plasmid was selected as 3:1

$$\frac{\text{Fragment size (bp)}}{\text{Vector size (bp)}} \times \frac{3}{1} \times 0.1\ \mu\text{g plasmid}$$

A control reaction was set up, containing all the reagents listed above except the insert. The ligation mixture was incubated at 16 °C overnight.

2.2.9 Identification of recombinant clones

Competent *E. coli* cells were transformed with 5 µL of ligation mixture according to the transformation procedure explained in section 2.2.6. The transformed *E. coli* cells were inoculated on agar plates containing LB medium with 100 µg/mL ampicillin. For blue-white colony selection, 10 µL of 100 mM IPTG and 50 µL of 2% X-gal (Appendix B) were spread on LB plates 30 minutes prior to inoculation of transformed cells and the plates were incubated at 37 °C for 30 minutes to let the media soak in IPTG and X-gal. Following the overnight incubation, a number of white colonies were picked up and plasmid isolation was done to check the presence of insert. Potential recombinant plasmids were then digested with suitable restriction enzymes before loading on an agarose gel to analyse the presence and the size of the insert fragment. If the vector used in ligation did not allow the use of the blue-white colony selection, all of the colonies after the transformation would be picked and plasmid isolations would be done.

Another important point to be considered in selection of recombinant clones is the orientation of the insert in the vector. In order to check the position of the insert, PCR (Section 2.2.4) was done using specific primers (Appendix E).

2.2.10 Transformation of *A. sojae*

2.2.10.1 *A. sojae* ATCC11906 (*pyr*G^{-})

A. sojae ATCC11906 (*pyr*G^{-}) strain, being a uridine auxotrophic mutant which is unable to produce the enzyme orotidine-5 monophosphate decarboxylase (*pyr*G), involved in the biosynthesis of uridine, was used for heterologous expression. The synthesis of the enzyme is prevented by a mutation within the *pyr*G locus. Consequently, such a system provided a higher transformation frequency. Strain ATCC11906, which displayed low proteolytic activity, was selected among other *A. sojae* strains and its proteolytic activity was further reduced by disrupting the most abundant alkaline protease coding gene *alp*A by Heerikhuisen *et al.* (2001).

2.2.10.2 Selection plasmid

In the co-transformation studies, pAMDSPYG plasmid was used as a selective marker. This plasmid includes *amdS* gene of *A. nidulans* and *pyrG* gene of *A. niger*. The *amdS* gene encodes an enzyme that confers a strain the ability to use acetamide and acrylamide as nitrogen and carbon sources. The auxotrophic marker *pyrG* gene encodes orotidine 5-monophosphate decarboxylase, which confers a *pyr*G^{-} strain the ability to grow in the absence of uridine.

2.2.10.3 Expression vector

The expression vector used in transformation was pAN52-4 (sequence accession number Z32750), the map of which is shown in Appendix C.2. It contains the constitutive promoter sequence of *A. nidulans gpdA* gene, encoding glyceraldehyde-3-phosphatedehydrogenase, terminator sequence of *A. nidulans trpC* gene, encoding an enzyme having role in tryptophan biosynthesis, and 24 amino acid-long signal and propeptide sequence of *A. niger glaA* gene encoding glucoamylase.

2.2.10.4 *A. sojae* transformation method

A. sojae transformation was carried out according to a procedure adopted from different protocols (Punt *et al*., 1987) using recombinant plasmid (pAN52-4 expression vector containing α-galactosidase gene) and pAMDSPYRG plasmid containing the *pyrG* selection marker, in a 1:10 ratio. Transformants were selected for uridine prototrophy.

The protocol is based on the preparation of protoplasts and subsequent PEG/$CaCl_2$-mediated DNA uptake. *A. sojae* ATCC11906 ($pyrG^-$) strain was grown on minimal medium agar plates (Appendix B) supplemented with 10 mM uridine and 10 mM uracil for 7 days at 30 °C. Spore suspension was prepared using saline/tween solution (Appendix B) and spores were counted using a Thoma haemocytometer, number of spores/mL was calculated as described in section 2.2.10.5.

500 mL flask containing 250 mL complete medium (Appendix B) supplemented with 10 mM uridine and 10 mM uracil was inoculated with $2x10^6$ spores/mL. After 18-hour growth at 30 °C at 200 rpm, mycelium was collected by filtration through nylon mesh and washed with lytic solution (Appendix B). The collected mycelium was resuspended in filter sterilized 20

mL lytic solution containing 40 mg/mL lysing enzyme (Appendix A). Protoplasts were prepared by incubating the lytic enzyme solution with mycelium at 30 °C for 3−5 hours with slow agitation. Protoplast formation was checked under microscope at 30-minute intervals.

Protoplasts were separated from mycelial debris by filtering through sterile glass wool. From this step on, protoplasts were kept on ice. Protoplast solution was then centrifuged at 2000 rpm for 5 minutes and the supernatant was carefully discarded. The pellet was resuspended in 5 mL STC solution (Appendix B) and the solution was pelleted by centrifugation as before. This washing step was performed twice, after which the protoplasts were resuspended in STC solution such that the concentration is $1x10^8$/mL. 200 µL of the protoplast suspension was added to a 50 mL centrifuge tube for each transformation reaction. Then, 20 µg of recombinant plasmid and 2 µg of pAMDSPYRG co-transformation plasmid were added and mixed gently. To this suspension, 50 µL of PEG buffer (Appendix B) was added, mixed gently, and incubated at room temperature for 20 minutes. After that, 2 mL of PEG buffer was added, mixed gently, and incubated at room temperature for 5 minutes. Then 4 mL STC solution was added to the tubes and tubes were mixed gently. Lastly, 25 mL of melted stabilized minimal medium top agar (Appendix B) was added to the tubes, mixed by inverting several times and the mixture was poured onto two 9 mm minimal medium agar plates. Plates were incubated for 3−4 days at 30 °C.

Obtained transformants were transferred to minimal medium agar plates and incubated at 30 °C until sporulation. Spores were suspended in a small volume of saline/tween solution and streaked onto minimal medium agar plates with a loop to obtain single spores. After growing at 30 °C until formation of small colonies, single colonies were transferred to minimal medium agar plates and incubated at 30 °C for 7 days. Glycerol stocks were prepared from these single colonies by adding 25% glycerol to saline/tween solution containing the purified spores.

2.2.10.5 Preparation of spore suspensions and inoculum

10 mL saline/tween solution was pipetted on the spore-mat. Spores were scraped off using a bend inoculation needle. The spore suspension was transferred to a sterile bottle with a sterile plastic Pasteur Pipette. The concentration of spores was determined by counting the sample diluted with saline/tween solution in a haemocytometer. The concentration of spores was calculated according to the following equation:

$$\frac{\text{Number of spores counted} \times 1000\ \text{mm}^3 \times \text{dilution}}{\text{Number of squares counted} \times \text{width}^2 \times \text{depth}} = \text{Number of spores / mL}$$

Where width: 0.05 mm^2, depth: 0.1 mm^2 for Thoma Haemocytometer.

2.2.11 α-Galactosidase activity assay

Appropriately diluted 0.25 mL of third day culture supernatant and 0.25 mL of 4 mM *p*NPαGal (Appendix B) were combined and the final volume was adjusted to 1 mL in 100 mM phosphate buffer, pH 4.5 (Appendix B) and the mixture was incubated at 50 °C for 8 minutes. As a blank solution, 0.25 mL of 4 mM *p*NPαGal was combined with 100 mM phosphate buffer, pH 4.5 to a final volume of 1 mL. The reactions were stopped by the addition of 3.5 mL of 0.2 M sodium tetraborate solution (Appendix B). The *p*-nitrophenol released was measured from the absorbance at 410 nm using Shimadzu UV-visible spectrophotometer, 1700 PharmaSpec and *p*-nitrophenol standard curve (Appendix G). One unit of enzyme activity is defined as the amount of enzyme required to liberate one µmole of *p*-nitrophenol per minute under the conditions specified above. The data presented for all α-galactosidase activity determinations were mean values of duplicate assays, in which the standard deviations always lay under 10%.

2.2.12 Determination of fungal biomass

Samples withdrawn from the cultivation were filtered through pre-weighed Whatman No. 1 filter paper and were washed 3−5 times with distilled water for fungal biomass determination. The mycelial pellets were dried to a constant weight at 60 °C.

2.2.13 SDS-PAGE

SDS-PAGE was done according to the standard protocol of Laemmli (1970). Electrophoresis system, Serva BlueFlash S, 15 x 28 x 8.5 cm was used, following the instruction manual of Blue Vertical and BioRad, were used.

2.2.13.1 Gel plate assembly

The spacers were placed on the edges of large gel plate and small gel plate was overlaid to create a sandwich. The glass plate sandwich was placed into the electrophoresis running unit, with the small plate innermost and affixed to the inner core running unit by inserting the wedges and pressing down. The running unit was placed on the silicon pads of the gel-casting stand. The cams were used to tighten the assembly down onto the silicon pads.

2.2.13.2 Gel pouring

The components needed for SDS-PAGE are given in Appendix B. Separating gel was prepared by mixing the components listed in Table 2.2 in a tube. TEMED (tetramethylethylenediamine) and freshly made APS (ammonium persulfate) were added before the gel was ready to pour to prevent polymerization in the tube. The separating gel mixture was poured between the plates, overlaid with water, and left for polymerization. After 30

minutes, the water was removed completely and the stacking gel prepared in the same way with the components listed in Table 2.3, was poured on separating gel.

The comb was inserted and the stacking gel was left for polymerization for about 30 minutes. Once the gel was polymerized, the comb was removed and wells were washed out with 1X running buffer.

Table 2.2 Separating gel preparation

Separating Gel (12.5%) Components	**Volume (mL)**
Separating gel buffer	1.2
30% Acrylamide stock	2.1
H_2O	1.7
APS (25%)	0.3
TEMED	0.003
Total	5

Table 2.3 Stacking gel preparation

Stacking Gel (7.5%) Components	**Volume (mL)**
Stacking gel buffer	0.6
30% Acrylamide stock	0.4
H_2O	1.4
APS (25%)	0.02
TEMED	0.002
Total	2.4

2.2.13.3 Sample preparations and electrophoresis

Sample-denaturing mix was prepared by mixing β-mercaptoethanol and sample buffer (Appendix B) in the ratio of 1:4. After the addition of 5 µL sample-denaturing mix to 15 µL of each sample, the samples were boiled for 5 minutes in a boiling water bath and allowed to cool. Denatured samples were centrifuged for 1 minute at maximum speed and were delivered to the base of the wells. The molecular weights of the samples were determined by comparing the relative mobilities of samples with the protein molecular weight markers (Appendix D) delivered to a spare well of the gel.

Constant voltage of 150 V was applied in electrophoresis system and the gel was run until the blue dye was migrated to the base of the gel.

2.2.13.4 Gel Staining

After SDS-PAGE, the gels were stained either with Coomassie Brilliant Blue R-250 or silver nitrate stain.

2.2.13.4.1 Coomassie Brilliant Blue Stain

After the electrophoresis, the gel was put in 100–150 mL Coomassie Brilliant Blue stain (Appendix B) and was warmed up to 50 °C in the microwave for several seconds. Then the gel was incubated by shaking for about 1 hour at room temperature. The stain solution was removed and the gel was washed with distilled water for a few times and was transferred into 100–150 mL destaining solution (Appendix B). Again, the solution was warmed up in the microwave for several seconds and was incubated by shaking at room temperature. The destaining solution was changed several

times until the background colour disappeared and the desired protein bands became visible on the gel.

2.2.13.4.2 Silver staining

After electrophoretic separation, the gel was placed in 100 mL fixer solution (Appendix B) for 1 hour to overnight. After that, the fixer solution was removed and the gel was washed three times with 100 mL of 50% ethanol for 20 minutes. After removing ethanol, the gel was treated with 100 mL pre-treatment solution (Appendix B) exactly for 1 minute. Then pre-treatment solution was removed and the gel was rinsed three times with water exactly for 20 seconds. Then, the gel was placed in 100 mL of silver nitrate solution (Appendix B) for 20 minutes. After removing silver nitrate solution, the gel was washed two times with water for 20 seconds exactly. Then 100 mL developing solution (Appendix B) was added. When the protein bands started to appear, reaction was slowed down by adding water. Once the desired band intensity was obtained, developing solution was discarded; the gel was washed two times with water for 2 minutes. Finally, the gel was kept in 100 mL stop solution (Appendix B) at least for 10 minutes and the gels were photographed on a light box.

2.2.14 Selection of the best carbon and nitrogen sources

Glucose, sucrose, molasses, lactose, galactose, maltose, fructose, starch, and cellulose at concentrations of 20 g/L were tested as the carbon sources in modified YpSs medium. Molasses, which was analysed by HPLC, had 40% sucrose and 2.85% raffinose content. Therefore, 50 g/L of molasses was used to obtain a similar sucrose concentration of 20 g/L.

The nitrogen sources, sodium nitrate ($NaNO_3$), ammonium nitrate (NH_4NO_3), potassium nitrate (KNO_3), ammonium acetate (CH_3COONH_4),

tryptone, peptone from pancreatically digested casein (peptone-C), peptone from pancreatically digested meat, and yeast extract at concentrations of 4 g/L were added to the modified ypSs medium. Other ingredients were kept in their original concentrations in modified YpSs medium

2.2.15 Optimization by response surface methodology

Box-Behnken design (BBD) was applied in response surface methodology (RSM). With respect to three independent variables (% molasses, % NH_4NO_3, and agitation speed) and two dependent variables (α-galactosidase activity, U/mL and biomass generation, mg/mL) were to be optimized by the experimental plan. The ranges were 4−12% for molasses, 0.5−1.5% for NH_4NO_3, and 125−325 rpm for agitation speed for each factor studied. The cultivations were performed in 250 mL Erlenmeyer flasks with 100 mL working volume at 30 °C. The coded and uncoded forms of independent factors are given in Table 2.4. Minitab *v*.15 (Minitab Inc., State College, PA) was exploited to analyse the experimental design given in Table 2.5. A set of 30 experiments were performed. The measurement of each response variable was given as the average of two replicates.

Table 2.4 Coded and uncoded variables of independent factors in RSM

Variables	**Symbols**	**Coded Levels**		
		−1 (Low)	0 (Medium)	+1 (High)
		Uncoded Levels		
Molasses (%)	M	4	8	12
NH_4NO_3 (%)	N	0.5	1	1.5
Agitation (Rpm)	A	125	225	325

A second order polynomial equation was applied to the data to correlate the production of α-galactosidase and biomass (*Y*) to the amount of molasses and NH_4NO_3 and agitation rate. The model equation for a 3-factor system is:

$$Y = b_0 + b_1X_1 + b_2X_2 + b_3X_3 + b_{11}X^2_1 + b_{22}X^2_2 + b_{33}X^2_3 + b_{12}X_1X_2 + b_{13}X_1X_3 + b_{23}X_2X_3$$

Where *Y*, is the predicted response, b_0, the intercept, b_1, b_2, b_3, linear coefficients, b_{11}, b_{22}, b_{33}, squared coefficients, b_{12}, b_{13}, b_{23}, interaction coefficients, and X_1, X_2, X_3, the independent variables used in this study. MINITAB ™ analysis of variance (ANOVA) was exploited for regression analysis of experimental data, response surface and contour plots, and determination of the optimum values for independent variables.

Table 2.5 Experimental design for optimization of α-galactosidase and biomass production using response surface methodology

Run	Carbon (% Molasses)	Nitrogen (% NH_4NO_3)	Agitation (rpm)	Y_1: α-galactosidase (U/mL)	Y_2: Biomass (mg/mL)
1	8	1.0	225	9.9	15.1
2	12	1.0	125	4.0	12.6
3	12	0.5	225	5.9	16.2
4	12	1.0	325	9.8	17
5	4	1.0	325	3.4	9
6	4	1.5	225	3.8	10.4
7	8	1.0	225	9.5	14.5
8	4	0.5	225	2.5	8.3
9	8	0.5	125	3.6	7.3
10	12	1.5	225	9.4	16.8
11	8	1.5	125	5.2	10.1
12	8	1.5	325	8.2	16
13	8	0.5	325	5.5	13.3
14	4	1.0	125	1.6	6.2
15	8	1.0	225	9.4	14.2

2.2.16 Effect of culture volume on production

After the optimization of culture conditions, the effect of culture volume on α-galactosidase production yield was studied to further improve production. The cultivations were carried out in 250, 1000, and 2000 mL Erlenmeyer Flasks with 100, 400, and 800 mL working volume, respectively. Cultures were incubated at 30 °C in a shaker incubator under the optimized conditions (10.5% molasses, 1.3% NH_4NO_3, and 276 rpm).

2.2.17 Purification of recombinant α-galactosidase

ÄKTA Prime FPLC system (Amersham Biosciences, Sweden) was used for α-galactosidase purification, according to a two-step purification technique adopted from Puchart *et al*., (2000) including anion exchange and hydrophobic interaction chromatography. Supernatant taken from the third day of cultivation was firstly filtered through Whatman No. 1 filter paper. Supernatant and all liquids used for purification were filtered through 0.45 µm-pore-size membranes (Millipore, USA) before use.

Anion exchange chromatography (AEC), which was performed in a 20 mL prepacked, ready to use HiPrep™ 16/10 Q XL Column (Amersham Biosciences, USA) was the first step of the purification. Column characteristics are provided in Appendix H. The filtrate was applied to HiPrep™ 16/10 Q XL column equilibrated with 50 mM sodium phosphate buffer, pH 6.0 (buffer A). 5 mL fractions were collected during elution at the flow rate of 0.5 mL/minute with an increasing gradient in the range of 0−0.5 M NaCl, prepared in buffer A. All fractions were checked for α-galactosidase activity.

α-Galactosidase-active fractions of AEC were pooled and applied to hydrophobic interaction chromatography (HIC) conducted in a pre-packed,

ready to use HiPrep™ 26/10 Desalting Column (Amersham Biosciences, USA). Column characteristics are provided in Appendix H. The HiPrep™ 26/10 desalting column was equilibrated with 1.3 M $(NH_4)_2SO_4$ in buffer A. Elution was done at the flow rate of 0.3 mL/minute and 3 mL fractions were collected. Adsorbed proteins were liberated from the carrier with linear decreasing gradient of 1.3−0 M $(NH_4)_2SO_4$ in buffer A. Fractions, which have α-galactosidase activity, were pooled and protein concentrations, specific activities, yields, and purification folds were calculated.

2.2.18 Determination of total protein concentration

The concentration of total protein was measured by the Lowry Method (Lowry *et al*., 1951) with the use of bovine serum albumin (BSA) as standard (Appendix I).

2.2.19 N-Deglycosylation of the recombinant α-galactosidase

N-Deglycosylation was performed by the N-Glycanase enzyme (Peptide-N-Glycosidase F) (ProZyme, USA). 100 µg of purified α-galactosidase sample was prepared in 45 µL of 1X reaction buffer. 2.5 µL of SDS / β-mercaptoethanol (final reaction concentration; 0.1% SDS, 50 mM β-mercaptoethanol) solution was added and the mixture was denatured by heating at 100 °C for 5 minutes. After cooling, 2.5 µL Tergitol-type NP-40 (final concentration 0.75%) and 2.5 µL N-Glycanase were added to the reaction mixture and incubated overnight at 37 °C. NetNGlyc 1.0 Server program was used for the prediction of N-glycosylation sites (N-X-S/T) (Gupta *et al*., 2004).

2.2.20 Enzyme kinetics of recombinant α-galactosidase

Kinetic studies were carried out using *p*NPαGal substrate at concentrations ranging from 0.1 to 3.5 mM. α-Galactosidase activity was measured under the standard assay conditions as specified in Section 2.2.11 and the kinetic constants K_m and V_{max} were determined from Lineweaver-Burk plot using the trial version of the GraphPad Prism *v*5.

2.2.21 Effect of pH on recombinant α-galactosidase activity and stability

To determine the effect of pH on α-galactosidase activity, the enzyme assays were performed at various pH values in the range of 2.5−8.0 using 50 mM of the following buffers: sodium citrate (pH 2.5, 3.0), sodium acetate (pH 4.0, 4.5) sodium phosphate (pH 4.0−8.0). Temperature, enzyme, and substrate concentrations were kept constant as stated in the standard assay condition (Section 2.2.11).

In order to determine the effect of pH on α-galactosidase stability, enzyme samples were incubated in the pH range of 2.5−8.0 for 2 and 4 hours. After incubations, the residual activities were determined by the standard activity assay method and were reported as the ratio of enzyme activity after pH treatment to the initial maximum activity at pH 4.5.

2.2.22 Effect of temperature on recombinant α-galactosidase activity and stability

Effect of temperature on α-galactosidase activity was determined in the range of 20−80 °C by assaying the enzyme activities at specified temperatures. pH, enzyme, and substrate concentrations were kept constant as stated in the standard assay condition (Section 2.2.11).

In order to determine the effect of temperature on α-galactosidase stability, enzyme samples were incubated at 20−80 °C for 1, 3, and 5 hours. After incubations, the residual activities were determined by the standard activity assay and were reported as the ratio of the enzyme activity after temperature treatment to the initial maximum activity at 50 °C.

2.2.23 Effects of additives on the recombinant α-galactosidase activity

In order to determine the effects of different metal ions and chemicals on α-galactosidase activity, enzyme samples were incubated in the presence of 1 mM of each agent for 90 minutes at room temperature. After incubations, the residual activities were determined by the standard activity assay as stated in Section 2.2.11 and were reported as the ratio of the enzyme activity after the treatment with additives to the initial maximum activity obtained in the absence of the additives.

2.2.24 Osmotic stress analysis

2.2.24.1 Osmotic stress treatment of recombinant *A. sojae* Ta1 strain

Recombinant *A. sojae* Ta1 strain was grown on complete medium agar (Appendix B). Shake flask cultures were prepared in 1 L Erlenmeyer flasks containing 200 mL complete medium and were incubated at 30 °C in a shaker incubator at 200 rpm. Fungal spores ($1x10^6$) from the stock cultures stored at 4 °C were inoculated into 5 mL pre-culture complete medium, which was transferred into the main culture after overnight incubation.

2.2.24.1.1 Preparation and growth of salt-adapted and non-adapted cultures

In order to expose non-adapted cells to osmotic stress, *A. sojae* Ta1 was transferred into complete medium containing either 1 M or 2 M of either potassium chloride (KCl), magnesium chloride ($MgCl_2$), magnesium sulfate ($MgSO_4$), sodium chloride (NaCl) or sodium sulfate (Na_2SO_4) as salinity agents. Medium was inoculated with pre-culture, which was grown in the absence of salt. As for the adapted cells, adaptation to high salt concentrations was achieved by a method based on the gradual acclimatization of *A. sojae* Ta1 to salts by gradually growing in the presence of increasing salt concentrations. First, *A. sojae* Ta1 was grown in complete broth medium containing 0.5 M salt for 3 days and then incubated on 0.5 M salt-containing agar plates for 3–5 days for spore formation. Spores of 0.5 M salt-adapted cultures were used to inoculate pre-culture medium containing 1 M salt. Next, cells were grown on 1 M salt-containing medium for 5 days and were incubated on 1 M salt-containing agar plates for 5–8 days to obtain salt-adapted spores. Finally, the spores of the cultures, adapted to 1 M salt, were used to inoculate 1 M salt-containing complete medium, after overnight pre-incubation at the same salt concentration. Adaptation to 2 M of any of the salts, as described above, resulted in un-healthy cells and lack of sporulation, and was thus, excluded.

2.2.24.1.2 Analysis of fungal growth in the presence of osmotic stress

To determine biomass generation, samples were collected at days 2, 4, 6, and 8, and were filtered through pre-weighed Whatman No. 1 filter paper and washed several times with distilled water, until salt was completely removed. Mycelial biomass was dried to a constant weight at 60 °C. Error bars in the figures related to biomass measurement represent the standard deviations from the mean of two independent experiments.

2.2.24.1.3 Analysis of fungal morphology in the presence of osmotic stress

To observe the effects of osmotic stress on fungal morphology, samples of fungal mycelia were collected from culture fluids at the end of 8-day cultivation and were analysed directly under the light microscope (Olympus BH2- WHK 10X/20L). Pictures were taken by Panasonic Lumix DMC-FS3.

2.2.25 Analysis of transgalactosylation activity of recombinant α-galactosidase

2.2.25.1 Transgalactosylation reaction

L-arabinose, *L*-fucose, *D*-fructose, *D*-xylose, *D*-Galactose, *D*-glucose, *D*-mannose, cellobiose, lactose, maltose, melibiose, and sucrose were used as acceptor sugar (Table 2.6). The donor sugar was *p*NPαGal, which is efficiently recognized by α-galactosidase and fast reacting substrate due to its good leaving group. As the donor sugar is more expensive than acceptor sugars, acceptor sugars were used in excess amounts to push the reaction towards synthesis instead of hydrolysis. Purified α-galactosidase was used in all transgalactosylation experiments. 0.5 U/mL purified α-galactosidase, 1 M acceptor sugar, and 0.25 M donor sugar were mixed in 100 mM sodium phosphate buffer, pH 4.5 and the mixture was incubated at 50 °C for 1 hour and the reaction was stopped by heating at 95 °C for 5 minutes.

2.2.25.2 Analysis of transgalactosylation products

After enzyme inactivation, the transgalactosylation reaction mixtures were monitored by thin layer chromatography (TLC) on silica-coated aluminium sheets (Merck, Darmstadt, Germany). The heated mixtures were diluted 50-fold with 100 mM sodium phosphate, pH 4.5 and 1 µl diluted aliquot was

loaded onto the TLC plate. *n*-Butanol:Ethanol:Water (10:8:7) solvent system was used as mobile phase. In order to visualize sugar spots, the TLC plates were dipped into the jar containing 0.2% (m/V) recorcin in 10% (V/V) H_2SO_4 in ethanol and dried 10 minutes at 100 °C (Puchart and Biely, 2005).

To confirm the transgalactosylation, 10 µl of the diluted aliquot was completely dissolved in 50:50 solution of water:ACN containing 0.1% formic acid and analysed by electrospray ionization-time of flight mass spectrometry (ESI-TOF MS). ESI-TOF MS was performed using Waters LCT (Waters Corporation, MA. USA). Samples were injected using a Waters Alliance auto-sampler in the mobile phase of 50:50 solution of water:ACN containing 0.1% formic acid at 0.1 mL/h flow rate. MS detection was performed in positive mode keeping the capillary voltage at 3 kV and capillary temperature of 200 °C. The data was analysed with Waters OpenAccess and Masslynx software.

Quantitative analysis of transgalactosylation reaction was performed by high-performance liquid chromatography (HPLC). HPLC was carried out by Varian Prostar HPLC System on Varian MetaCarb 87H Column (300 X 7.8 mm) coupled to ProStar 350 refractive index detector. 0.008 N H_2SO_4 was used as mobile phase. 50 µL samples were injected and eluted at a flow rate of 0.5 mL/min at 35 °C. Varian Star Workstation Software processed data obtained from HPLC. Quantitative determination was carried out using calibration curves of the corresponding acceptor sugar as the reference. The yield was calculated as the ratio of transgalactosylated acceptor amount to initial acceptor amount.

Table 2.6 Donor and acceptor substrates used in transgalactosylation reactions

Substrates	Category	Molar mass (g/mol)
*p*NPαGal	donor - chromogenic substrate	301.25
Galactose	acceptor: monosaccharide - hexose	180.16
Glucose	acceptor: monosaccharide - hexose	180.16
Mannose	acceptor: monosaccharide - hexose	180.16
Fucose	acceptor: monosaccharide - deoxyhexose	164.16
Arabinose	acceptor: monosaccharide - aldopentose	150.13
Xylose	acceptor: monosaccharide - aldopentose	150.13
Cellobiose	acceptor: disaccharide: glucose-β-(1,4)-glucose	342.30
Lactose	acceptor: disaccharide: galactose-β-(1,4)-glucose	342.30
Maltose	acceptor: disaccharide: glucose-α-(1,4)-glucose	342.30
Melibiose	acceptor: disaccharide: galactose-α-(1,6)-glucose	342.30
Sucrose	acceptor: disaccharide: glucose-α-(1,2)-fructose	342.30

CHAPTER 3

RESULTS AND DISCUSSIONS

3.1 Overall experimental strategy of the study

In this study, it was aimed to produce industrially important α-galactosidase enzyme from a human pathogen, *A. fumigatus,* in a GRAS organism, *A. sojae.* The experimental strategy of the study is shown in Figure 3.1.

In the early stages of the study, *agl*B gene of *A. fumigatus* was cloned onto pAN52-4 expression vector bearing *gpd*A promoter. The newly formed recombinant plasmid was called as pANaglB. pANaglB was transformed into *A. sojae* ATTCC11906 host strain and the *A. sojae* containing pANaglB was named as *A. sojae* Ta1. After the analysis of *A. sojae* Ta1 transformants for α-galactosidase production, cultivation conditions were optimized through response surface methodology using Box-Behnken design. Salt stress was used to induce α-galactosidase production by *A. sojae* Ta1 by taking the advantage of the fact that the *gpd*A promoter is induced by osmotic stress (Redkar *et al*., 1998). The recombinant enzyme was purified for kinetic analyses and characterization of the enzyme. Finally, the purified enzyme was used in transgalactosylation application.

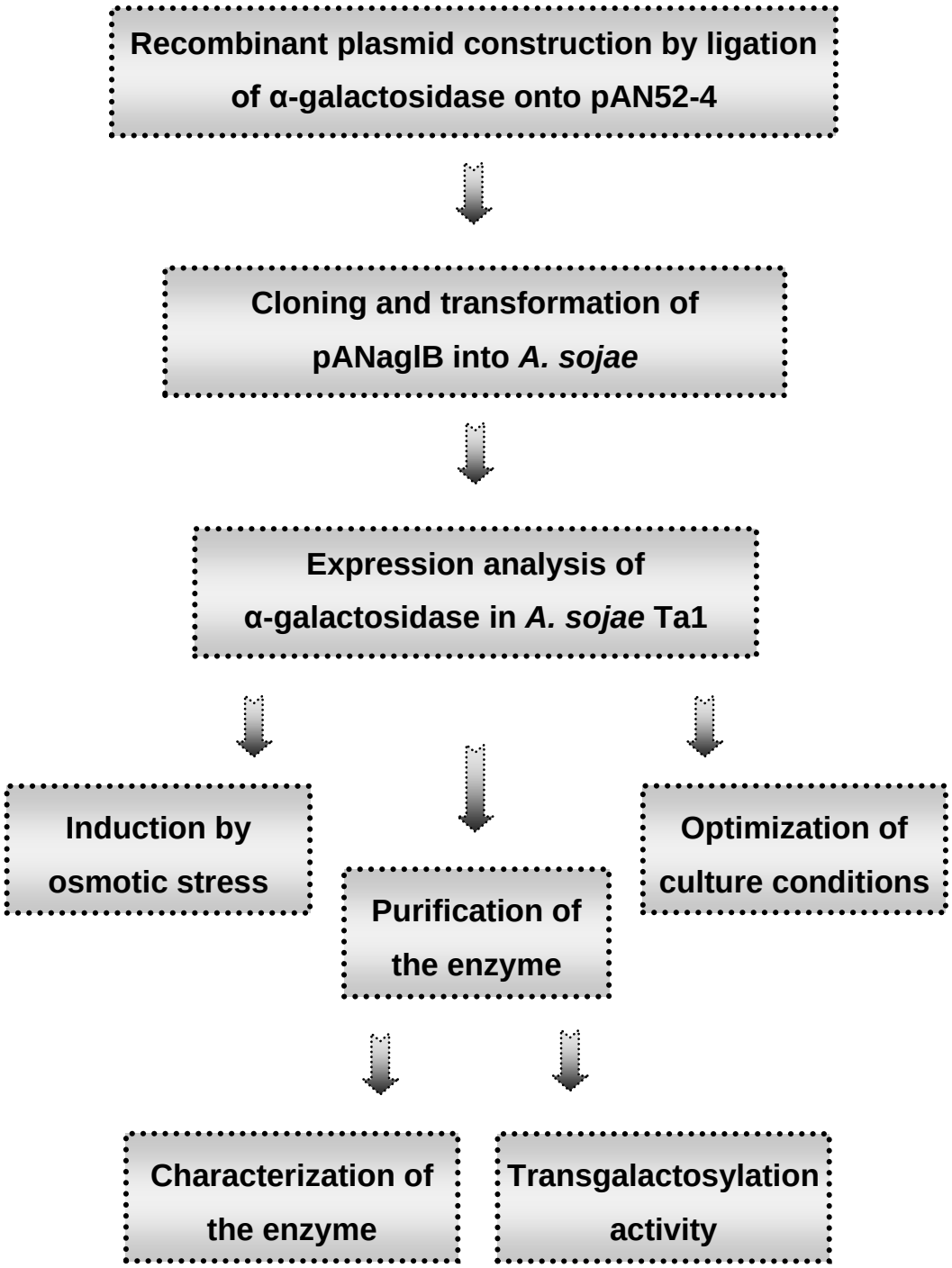

Figure 3.1 Flow chart of the experimental strategy

3.2 Ligation of α-galactosidase gene (*agl*B) onto vector pAN52-4 and transformation into *E. coli* XL1 Blue MRF′

In previous studies, *A. fumigatus* α-galactosidase gene (*agl*B) was isolated and inserted into pUC 19 cloning vector (Appendix C.1) by PCR-cloning method using specific primers (Appendix E) by Söyler (2004). During the present study, pUC 19 vector containing *agl*B gene was digested with HindIII enzyme to obtain the previously inserted *agl*B gene. It was amplified by PCR. The expression vector pAN52-4 and the PCR-amplified gene fragment (*agl*B) were both digested with the same restriction enzyme, HindIII. The *agl*B gene fragment was ligated onto vector pAN52-4 and cloned into *E. coli* XL1 Blue MRF′.

The recombinant clones were selected and plasmid DNAs were isolated from recombinant colonies as described in Section 2.2.1. After plasmid isolation and purification, the efficiency of the ligation was confirmed by restriction enzyme digestion. Following HindIII digestion, two anticipated bands [insert, *agl*B (1622 bp) and vector, pAN52-4 (5748 bp)] were analysed by agarose gel electrophoresis as shown in Figure 3.2.

Recombinant plasmid for the expression of *agl*B of *A. fumigatus* was named as **pANaglB**. Expression was achieved under the control of *A. nidulans* glyceraldehydes-3-phoshate dehydrogenase (*gpd*A) promoter. The signal sequence of *agl*B was replaced by the signal and prosequences of *A. niger* glucoamylase gene (*gla*A). Major transcription start site, poly A tail, HindIII cut site used to insert the gene, terminator sequence of *A. nidulans* trpC gene, and signal and pro sequences of *A. niger gla*A gene are illustrated on the drawing provided in Figure 3.3.

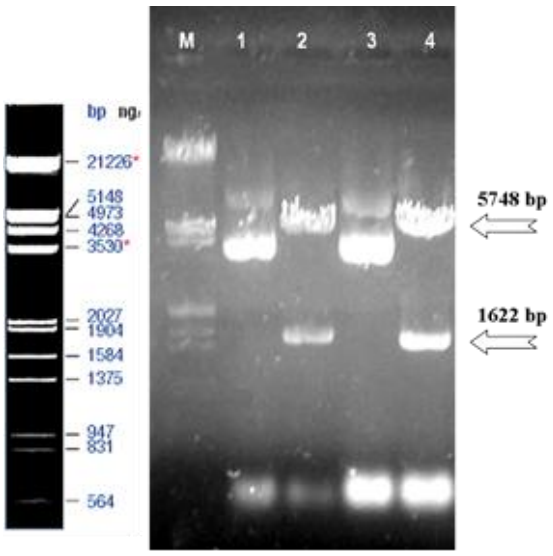

Figure 3.2 Restriction digestion of recombinant plasmid (pANaglB) with Hind III. Lane 1 and 3: isolated pANaglB; lane 2 and 4: Hind III-cut pANaglB; lane M: Lambda DNA/EcoRI + HindIII marker (Appendix D)

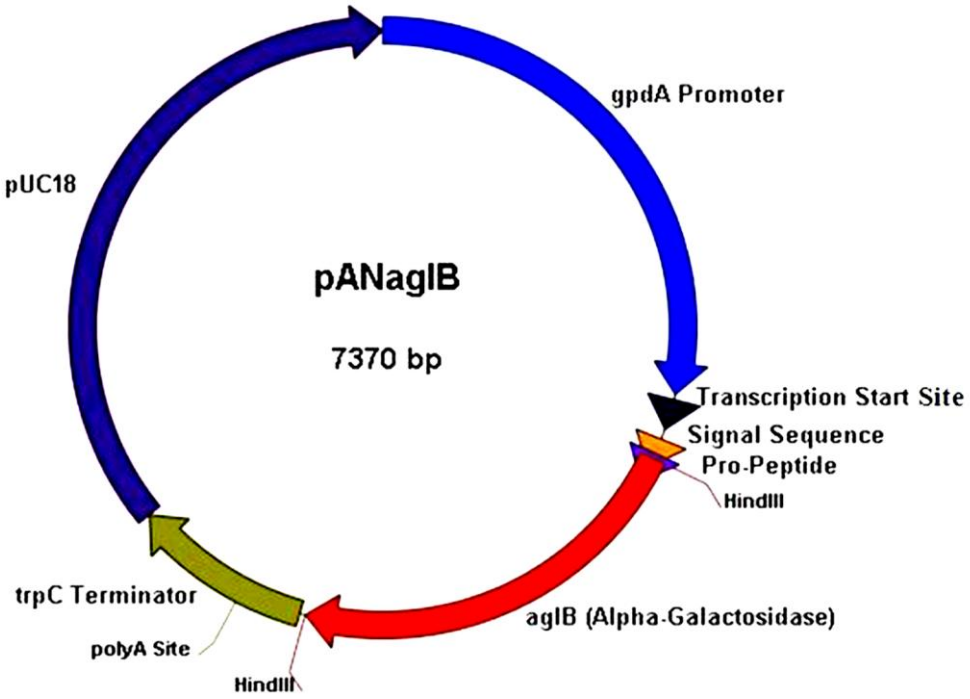

Figure 3.3 Schematic representation of recombinant plasmid, pANaglB for the expression of *agl*B of *A. fumigatus*. Promoter sequence of *A. nidulans gpd*A gene, major transcription start site, *poly A* tail, HindIII cut site used to insert the gene, terminator sequence of *A. nidulans trp*C gene, and signal and pro sequences of *A. niger gla*A gene are indicated.

The cloned gene *(agl*B) was sequenced with gene bank accession number, FJ843023.1. Nucleotide and amino acid sequences of *agl*B are provided in Appendix F. Results of the amino acid sequence alignment of native and recombinant α-galactosidase is provided in Appendix F.

The orientation of the insert was confirmed by PCR using aglB-specific primers, pB1 (forward primer) and pA2 (reverse primer), and vector-specific primer, pV1 (Appendix E).

If the insert was in the correct orientation,

- PCR with pB1 and pA2 primers should yield a fragment of 1622 bp (1)
- PCR with pB1 and pV1 primers should yield a fragment of 5748 bp (2)
- PCR with pA2 and pV1 primers should not give any fragment (3)

After PCR amplification, it was seen that the *agl*B gene on the vector pAN52-4 was in the correct orientation (Figure 3.4). Among the recombinant plasmids, pANaglB (A-D) shown in Figure 3.4, pANaglB-B was chosen for sequence analysis. The cloned gene (*agl*B) was sequenced with gene bank accession number (FJ843023) using primers given in Table E.2. The nucleotide sequence is given in Appendix F.1.

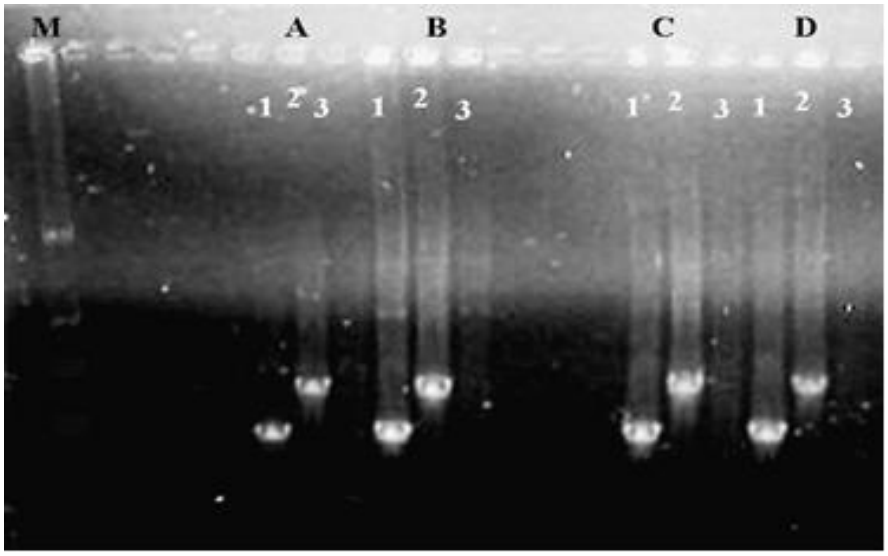

Figure 3.4 A−D are 4 different recombinant plasmids. Each lane 1, the result of PCR with pB1 and pA2 primers yielding 1622 bp PCR product; Each lane 2, the result of PCR with pB1 and pV1 primers yielding 5748 bp PCR product; Each lane 3, the result of PCR with pA2 and pV1 primers yielding no PCR product; Lane M, Molecular size marker, λ DNA/EcoRI + HindIII (Appendix D).

3.3 Transformation into *A. sojae* and screening

3.3.1 Protoplast transformation and selection of transformants

In the first step of co-transformation, *A. sojae* ATCC11906 protoplasts were formed according to the procedure described in section 2.2.10.4. Stages during formation of the protoplasts from *A. sojae* mycelia are shown in Figure 3.5. These protoplasts were transformed with a mixture of pAN*agl*B and selective plasmid pAMDSPYRG in a ratio of 10:1.

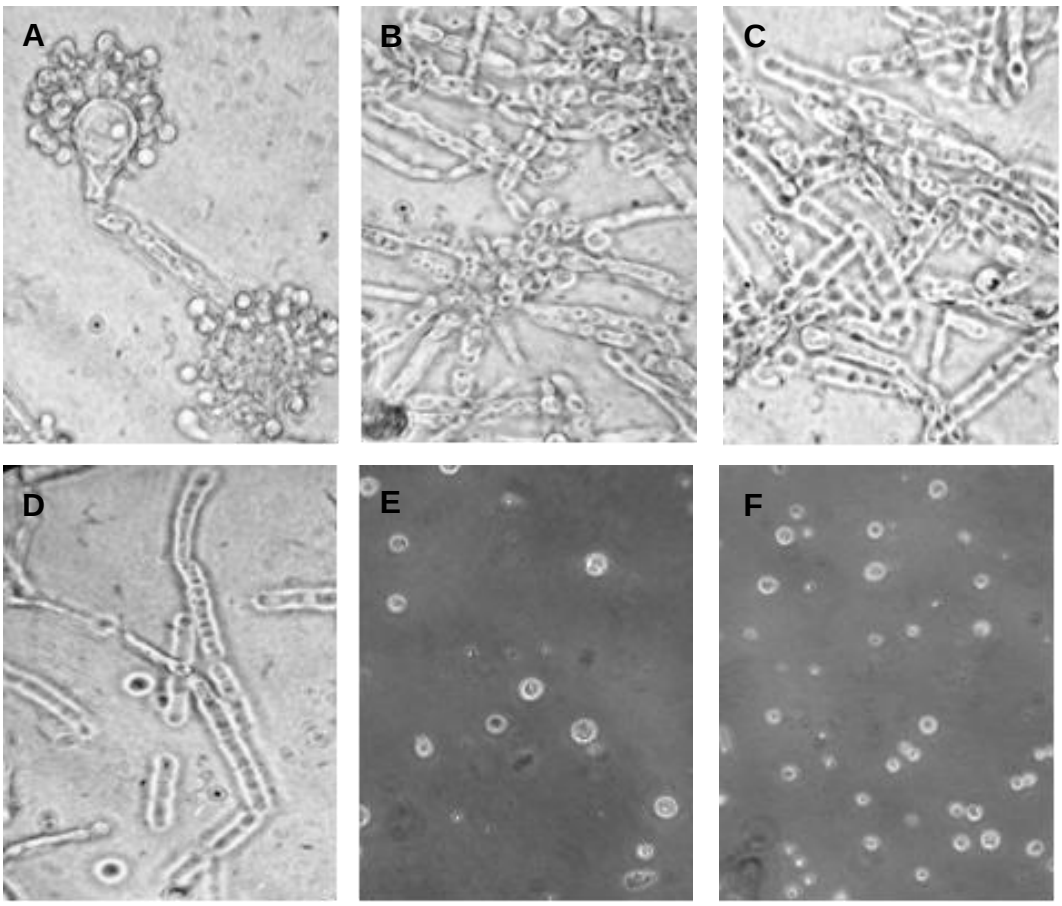

Figure 3.5 Protoplast formation from the mycelium of *A. sojae* ATCC11906 (*pyr*G^{-}) resuspended in the lytic solution (A−F). Samples were taken at 30 minutes intervals.

pAN52-4 does not have a selectable marker gene for the selection of transformants. Therefore, a selection vector, pAMDSPYRG, was needed to select the recombinant cells. pAMDSPYRG incorporates the ability to use acetamide and acrylamide as nitrogen and carbon sources and to produce uridine. Therefore, transformants could be selected for their abilities to grow on minimal medium without uridine supplementation.

3.3.2 Screening of α-galactosidase activity and comparison

The recombinant *A. sojae* cells that could grow in the absence of uridine and uracil might have only the selection marker but not the expression vector. To confirm the presence of *agl*B gene of *A. fumigatus* in the recombinant *A. sojae* cells, activity screening was performed. Recombinant *A. sojae* strain expressing α-galactosidase gene of *A. fumigatus* was named as ***A. sojae* Ta1** from this point on.

Since α-galactosidase gene was cloned onto integrative vector pAN52-4 possessing the constitutive and strong *gpd*A promoter, induction of α-galactosidase production in *A. sojae* Ta1 was not needed and expression was possible on simple carbon sources like glucose. On the other hand, *A. fumigatus* should be grown on a medium containing an inducer like locust bean gum (LBG) to be able to express α-galactosidase.

Figure 3.6 is the graph presenting the time course comparison of extracellular α-galactosidase activities of the control strain, *A. sojae* ATCC11906, *A. sojae* Ta1, and *A. fumigatus*. After 3 days of incubation, 2.45 U/mL α-galactosidase was produced by *A. sojae* Ta1 that was nearly 3-fold higher than the production of α-galactosidase by *A. fumigatus* (0.85 U/mL). In non-recombinant *A. sojae* strain, α-galactosidase activity was not observed.

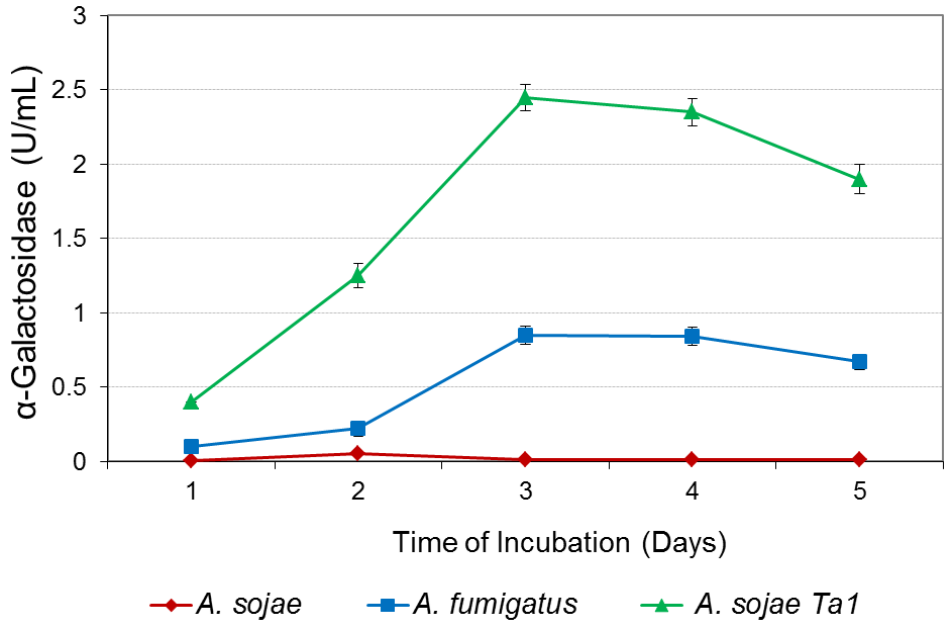

Figure 3.6 Comparison of α-galactosidase secretion by *A. fumigatus* IMI 385708 grown on medium containing 0.5% LBG, *A. sojae* ATCC11906 (control), and *A. sojae* Ta1 grown on YpSs medium containing 2% glucose

3.3.3 Analysis of protein profiles

Extracellular protein production of *A. fumigatus* grown on LBG, untransformed *A. sojae* ATCC11906 grown on glucose, and *A. sojae* Ta1 grown on glucose containing media were compared. Culture supernatants from the third day of cultivations were collected by filtration through Whatman No. 1 filter paper and concentrated 2-fold in vacuum evaporator. The samples were subjected to SDS-PAGE analysis followed by silver nitrate staining (Figure 3.7).

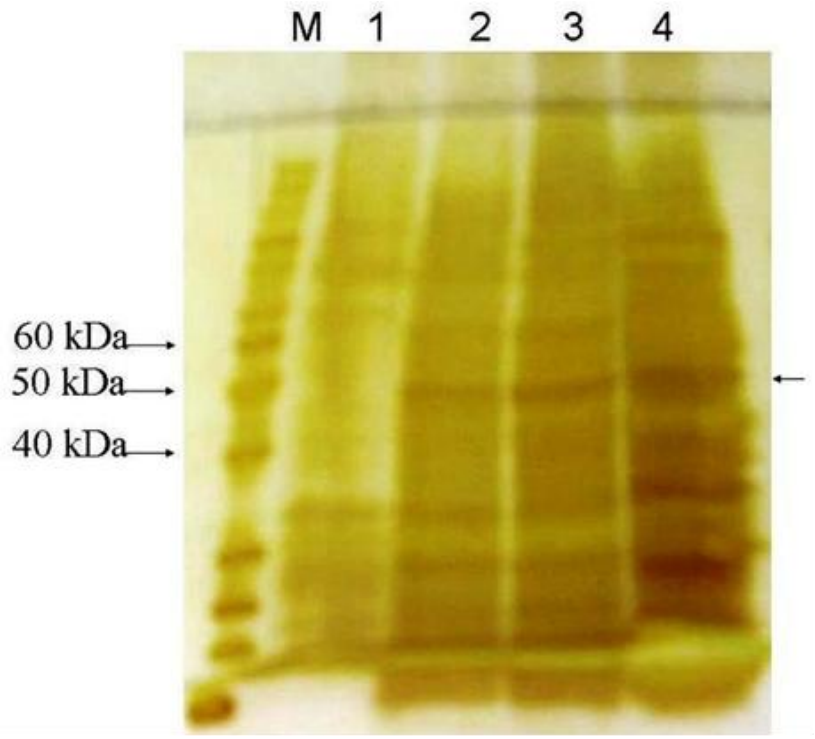

Figure 3.7 SDS-PAGE of culture supernatants. Lane 1, *A. sojae* ATCC11906 (*pyr*G⁻); lanes 2 and 3, *A. sojae* Ta1; lane 4, *A. fumigatus*; lane M, PageRuler™ unstained protein ladder (Appendix D.2.1)

According to the results, an explicit protein band corresponding to α-galactosidase was obtained in *A. sojae* Ta1, while no protein band around this position was seen in non-recombinant *A. sojae*. As *A. fumigatus* was induced with LBG, many protein bands likely belonging to other hydrolytic enzymes were observed in *A. fumigatus* in addition to α-galactosidase (Figure 3.7).

The expression system applied in this work was quite effective and *A. sojae* Ta1 transformants with long-term stability were obtained by the use of pAN52-4, which integrates into the fungal genome. This system allowed high-level heterologous expression of α-galactosidase by *A. sojae* Ta1 without polymeric substrate. The use of strong promoters derived from housekeeping genes, such as the fungal glyceraldehyde-3-phosphate

dehydrogenase gene, has the advantage of constitutive, growth-associated production of heterologous proteins. Conversely, *A. fumigatus* needs an inducer; one of the best is LBG for α-galactosidase production. Nevertheless, LBG increases the viscosity of the medium and *A. fumigatus* excretes different enzymes to hydrolyse LBG, causing a mixture of enzymes, perhaps also including other α-galactosidases. This complicates purification process and shows that the observed α-galactosidase activity from the culture supernatants of *A. fumigatus* is the total effect of different α-galactosidases. In the genome of *A. fumigatus* there are 6 putative α-galactosidase genes (Figure 1.9) (Gilsenan *et al*., 2009). Thus, the observed 3-fold increase in α-galactosidase production by *A. sojae* Ta1 is likely to be higher than the observed level.

The level of α-galactosidase production achieved by recombinant *A. sojae* Ta1 (2.45 U/mL) is higher than those reported in the literature, including α-galactosidases from *Gibberilla* sp. (1.42 U/mL) (Cao *et al*., 2009b), *Rhizopus* sp. (1.69 U/mL) (Cao et al., 2009a), which were expressed in *E. coli* and α-galactosidase from Bispora sp. (1.52 U/mL) expressed in *Pichia pastoris* (Wang *et al*., 2010) but still lower than the α-galactosidases from *Rhizomucor miehei* (11.03 U/mL) (Katrolia *et al*., 2012) and *Absidia corymbifera* (18.7 U/mL) (Baik *et al*., 2000), which were expressed in *E. coli* and *Penicillium* sp. α-galactosidase (6.03 U/mL) (Mi *et al*., 2007) expressed in *Pichia pastoris*.

From the industrial point of view, higher enzyme production is not the only benefit of this recombinant system, which also offered several other benefits for enzyme industry such as the use of a safe organism instead of an opportunistic human pathogen, easy purification and product recovery by the elimination of LBG use in the cultivation, and high product purity. In industrial perspective of enzyme production, the economy is another important point to consider and can be addressed by the optimization of the bioprocess.

3.4 Optimization of heterologous α-galactosidase production

3.4.1 Selection of best carbon and nitrogen sources

Among the various carbon sources studied, maximal α-galactosidase production, with 4.5 U/mL activity, was obtained after 3-days of incubation with 50 g/L (similar sucrose concentration of 20 g/L) of molasses as the sole carbon source ($p<0.05$) (Figure 3.8).

It was likely to obtain maximal α-galactosidase production with molasses, which contains 40% sucrose, because of beneficial effects of the complex composition of this carbon source, which contains trace elements such as, magnesium, potassium, sodium, calcium, iron, copper (El-Abyad *et al*., 1992) and trace amounts of other carbohydrates, in addition to the sucrose as the major carbohydrate. Molasses, a by-product of beet sugar industry, was thus chosen as carbon source for media optimization.

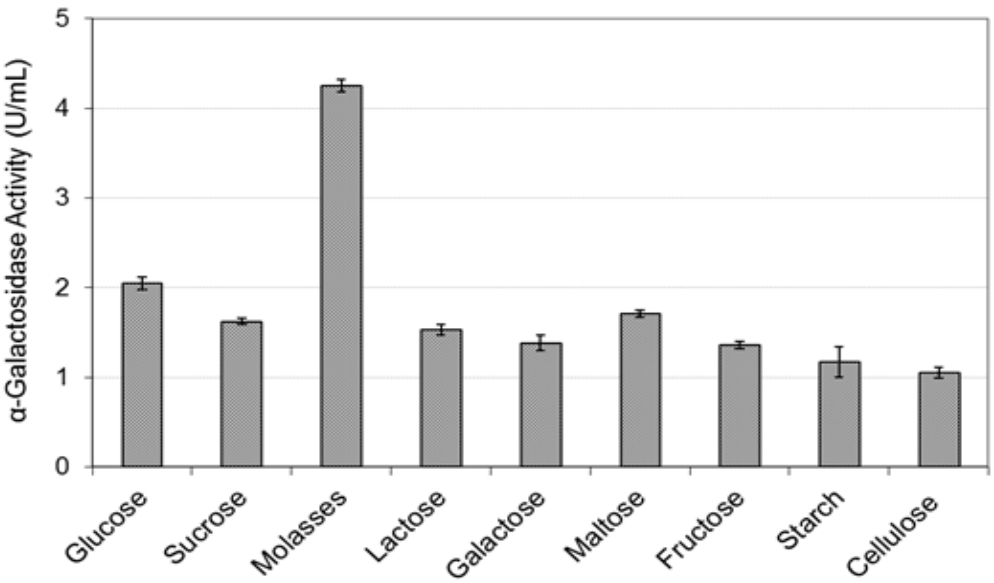

Figure 3.8 Effect of carbon sources (2%) on α-galactosidase production by *A. sojae* Ta1 grown in 100 mL YpSs medium at 30 °C and 155 rpm.

The difference in α-galactosidase production with different nitrogen sources was insignificant ($p>0.05$). Since the highest yields were obtained with $NaNO_3$, NH_4NO_3, and peptone-C, and by taking into account the cost of these sources, NH_4NO_3 was chosen as the best nitrogen source for optimization by RSM.

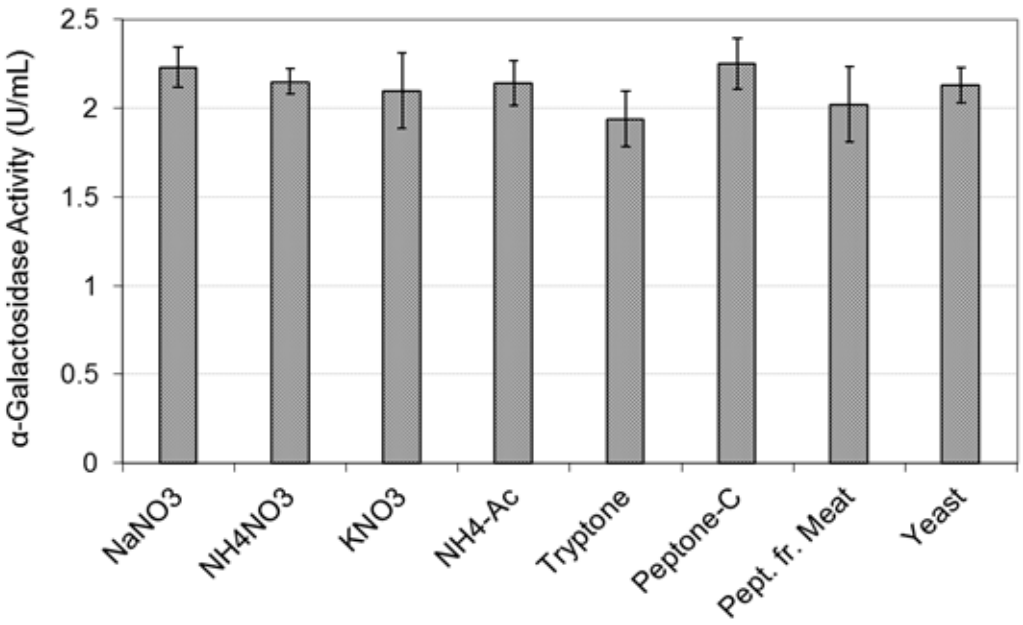

Figure 3.9 Effect of nitrogen sources (0.4%) on α-galactosidase production by *A. sojae* Ta1 grown in 100 mL YpSs medium at 30 °C and 155 rpm

3.4.2 Box-Behnken design and response surface methodology

The α-galactosidase production by recombinant *A. sojae* Ta1 in submerged culture was optimized using Box-Behnken design (BBD) of response surface methodology. The results of BBD experiments to determine the effects of concentrations of molasses, NH_4NO_3, and agitation speed are shown in Table 2.5.

The coefficients of regression equation obtained after ANOVA for α-galactosidase production and biomass generation are presented in Table 3.1 and 3.2, respectively. Thus, the production of α-galactosidase is best predicted by the model equation:

$$Y_1 = 9.5500 + 2.2194\ M + 1.1272\ N + 1.5472\ A - 2.5216\ M^2 - 1.5834\ N^2 - 2.2972\ A^2 + 0.9887\ M\ A$$

The production of biomass is best predicted by the model equation:

$$Y_2 = 14.625 + 3.6581\ M + 1.0284\ N - 2.4234\ A - 2.2588\ A^2$$

where Y_1; predicted α-galactosidase production, Y_2; predicted biomass production, the symbols, M, N, A, are the coded variables of molasses concentration, NH_4NO_3 concentration, and agitation speed, respectively.

The coefficient of determination (R^2) was calculated as 0.94 for α-galactosidase production and 0.89 for biomass generation. The closer the R^2 value is to 1.0, the stronger the model is. This implied that the two model equations were adequately fit to the data. The pred R^2 of 0.88 for α-galactosidase production is in good agreement with adj R^2 of 0.91 (Table 3.1). This proved a good agreement between the experimental and predicted values for galactosidase production.

Table 3.1 Estimated regression coefficients of multiple determinations (R^2) for α-galactosidase production

TERM	COEF	SE COEF	T	P
Constant	9.5500	0.3577	266701	0.000
Molasses	2.2194	0,2190	10,133	0.000
NH_4NO_3	1.1272	0.2190	5.146	0.000
Agitation	1.5472	0.2190	7.064	0.000
Molasses*Molasses	−2.5216	0.3224	−7.821	0.000
NH_4NO_3*NH_4NO_3	−1.5834	0.3224	−4.912	0.000
Agitation*Agitation	−2.2972	0.3224	−7.126	0.000
Molasses*NH_4NO_3	0.5350	0.3097	1.727	0.100
Molasses*Agitation	0.9887	0.3097	3.192	0.005
NH_4NO_3*Agitation	0.2931	0.3097	0.946	0.355
S = 0.876081 PRESS = 29.4913				
R^2 = 93.98% R^2(pred) = 88.43% R^2(adj) = 91.27%				

Table 3.2 Estimated regression coefficients of multiple determinations (R^2) for biomass production

TERM	COEF	SE COEF	T	P
Constant	14.6250	0.6143	23.810	0.000
Molasses	3.6581	0.3761	9.725	0.000
NH_4NO_3	1.0284	0.3761	2.734	0.013
Agitation	2.4234	0.3761	6.443	0.000
Molasses*Molasses	−1.0369	0.5537	−1.873	0.076
NH_4NO3*NH_4NO_3	−0.6712	0.5537	−1.212	0.240
Agitation*Agitation	2.2588	0.5537	4.080	0.001
Molasses*NH_4NO_3	−0.4019	0.5320	−0.755	0.459
Molasses*Agitation	0.4831	0.5320	0.908	0.375
NH_4NO_3*Agitation	−0.0425	0.5320	−0.080	0.937
S = 1.50460 PRESS = 112.303				
R^2 = 89.17% R^2(pred) = 73.14% R^2(adj) = 84.30%				

The magnitudes of the model coefficients in Table 3.1 showed that molasses had a more prominent effect on α-galactosidase production than NH_4NO_3 and agitation speed. On the contrary, molasses, NH_4NO_3, and agitation speed had negative quadratic effects (the magnitudes of molasses' and agitation speed's effects are close to each other). A positive value shows an increase in the response if the corresponding variable is increased to higher level, while the negative value indicates that a better response is obtained at low levels of the variable. For the interactions, a positive value indicates that the response increases if both variables change to the same level, low or high. A negative value indicates an increase in the

response if the variables change in opposite directions (one variable increases to a high level and the other decreases to a low level) (Martendal *et al*., 2007). The interactive effects were all positive with that of molasses and agitation speed presenting the highest effect. The other interactive effects had higher *p* values (p>> 0.05) and were statistically insignificant. All the main factors were found to have significant impact on enzyme and biomass production Tables 3.1 and 3.2. However, the statistical results indicated that only the interaction of molasses and agitation speed (M*A) was significant. The interaction of these two different variables can be explained by the following example; for 4% molasses, an increase in agitation speed from 125 rpm to 325 rpm causes enzyme activity to increase from 1.6 U/mL to 3.4 U/mL (NH_4NO_3 is fixed at 1%). At higher amounts of molasses, i.e. 12%, the same change of agitation speed increases enzyme activity from 4 U/mL to 9.8 U/mL. The extent of increase in former case is narrower than the latter since molasses concentration is higher in the latter case and molasses has individually significant impact on enzyme activity as reported in Table 3.1. However, the same changes did not give such results for biomass, but yielded parallel increases in biomass, which is an indication of no interaction of the two variables Table 3.2.

The results of variance analysis shown in Table 3.3 indicated that the model had significant linear, quadratic, and interaction effects ($p<0.05$) for α-galactosidase production. In the case of variance analysis of biomass generation shown in Table 3.4, the model had significant linear and quadratic effects ($p<0.05$) but insignificant interaction effects ($p>0.05$). The results of variance analysis for both α-galactosidase and biomass production also revealed that the models were adequate in predicting α-galactosidase and biomass production due to insignificant lack of fit ($p>0.05$).

Table 3.3 Analysis of variances for α-galactosidase production using coded values

SOURCE	DF	SEQ SS	ADJ SS	ADJ MS	F	P
Regression	9	239.518	239.518	26.6132	34.67	0.000
Linear	3	137.439	137.439	45.8132	59.69	0.000
Square	3	91.281	91.281	30.4269	39.64	0.000
Interaction	3	10.798	10.798	3.5994	4.69	0.012
Residual Error	20	15.350	15.350	0.7675		
Lack-of-Fit	3	1.702	1.702	0.5675	0.71	0.561
Pure Error	17	13.648	13.648	0.8028		
Total	29	254.869				

Table 3.4 Analysis of variances for biomass generation using coded values

SOURCE	DF	SEQ SS	ADJ SS	ADJ MS	F	P
Regression	9	372.804	372.804	41.423	18.30	0.000
Linear	3	325.002	325.002	108.334	47.85	0.000
Square	3	44.629	44.629	14.876	6.57	0.003
Interaction	3	3.174	3.174	1.058	0.47	0.708
Residual Error	20	45.276	45.276	2.264		
Lack-of-Fit	3	6.818	6.818	2.273	1.00	0.415
Pure Error	17	38.458	38.458	2.262		
Total	29	418.080				

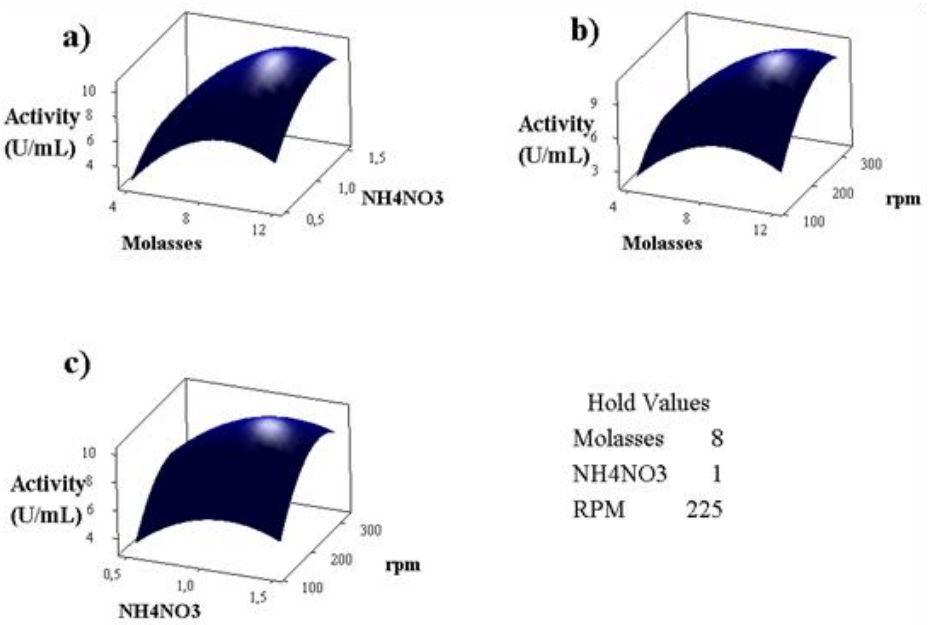

Figure 3.10 Response surface plots showing the effect of (a) Molasses and NH_4NO_3, (b) Molasses and Agitation speed, and (c) NH_4NO_3 and Agitation speed on α-galactosidase production

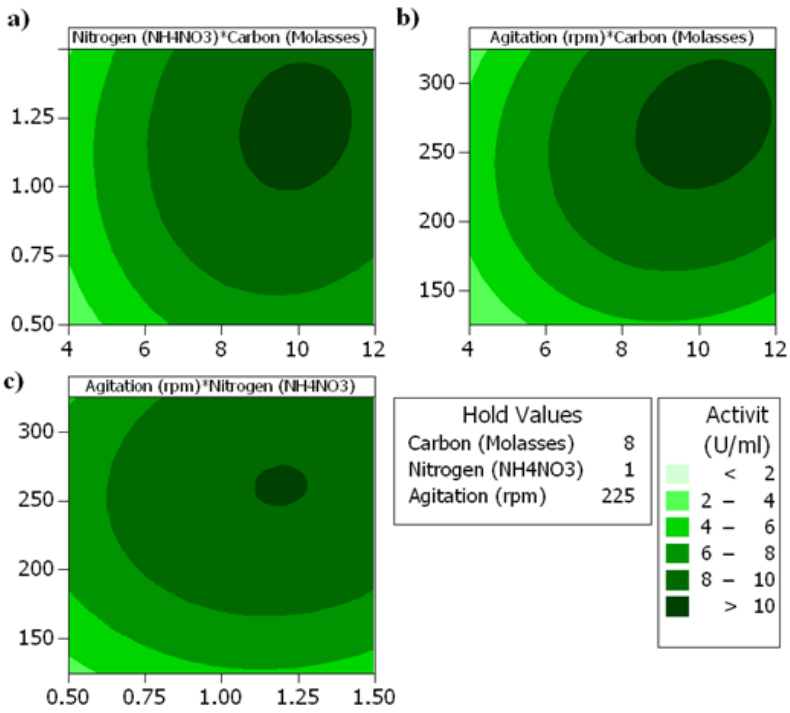

Figure 3.11 Contour plots showing the effect of (a) Molasses and NH_4NO_3, (b) Molasses and Agitation speed, and (c) NH_4NO_3 and Agitation speed on α-galactosidase production

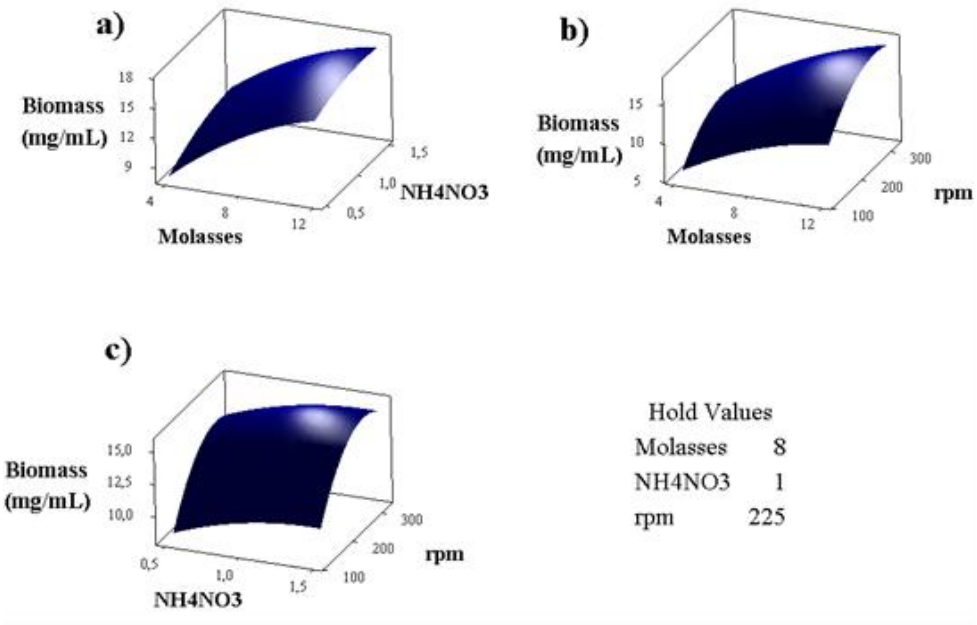

Figure 3.12 Response surface plots showing the effect of (a) Molasses and NH_4NO_3, (b) Molasses and Agitation speed, and (c) NH_4NO_3 and Agitation speed on biomass generation

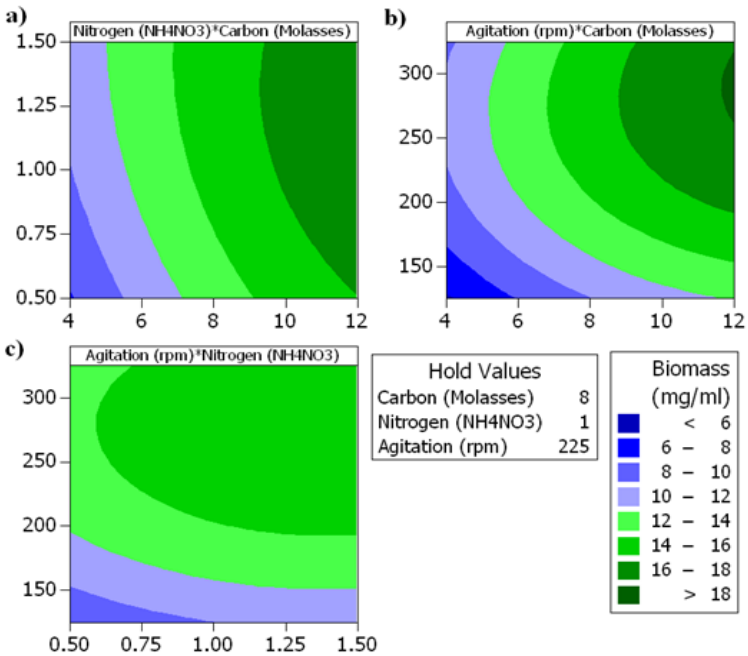

Figure 3.13 Contour plots showing the effect of (a) Molasses and NH_4NO_3, (b) Molasses and Agitation speed, and (c) NH_4NO_3 and Agitation speed on biomass generation

Figures 3.10 and 3.11 represent the response surface and contour plots, respectively, for α-galactosidase production and Figures 3.12 and 3.13 represent the response surface and contour plots, respectively, for biomass generation at varying concentrations of a) molasses vs. NH_4NO_3 b) molasses vs. agitation speed and c) NH_4NO_3 vs. agitation speed, respectively. The third factor, in all cases, was held constant at the centre point (i.e. agitation speed 225 rpm, NH_4NO_3 1%, and molasses 8%, respectively).

Response surface and contour plots help to understand the interaction between the variables and the optimum conditions required for α-galactosidase and biomass production. Surface plots in Figures 3.10 and 3.12 showed the peaks, which suggested that the optimum points were within the design frontiers and it was simple to find the optimum levels of each of the three variables for a maximum response from these peaks.

All surface and contour plots showed that as the levels of the variables increased, α-galactosidase production and the biomass generation increased up to a certain level. For α-galactosidase production, both surface and contour plots in Figures 3.10 and 3.11 showed that α-galactosidase activity higher than 10 U/mL was achieved when the molasses and NH_4NO_3 concentrations and agitation speed reached slightly beyond the 10%, 1.25% 250 rpm levels, respectively. The maximum biomass production, shown in Figures 3.12 and 3.13 was obtained beyond 18 mg/mL with approximately 12% molasses and 300 rpm agitation speed. The biomass production seemed rather independent of NH_4NO_3 concentrations after 0.6% NH_4NO_3 level. This could also be seen in Table 3.2; the less effective factor on biomass production was NH_4NO_3 when the *p* values are considered. Subsequent increase either did not affect or caused adverse effect on responses.

The possible reasons for the decrease in enzyme yield beyond the optimum levels of the variables could be non-optimal growth, direct/indirect effects on the gene expression level of the enzyme, carbon or nitrogen catabolite repression (Lockington *et al*., 2002), lower levels of oxygen and nutrient transport and shear stress caused by high agitation rates, (El-Enshasy *et al*., 2006).

The shapes of the contour plots, which could be circular, elliptical, or saddle, provide another tool to point out the significance of the interactions between the variables. A circular contour plot shows negligible interaction, while elliptical or saddle contour plot point out significant interaction between the corresponding variables (Murthy *et al*., 2000). In Figure 3.11 (B), the contour plot showed significant interaction between Molasses-Agitation with the more elliptical shape than the others. In the other contour plots in Figure 3.12, the shapes of the contour plots are rather circular, and Molasses-NH_4NO_3 and NH_4NO_3-Agitation speed interactions could be assumed as negligible for α-galactosidase production. In Figure 3.13, all of the contour plots indicate negligible interaction between the variables for biomass generation. This can also be confirmed from the *p* values presented in Table 3.2.

Using the “response optimizer” option of Minitab *v.*15, the optimum values of the three factors studied were found as 10.5% molasses (w/v), 1.3% NH_4NO_3 (w/v), and 276 rpm agitation speed. To validate the model, the experiments were performed for α-galactosidase production by using the obtained optimized culture conditions in triplicate. When these conditions were used in cultivations, the observed activity and biomass levels were 10.4 U/mL and 15 mg/mL, which were very close to the corresponding predicted values of 10.8 U/mL and 15 mg/mL, respectively.

As a result of optimizing culture conditions, a 4-fold increase in α-galactosidase activity and 2-fold increase in biomass generation were obtained. Therefore, when compared to the production of α-galactosidase by *A. fumigatus* IMI 385708, at least 12-fold increase was achieved without the need of induction and by using a cheap industrial by-product, namely molasses.

Figure 3.14 shows the comparison of the highest extracellular α-galactosidase activities in culture supernatants of *A. fumigatus* IMI 385708 grown on YpSs medium containing 0.5% locust bean gum (LBG) and *A. sojae* Ta1 grown under basal (in YpSs medium containing 2% glucose and 0.4% yeast extract at 155 rpm) and optimized (in YpSs medium containing 10.5% molasses and 1.3% NH_4NO_3 at 276 rpm) cultivation conditions.

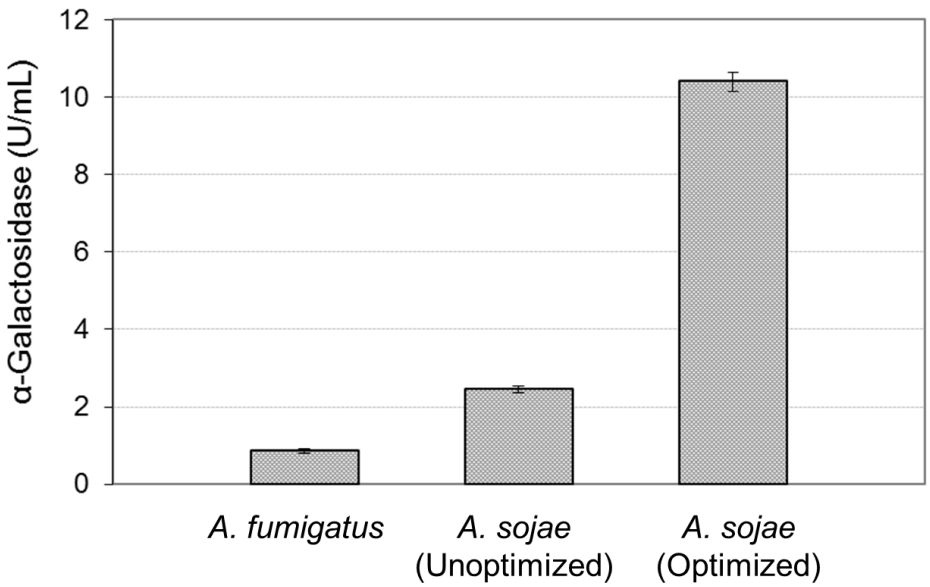

Figure 3.14 Comparison of the highest extracellular α-galactosidase activities of *A. fumigatus* IMI 385708 grown on 0.5% LBG, *A. sojae* Ta1 grown under unoptimized basal culture conditions (2% glucose, 0.4% yeast extract, 155 rpm), and *A. sojae* Ta1 grown under optimized culture conditions (10.5% molasses, 1.3% NH_4NO_3, 276 rpm) on the third day of the cultivation in modified YpSs medium.

Improvement of α-galactosidase production by optimizing culture conditions has been reported recently in different studies and compared in Table 3.5. The achieved maximum production yields by *Thermomyces lanuginosu*s on galactomannan (Svastits-Dücső *et al*., 2009) and by *Lactobacillus agilis* on soybean vinasse (Sanada *et al*., 2009) were lower than our value achieved by *A. sojae* Ta1. In *A. sojae* Ta1, the heterologous production of α-galactosidase reached 10.4 U/mL without any inducer. Galactomannans and soybean vinasse, which contains considerable amount of raffinose (22%), and stachyose (11%), induced α-galactosidase production. However, the molasses used for *A. sojae* Ta1 contained only 2.85% raffinose. This sucrose concentration was tested on the host *A. sojae* ATCC11906 (*pyr*G^{-}) and it was not enough to induce α-galactosidase production.

Table 3.5 α-Galactosidase production by different strains after optimization

Organism	Substrate	Induction	Activity	References
*T. lanuginosu*s	galactomannan	**+** galactomannan	6 U/mL	Svastits-Dücső *et al*., 2009
L. agilis	soybean vinasse	**+** raffinose (22%), stachyose (11%)	7.6 U/mL	Sanada *et al*., 2009
A. sojae Ta1	molasses	**–** raffinose (2.85%)	10.4 U/mL	This thesis

3.5 Effect of culture volume on production

Effect of culture volume on α-galactosidase production was performed with 100, 400, and 800 mL working volume in 250, 1000, and 2000 mL flasks, respectively. Incubations were performed under optimized conditions (10.5% molasses (w/v), 1.3% NH_4NO_3 (w/v), and 276 rpm agitation speed).

As shown in Figure 3.15, the highest α-galactosidase activity, 15 U/mL, was observed in the cultivation performed in 800 mL working volume in 2000 mL Erlen Mayer flask.

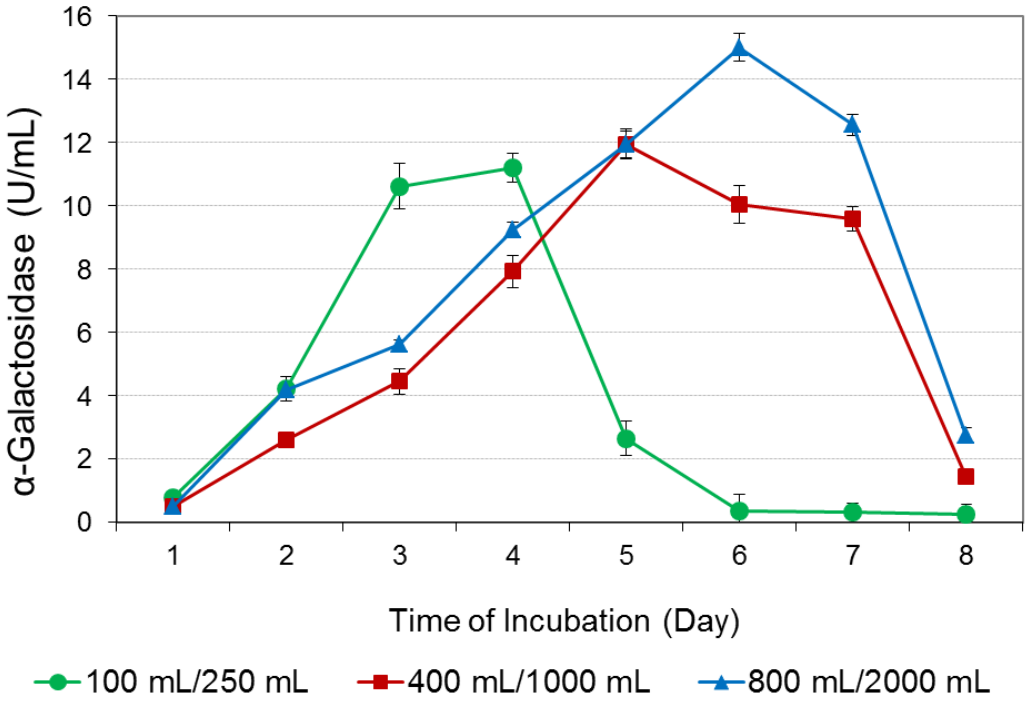

Figure 3.15 Effect of culture volume on recombinant α-galactosidase production by *A. sojae* Ta1 under optimized conditions (10.5% molasses, 1.3% NH_4NO_3, and 276 rpm)

The highest enzyme activity was obtained in the highest culture volume tested, on the other hand, the time required to reach maximum productivity in that cultivation was prolonged from 4 days (for the lowest culture volume) to 6 days (for the highest culture volume). Higher culture volumes to further increase the production was not practical under laboratory conditions considering the availability of incubator and flask volumes. However, this production trend gives rise to thought that the larger the culture volume, the higher the α-galactosidase productivity. On the other hand, the time required to reach maximal activity increases as the culture volume increases.

3.6 Purification and N-Deglycosylation of recombinant α-galactosidase

α-Galactosidase purification was performed using a two-step column chromatography technique including anion exchange and hydrophobic interaction chromatography. α-Galactosidase activities were followed in the eluted fractions and specific activity, yield, and the degree of purification were calculated.

In the first step of purification, anion exchange chromatography (AEC), most of the protein was not trapped on the column. α-Galactosidase was adsorbed on the column and was eluted after application of a linear NaCl gradient. Eluted fractions were followed and checked for α-galactosidase activity. The highest α-galactosidase activities were detected in the fractions 16−21. However, these fractions did not give a single band on SDS-PAGE shown in the Figure 3.16; a few minor bands on SDS-PAGE gel were observed. Therefore, the second, hydrophobic interaction, chromatography was performed.

In the second purification step, hydrophobic interaction chromatography (HIC), while other proteins were adsorbed on the column, α-galactosidase was not trapped on the column and eluted in early fractions (1−10). These α-galactosidase active fractions were pooled.

Before and after purification the total protein concentrations measured by Lowry (1951) method (Appendix I) were 1.76 mg/mL (crude extract) and 0.1 mg/mL (HIC).

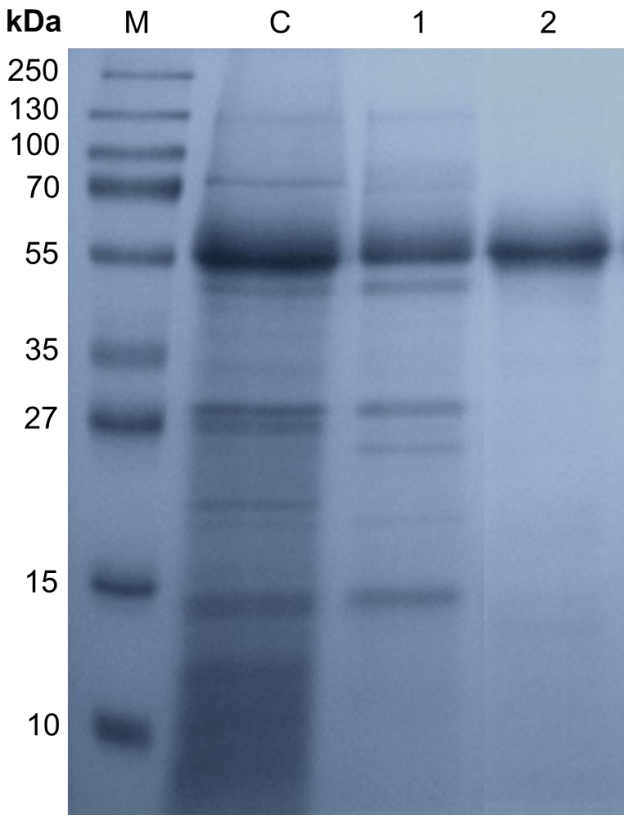

Figure 3.16 SDS-PAGE of the recombinant α-galactosidase purification steps after staining with Coomassie Brilliant Blue G-250. Lane M: PageRuler™ prestained protein ladder plus (Appendix D.3); lane C: culture supernatant, lane 1: recombinant α-galactosidase purified by AEC; lane2: recombinant α-galactosidase purified by HIC

Results of the two-step column chromatography technique including anion exchange and hydrophobic interaction are shown in Figure 3.16 and Table 3.6. Recombinant α-galactosidase produced by *A. sojae* was purified 18.7 times with the overall yield of 56%.

In a previous study, native α-galactosidase produced by *Aspergillus fumigatus* 385708 on locust bean gum, was purified by DEAE Sepharose and Phenyl Sepharose chromatography and the yield was 17.8% with 1596-fold purification (Puchart *et al*., 2000). This difference may be attributed to the fact that native α-galactosidase was produced on complex medium

containing locust bean gum. This was required for inducing α-galactosidase production. Here, as *A. sojae* Ta1 produce α-galactosidase continuously under the control of a constitutive *gpd*A promoter and does not need to be induced, it was cultivated on much more clear YpSs medium (Appendix B) containing glucose as the sole carbon source and the extracellular enzyme was more efficiently purified with 56% yield. Although the specific activity of native α-galactosidase was previously determined as 266.6 U/mg by Puchart *et al*. (2000), the specific activity of recombinant α-galactosidase was 64.7 U/mg.

Table 3.6 Summary of the purification of recombinant α-galactosidase from *A. sojae* Ta1 by anion exchange (AEC) and hydrophobic interaction chromatography (HIC)

Steps	Volume (mL)	Protein Conc. (mg/mL)	Total protein (mg)	Activity (U/mL)	[1*]Specific activity (U/mg)	Total activity (U)	[2*]Yield (%)	[3*]Degree of Purification
Crude Extract	57	1.76	100.3	6.1	3.46	347	100	1
AEC	30	0.14	4.2	6.8	48.57	204	58.78	14
HIC	30	0.1	3	6.47	64.7	194	56	18.7

[1*]Specific Activity (U/mg protein): α-Galactosidase activity (U/mL)/Protein concentration (mg/mL)
[2*]Yield (%): [Total α-galactosidase activity (U/mL)/Crude total α-galactosidase activity (U/mL)] x 100
[3*]Degree of Purification: Specific α-galactosidase activity (U/mg)/Crude specific α-galactosidase activity (U/mg)

α-Galactosidase encoded by *agl*B gene of *A. fumigatus* (Acc. No. ACO72591) has a calculated molecular weight of 49 kDa and 4 potential N-glycosylation sites in the amino acid sequence of the mature protein. The molecular mass of the native enzyme (Puchart *et al*., 2000), was reported as 57 kDa. Indeed, the recombinant enzyme also appeared as 57 kDa on SDS-PAGE, however, after treatment with N-glycanase, the molecular weight of the protein band decreased to *c.*50 kDa (Figure 3.17) supporting the presence of N-glycosylation, and indicating that the recombinant α-galactosidase produced in *A. sojae* Ta1 has undergone posttranslational processing similar to that of the native enzyme. N-Deglycosylation is very common in fungal proteins (Limongi *et al*., 1995; Panchal and Wodzinski, 1998).

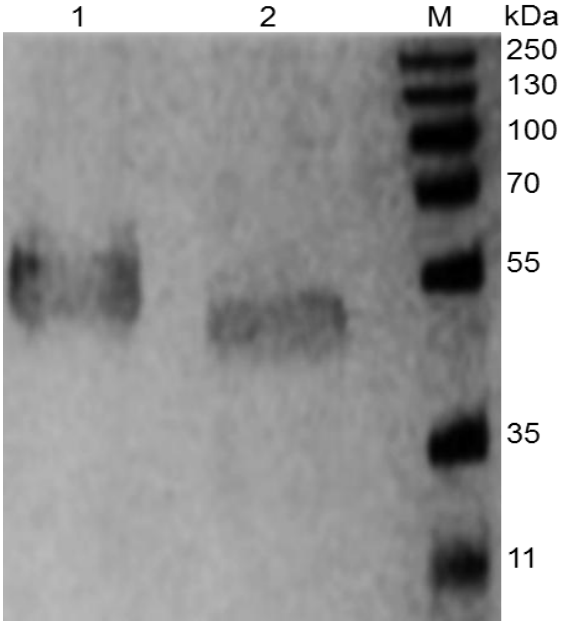

Figure 3.17 N-deglycosylation of recombinant α-galactosidase; lane 1: purified recombinant α-galactosidase, lane 2: purified recombinant α-galactosidase after N-glycanase treatment.

3.7 Kinetic analysis of recombinant α-galactosidase

Kinetic studies were performed using *p*NPαGal as substrate at concentrations ranging from 0.1 to 3.5 mM. The results of kinetic parameters followed Michaelis-Menten kinetics. Simple Michaelis-Menten kinetics has been reported for several Aspergilli (Zapater *et. al*., 1990, Neustroev *et. al*., 1991). Michaelis-Menten and Lineweaver Burk curves of α-galactosidase activity are shown in Figure 3.18 and Figure 3.19, respectively.

The V_{max} and K_m values of recombinant α-galactosidase for the hydrolysis of *p*NPαGal were 78±2 U/mg protein and 0.45±0.04 mM, respectively. Comparison of these results with the native form of the enzyme showed that while K_m values of the native form (0.5 mM) and recombinant form were similar, recombinant form had higher V_{max} than the native form (52.4 U/mg protein) (Puchart *et al*., 2000). The exact reason behind these differences is not known, however, it might emerge from the differences in purification procedures.

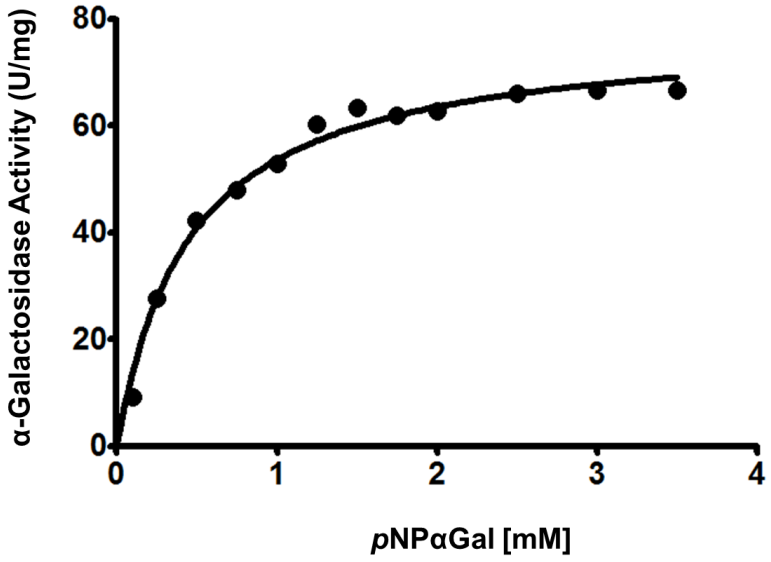

Figure 3.18 Michaelis-Menten curve of recombinant α-galactosidase

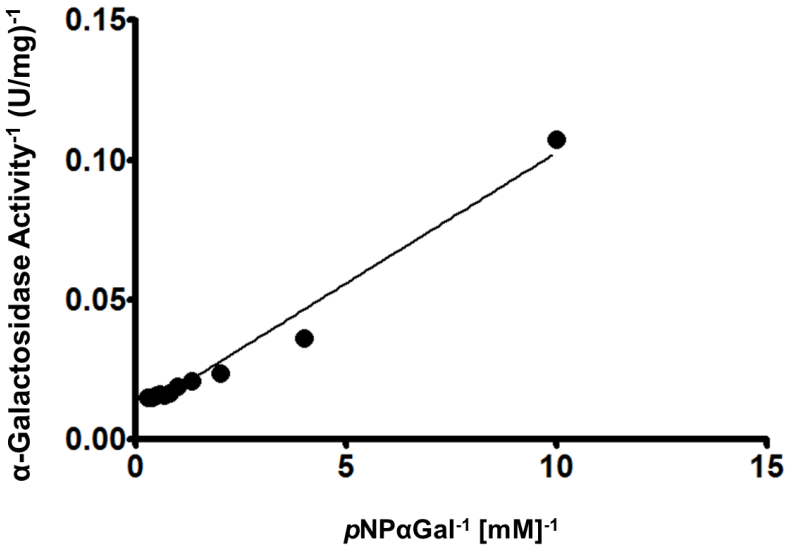

Figure 3.19 Lineweaver Burk plot of recombinant α-galactosidase activity

3.8 Effect of pH on recombinant α-galactosidase activity and stability

The effect of pH on recombinant α-galactosidase activity and stability were determined in a pH range of 2.5−8.0 under standard assay conditions. α-Galactosidase was most active between pH 4−6. The highest α-galactosidase activity was observed at pH 4.5 as shown in Figure 3.20. Previously, the native α-galactosidase was also reported to be most active between pH 4.5−5 (Puchart *et al*., 2000). This slightly acidic pH optimum is characteristic for fungal glycosyl hydrolases (Dey and Pridham, 1972).

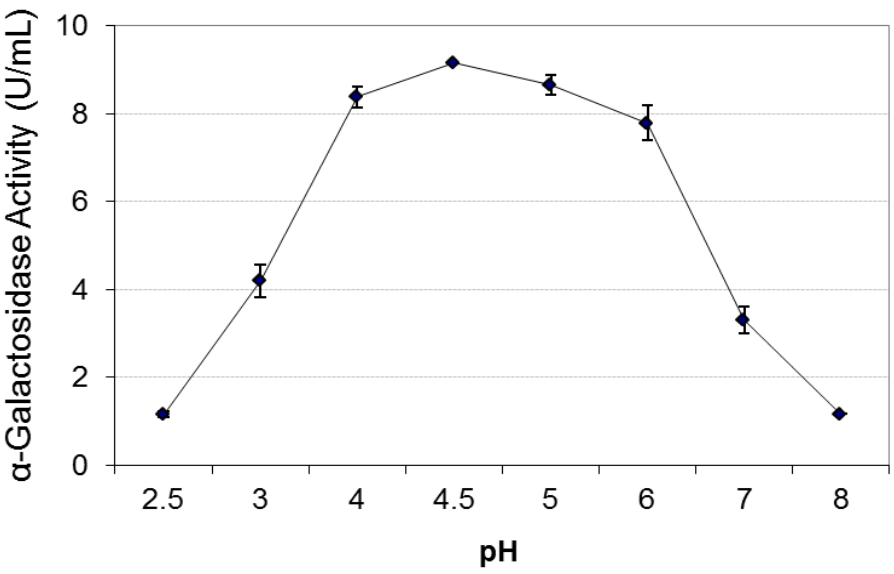

Figure 3.20 pH-dependence of recombinant α-galactosidase activity

Figure 3.21 shows the retained recombinant α-galactosidase activity after 2 and 4 h incubations at different pH values. α-Galactosidase was most active around pH 4.5 and retained *c.*60% of its activity in the pH range of 4−6 after 2 h incubation. However, after 4 h incubation the preserved activity percentages were only in the range of 12−27%.

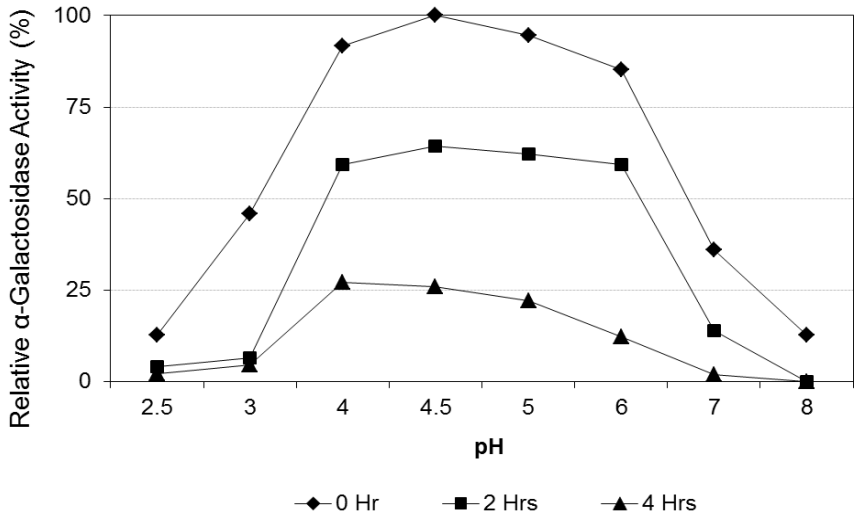

Figure 3.21 pH-dependence of recombinant α-galactosidase stability

3.9 Effect of temperature on recombinant α-galactosidase activity and stability

The effect of temperature on recombinant α-galactosidase activity and stability were determined in a temperature range of 20−80 °C under standard assay conditions. α-Galactosidase was most active between 50−60 °C as shown in Figure 3.22.

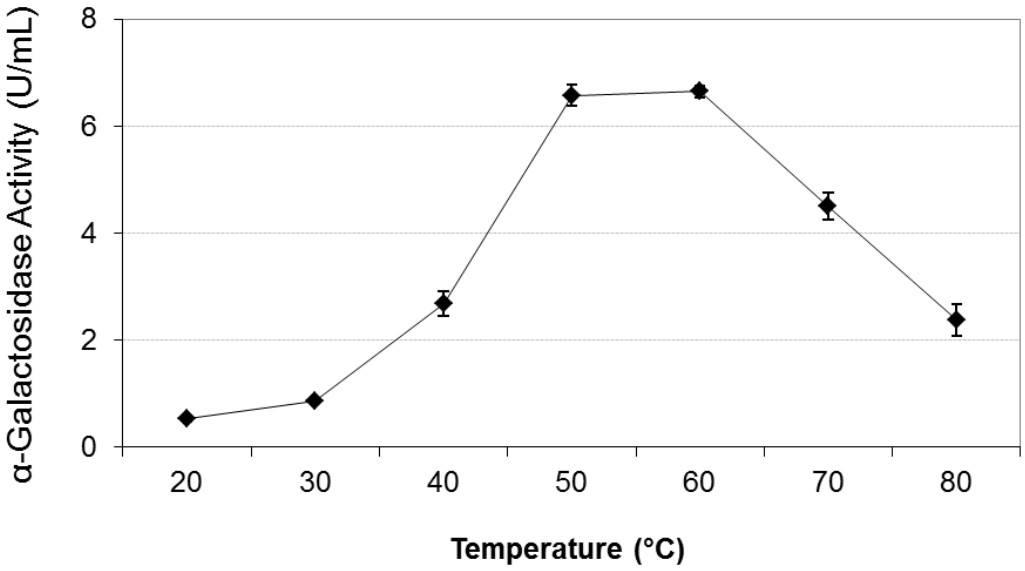

Figure 3.22 Temperature-dependence of recombinant α-galactosidase activity

Figure 3.23 shows the retained α-galactosidase activity after 1, 3, and 5 h incubations at different temperatures. More than 60% of activity was retained up to 50 °C even after 5 h incubation. After this temperature, α-galactosidase lost its stability sharply. Although α-galactosidase was most active in a temperature range of 50−60 °C, it could preserve only 8% of its activity after 1 h incubation at 60 °C. On the other hand, the retained activities were around 75% even after 5 h incubation at temperatures up to 40 °C.

The observed temperature optimum and temperature stability of the recombinant enzyme were lower than the native enzyme (65-70 °C) but were higher than the values reported for α-galactosidases from many other fungal sources (Kotwal *et. al*., 1998; Mi *et. al*., 2007). However, thermostability of the neither native nor recombinant enzyme could reach α-galactosidases from extremophilic bacteria *Thermotoga neapolitana* (Duffaud *et al*., 1997) and *T. maritima* (Liebl *et. al*., 1998).

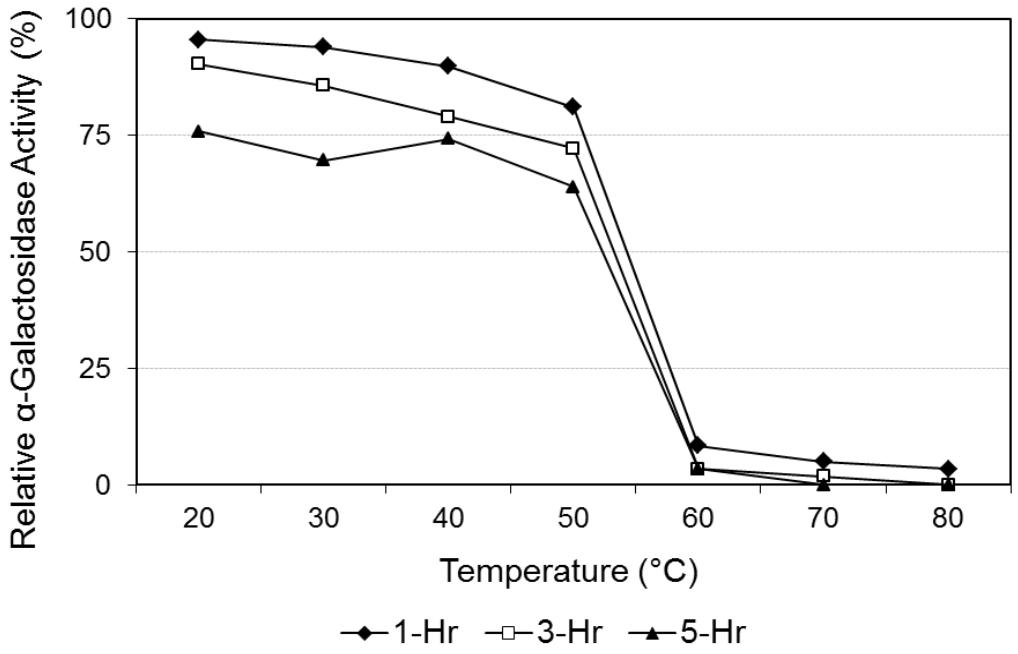

Figure 3.23 Temperature-dependence of recombinant α-galactosidase stability

3.10 Effect of additives on recombinant α-galactosidase activity and stability

The effects of metal ions and different protein denaturing agents on recombinant α-galactosidase activity were analysed by measuring the residual activity after incubation of enzyme with 1 mM of each reagents for 90 minutes. Results are summarized in Figure 3.24.

Recombinant α-galactosidase activity was not significantly affected by most of the metal cations (Ca^{2+}, Sr^{2+}, Zn^{2+}, Cu^{+2}, Co^{2+}, Cd^{2+}, Ba^{2+}, Cr^{3+}, B^{3+}), the metal chelating agent, EDTA, and the detergent, SDS. The change in the relative α-galactosidase activity remained under ±10% after the incubation with them. Not being affected by the metal chelating agent, EDTA may indicate that α-galactosidase was not a metalloenzyme.

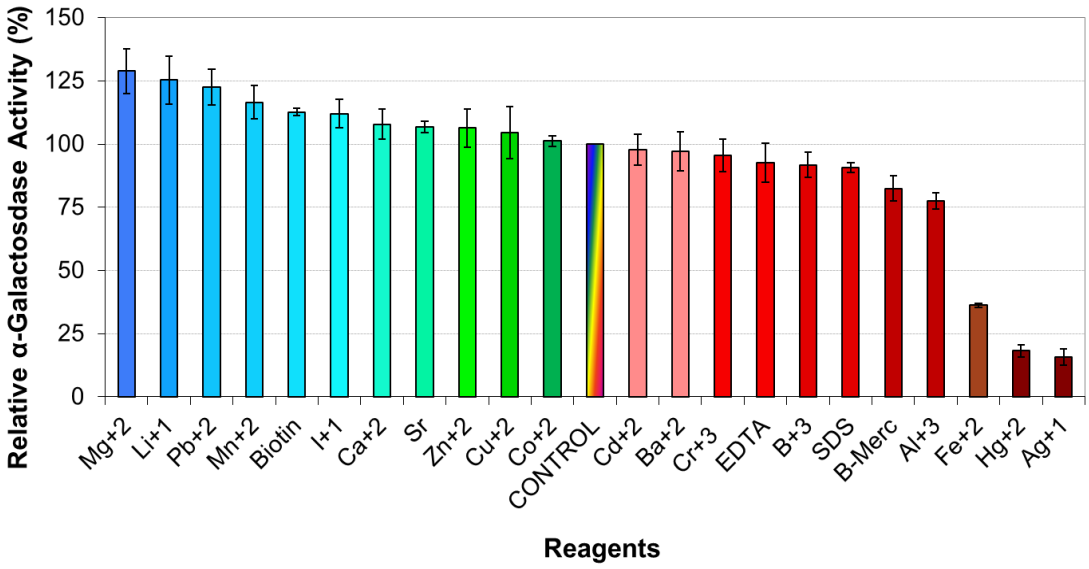

Figure 3.24 Effects of additives on recombinant α-galactosidase activity

Ag^{+1} and Hg^{2+} extremely inactivated α-galactosidase activity with 16 and 18% residual activities, respectively. The inhibition of α-galactosidases with Ag^{+1} and Hg^{2+} was reported previously (Zapater *et al*., 1990) and suggests reaction with thiol groups of histidine near the active site (Dey and Pridham, 1972). Fujimoto *et al.* (2003) also reported inactivation with Ag^{+1} and Hg^{2+}, which attack the cysteine residues in the active site and prevent substrate binding in the catalytic pocket of α-galactosidase. The Fe^{2+} also highly inhibited the activity up to 36% residual activity.

Mg^{+2}, Li^{+1}, Pb^{+2}, Mn^{+2}, biotin and I^{+1} enhanced the enzyme activity to varying degrees (29, 25, 22, 16, 12, 12%, respectively). Activation with Mg^{+2} and Mn^{+2} agreed with the results obtained for α-galactosidase from *Thermomyces lanuginosus* (Rezessy-Szabó *et al*., 2007). The cysteine-inhibitor, β-mercaptoethanol and a reactive chemical element, Al^{+3} slightly inhibited α-galactosidase activity (82% and 78%, respectively).

3.11 Effect of osmotic stress

Despite the constitutive nature of glyceraldehyde triphosphate dehydrogenase (*gpd*A) promoter, it was reported by Redkar *et al*. (1998) to be transcriptionally activated by osmotic signals. It was envisaged that these findings could be of value in further enhancing heterologous protein production in *A. sojae*, under the control of the *gpd*A promoter, and specifically, the production of α-galactosidase. Accordingly, in this study salt stress was used as an agent for enhancing the heterologous production of α-galactosidase by *A. sojae* Ta1. Either salts were added directly into growth medium, to generate salt shock, or cells were first adapted to salt. Salt-adapted and non-adapted cultures of *A. sojae* Ta1 were grown in the presence of various salts, and growth, α-galactosidase production, and morphology were analysed, as described in section 2.2.23.

Salt-adapted and non-adapted *A. sojae* Ta1 cells were grown in complete medium in the presence of different salts at either 1 M or 2 M. In order to eliminate other stresses and to analyse only the effect of salt stress, complete medium was chosen for cultivation over the simple YpSs medium (Appendix B), which might be inefficient under salt stress conditions, and optimized YpSs medium (Section 3.4), which might result in carbon and/or nitrogen catabolite repression due to high amounts of carbon (10.5% molasses) and nitrogen (1.3% NH_4NO_3) sources. In addition, as the agitation speed of the cultivations, 200 rpm was used instead of 276 rpm, which was determined by RSM, to avoid any possible shear stress.

3.11.1 Effect of salt stress on fungal growth

Based on biomass data obtained at the end of 8-day cultivations, salt addition had a negative effect on fungal growth in both non-adapted and salt-adapted cells (Figure 3.25). This effect was mainly influenced by the nature and concentration of the salinity agent used.

Non-adapted *A. sojae* Ta1 cells showed higher tolerance to KCl, and NaCl and lower to $MgSO_4$, and Na_2SO_4-stress. Cells could not survive in the presence of either 1 or 2 M $MgCl_2$ and 2 M Na_2SO_4. In general, growth significantly decreased as the concentration of salt was increased from 1 M to 2 M (Figure 3.25).

Among cultures adapted to 1 M of each of the salt used, a significant improvement was observed in growth especially on $MgCl_2$ and Na_2SO_4 (Figure 3.25). Growth on $MgSO_4$, NaCl, and KCl were not significantly different from the non-adapted cultures. Biomass generation on 1 M Na_2SO_4 was almost 2-fold in adapted cultures, compared to non-adapted cultures. Thus, gradual adaptation to salt stress resulted in an improvement of fungal growth.

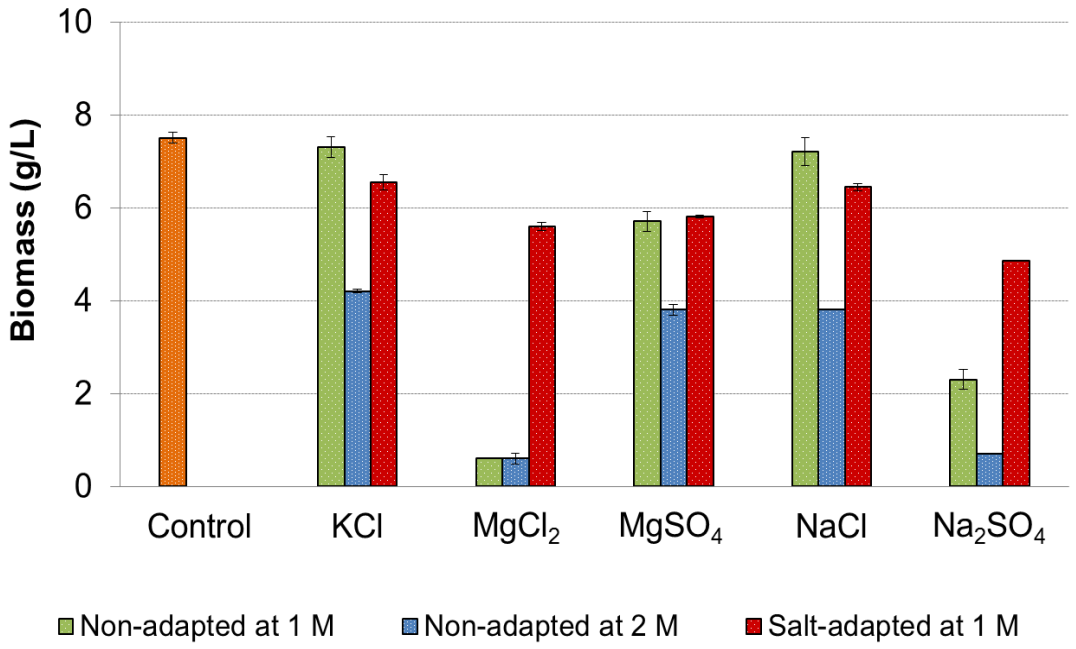

Figure 3.25 Effect of osmotic stress on the growth of *A. sojae* Ta1 in salt non-adapted cultures grown at 1 M (green) and at 2 M (blue), and salt-adapted cultures grown at 1 M (red), at the end of 8 days of cultivation at 30 °C in 2% glucose containing complete medium at 200 rpm. Error bars represent the standard deviations from the mean of two independent experiments.

These results are in accord with those in the literature. For example, Nikolaou *et al*. (2009) showed that the growth rates of *A. fumigatus* and *A. nidulans* were decreased by 54% and 65%, respectively, at 1 M NaCl and complete inhibition of growth took place at 2 M NaCl in *A. fumigatus* and at 3 M NaCl in *A. nidulans* cells. Raffaello *et al*. (2012) also observed stronger growth inhibition of *Heterobasidion annosum* in the presence of divalent salts like $MgCl_2$ and $CaCl_2$ compared to the same concentrations of monovalent salts like KCl and NaCl. In our study, salt adaptation somewhat improved growth as compared to the non-adapted cells, especially in the presence of $MgCl_2$ and Na_2SO_4.

3.11.2. Effect of salt stress on α-galactosidase production by non-adapted *A. sojae* Ta1

The influence of salt stress on α-galactosidase excretion was analysed by growing fungal cultures over 8 days of cultivation in the presence of 1 or 2 M of each salt. The pre-cultures, used to inoculate main cultures, were grown in the absence of salt stress, as described in section 2.2.23.1. Here the aim was to allow spores to germinate under normal conditions and expose mycelia to a sudden osmotic stress.

In general, α-galactosidase production displayed a different trend upon salt-stress in both non-adapted and salt-adapted cells, namely maximum productions were observed at day 6, instead of the 3rd day, as observed in the control culture.

Compared to the control (7.3 U/mL), the highest increase in volumetric α-galactosidase production was obtained in the presence of NaCl, which is also the cheapest among all other salts used in this study. Increase in α-galactosidase production was *c*.3-fold (22.7 U/mL) with 1 M NaCl (Figure 3.26), followed by *c*.2.5-fold increase in the presence of 1 M KCl (18 U/mL) (Figure 3.27), *c*.2.3-fold in the presence of 1 M $MgSO_4$ (17 U/mL) (Figure 3.28), and *c*.2-fold with 1 M Na_2SO_4 (15.3 U/mL) (Figure 3.29). No α-galactosidase activity was observed in the presence of $MgCl_2$, which caused complete growth inhibition in non-adapted cells.

Extracellular α-galactosidase activities were lower at 2 M, which is attributed to a decrease in growth (Figure 3.25), rather than a decrease in the activation of transcription of the *gpd*A promoter. Nevertheless, activities were still higher than the control, except at 2 M Na_2SO_4, which completely inhibited growth.

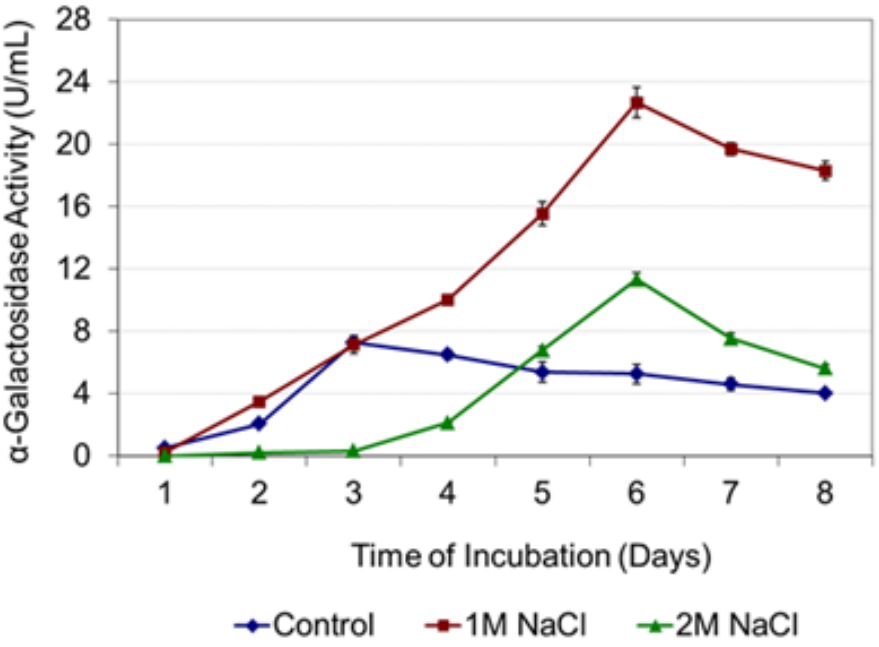

Figure 3.26 α-Galactosidase production by non-adapted *A. sojae* Ta1 in the presence of 1 M and 2 M NaCl. Error bars represent the standard deviations from the mean of two independent experiments.

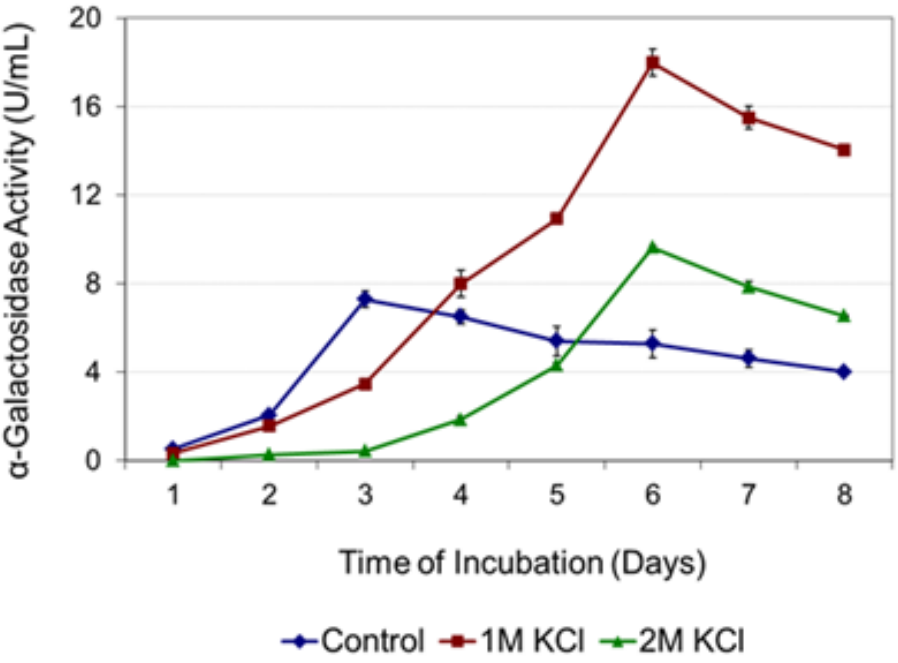

Figure 3.27 α-Galactosidase production by non-adapted *A. sojae* Ta1 in the presence of 1 M and 2 M KCl. Error bars represent the standard deviations from the mean of two independent experiments.

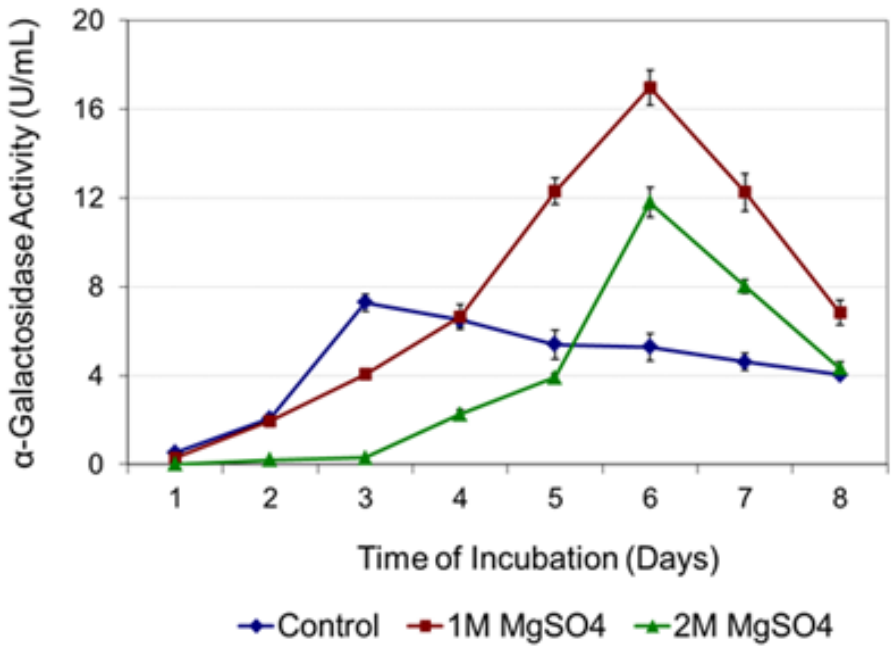

Figure 3.28 α-Galactosidase production by non-adapted *A. sojae* Ta1 in the presence of 1 M and 2 M $MgSO_4$. Error bars represent the standard deviations from the mean of two independent experiments.

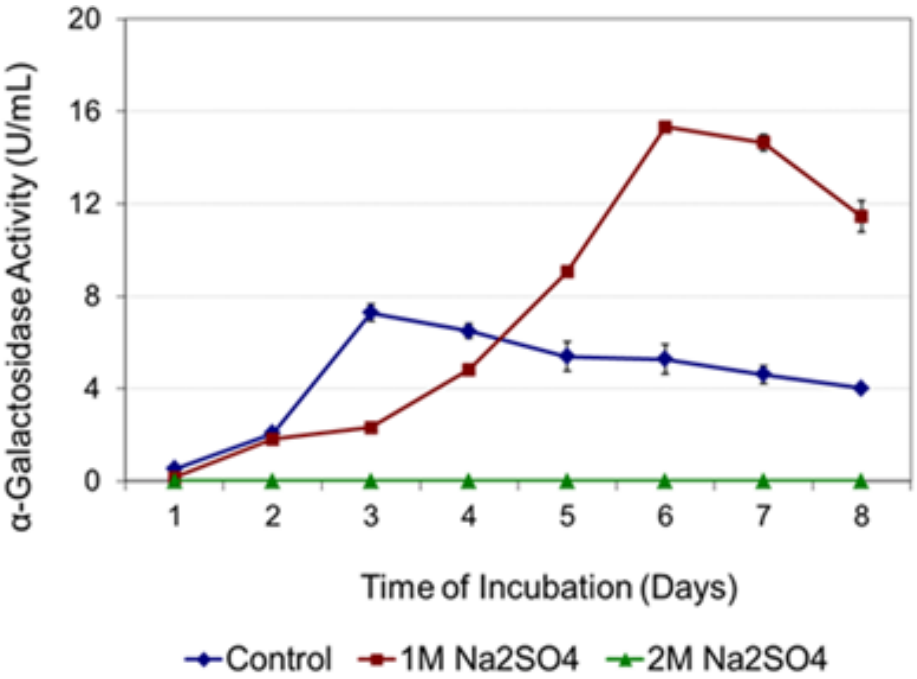

Figure 3.29 α-Galactosidase production by non-adapted *A. sojae* Ta1 in the presence of 1 M and 2 M Na_2SO_4. Error bars represent the standard deviations from the mean of two independent experiments.

3.11.3 Effect of salt stress on α-galactosidase production by salt-adapted *A. sojae* Ta1

A. sojae Ta1 was gradually adapted to 1 M of each of the salts tested, as described in section 2.2.23. Cultures were then grown in the presence of 1 M of each of the salt for 8 days and α-galactosidase activity in the growth medium was analysed. Results are shown in Figure 3.30. Accordingly, highest increase in α-galactosidase production was at 1 M NaCl (*c.*2.64-fold), which was followed by KCl (*c*.2.36-fold), $MgSO_4$ (*c.*1.5-fold), Na_2SO_4 (*c*.1.42-fold), and $MgCl_2$ (*c*.1.4-fold).

According to the results, similar to non-adapted cultures, NaCl and KCl resulted in the highest increase in α-galactosidase production, which was followed by the others in the same order, except for $MgCl_2$, which enhanced enzyme production, similar to Na_2SO_4. When adapted and non-adapted cultures are compared, on the one hand, a sudden salt stress appears to cause higher induction of the *gpd*A promoter; on the other hand, growth is improved by adaptation to salt, especially on $MgCl_2$ and Na_2SO_4.

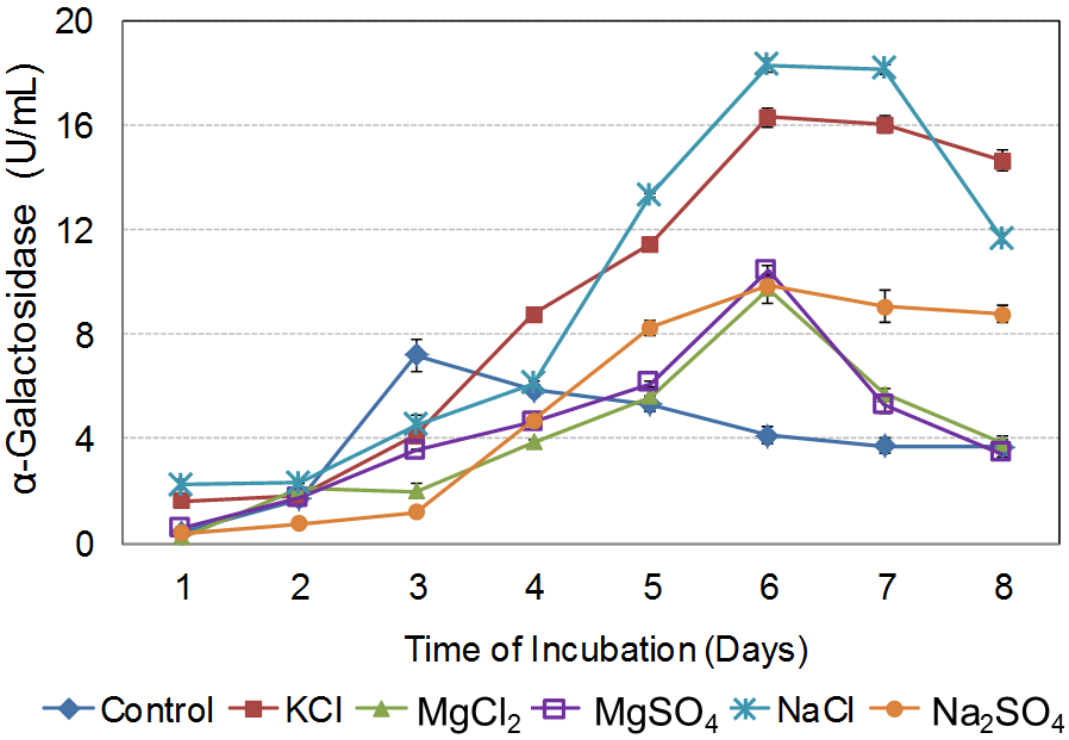

Figure 3.30 α-Galactosidase production by salt-adapted *A. sojae* Ta1 in the presence of 1 M KCl, $MgCl_2$, $MgSO_4$, NaCl, and Na_2SO_4. Error bars represent the standard deviations from the mean of two independent experiments.

To analyse biomass-based enzyme production (U/mg biomass), result of the biomass measurement of the day, when the highest enzyme productivity reached, was used. Biomass measurement of day 4 for control culture and day 6 for the salt-treated cultures were used to analyse biomass-based enzyme productions. Compared to the control culture (1 U/mg biomass), the most pronounced enhancement in biomass-based enzyme productivity was observed in the presence of 1 M Na_2SO_4 (Figure 3.31) by non-adapted cells. Although biomass reduction was approximately 70% (Figure 3.25), enzyme production increased 2-fold (Figure 3.29), and therefore, an overall 6.67-fold increase (6.67 U/mg biomass) was achieved in biomass-based α-galactosidase production on Na_2SO_4, which was followed by 1 M NaCl (3.1-fold by both non-adapted and NaCl-adapted cells), 1 M $MgSO_4$ (3-fold by

non-adapted cells), and 1 M KCl (2.5-fold by non-adapted and 2.8-fold by KCl-adapted cells (Figure 3.31) .

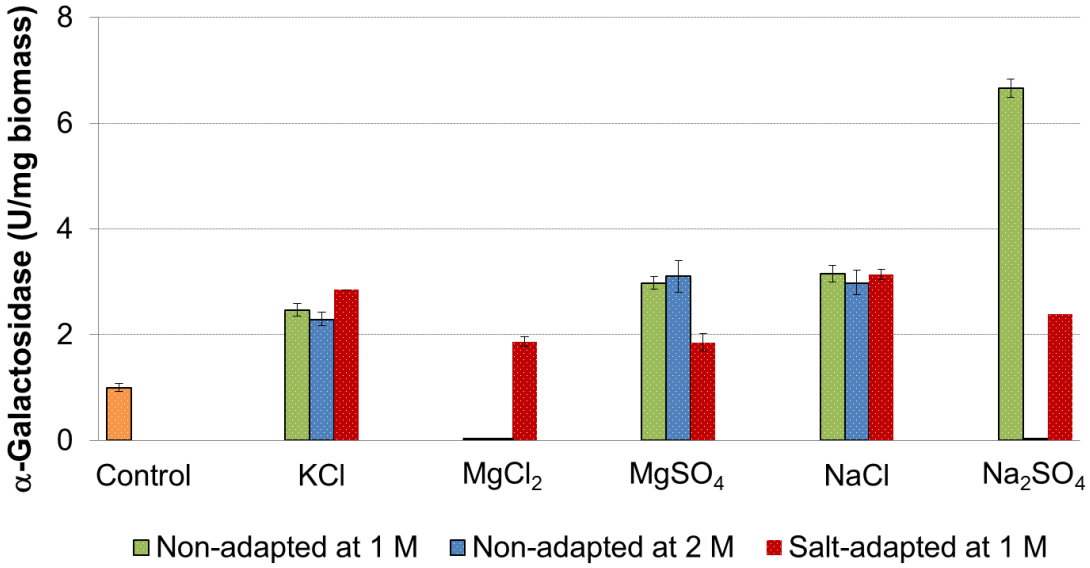

Figure 3.31 Biomass-based α-galactosidase production by *A. sojae* Ta1. Salt non-adapted cultures grown at 1 M (green) and at 2 M (blue), and salt-adapted cultures grown at 1 M (red) of each salt in 2% glucose containing complete medium at 30 °C at 200 rpm. Error bars represent the standard deviations from the mean of two independent experiments.

Adaptation to salt changed fungal biomass yield depending on the applied salt. $MgCl_2$ and Na_2SO_4-adapted cultures yielded higher fungal biomass than the non-adapted counterparts did, however; their biomass yields were still lower than the NaCl and KCl-adapted cells. In the case of NaCl and KCl-adapted cultures, lower biomass generations were observed in adapted cultures compared to the non-adapted cells. This might be due to either an adaptive strategy in order to withstand such unfavourable stress conditions by reducing volume and growth rate (Albertyn *et al*., 1994) after reaching sufficient biomass, or the energy expenditure of salt-adapted cultures. Adapted cells under stress conditions use available ATP for exclusion or compartmentalization of salt ions and for the synthesis of compatible

osmolytes and essential proteins conferring salt tolerance (Redkar *et al*., 1996b). On the other hand, α-galactosidase production was more induced in non-adapted cultures, which might be due to higher triggering effects of acute osmotic shock on *gpd*A promoter, which was previously shown to be induced by osmotic signals by Redkar *et al*. (1995). In the case of $MgCl_2$ and Na_2SO_4-adapted cultures, first, cell growth was improved in the presence of salt with the help of adaptation period and growth-associated α-galactosidase production took place once sufficient biomass was formed, and then compared to the control culture, up to 1.4-fold increase in α-galactosidase production was achieved by osmotic induction.

The maximum increase with 3-fold in volumetric α-galactosidase production in non-adapted *A. sojae* Ta1 cells was achieved in the presence of 1 M NaCl. In previous studies, NaCl was shown to enhance secretion of both glucose oxidase by *A. niger* (Fiedurek, 1998a) and β-galactosidase by *Penicillium notatum* (Fiedurek, 1998b). Neither of the enzymes were recombinant, so they were produced under the control of their own promoters. Fiedurek achieved 2.1-fold increase in glucose oxidase and 1.9-fold increase in β-galactosidase volumetric enzyme production by applying osmotic shock with 1.2 M and 0.4 M NaCl, respectively. Redkar *et al*. (1998) obtained 8.4-fold increased GUS specific activity by the expression of *uid*A gene under the control of *A. nidulans gpd*A promoter in Na_2SO_4-adapted *A. nidulans* culture with the use of 2 M Na_2SO_4.

The level of recombinant α-galactosidase production achieved by 1 M NaCl stress (22.7 U/mL) in *A. sojae* Ta1 is higher than those reported in the literature, including α-galactosidases from *Gibberilla* sp. (1.42 U/mL) (Cao *et al*., 2009b), *Rhizopus* sp. (1.69 U/mL) (Cao et al., 2009a), *Rhizomucor miehei* (11.03 U/mL) (Katrolia *et al*., 2012), and *Absidia corymbifera* (18.7 U/mL) (Baik *et al*., 2000) which were expressed in *E. coli* and Bispora sp. (1.52 U/mL) (Wang *et al*., 2010) and *Penicillium* sp. α-galactosidase (6.03 U/mL, shake-flask) (Mi *et al*., 2007) expressed in *Pichia pastoris.*

3.11.4 Effect of osmotic stress on fungal morphology

Osmotic stress is known to be linked to fungal morphogenesis (Duran *et al*., 2010). In agitated submerged cultures, filamentous fungi generally grow either in the form of freely dispersed filaments (hyphae) or in compact spherical mycelial pellets. Besides, some other intermediary growth forms like fluffy mycelia (diffuse mycelia), clumpy mycelia (aggregated mycelia), looser and more hairy pellets, can also be recognized (Thomas and Paul, 1996). The favoured fungal morphology varies from one product to another and affects the productivity of the fermentation process by changing viscosity of the broth medium, oxygen transfer to the inner parts of the pellets, or the number of active mycelial tips (Peberdy, 1994; Allen and Robinson, 1990).

The effect of salt stress on *A. sojae* Ta1 morphology could be observed at macroscopic and microscopic levels (Figure 3.32 and 3.33). In general, salt addition strongly reduced pellet formation, especially at 2 M. Salt-added cultures resulted in a relatively more dispersed filamentous growth or clumpy mycelial growth.

A pellet form between clumpy and compact pellet structure in 1 M KCl, NaCl, and $MgSO_4$ (Figure 3.32.a, c, and d) were observed. In 2 M KCl, 2 M NaCl, and 1 M Na_2SO_4 containing cultures clumpy mycelia were observed (Figure 3.32.b, f, and h). While pellet size was reduced slightly at 1 M $MgSO_4$ (Figure 3.32.d), fungus failed to form pellet structure and showed only fluffy mycelial growth form with dispersed filaments at 2 M $MgSO_4$ (Figure 3.32.g). As complete inhibition of growth took place in the presence of 1 M and 2 M $MgCl_2$ and 2 M Na_2SO_4 in non-adapted cultures, pictures are not included to the Figure 3.32.

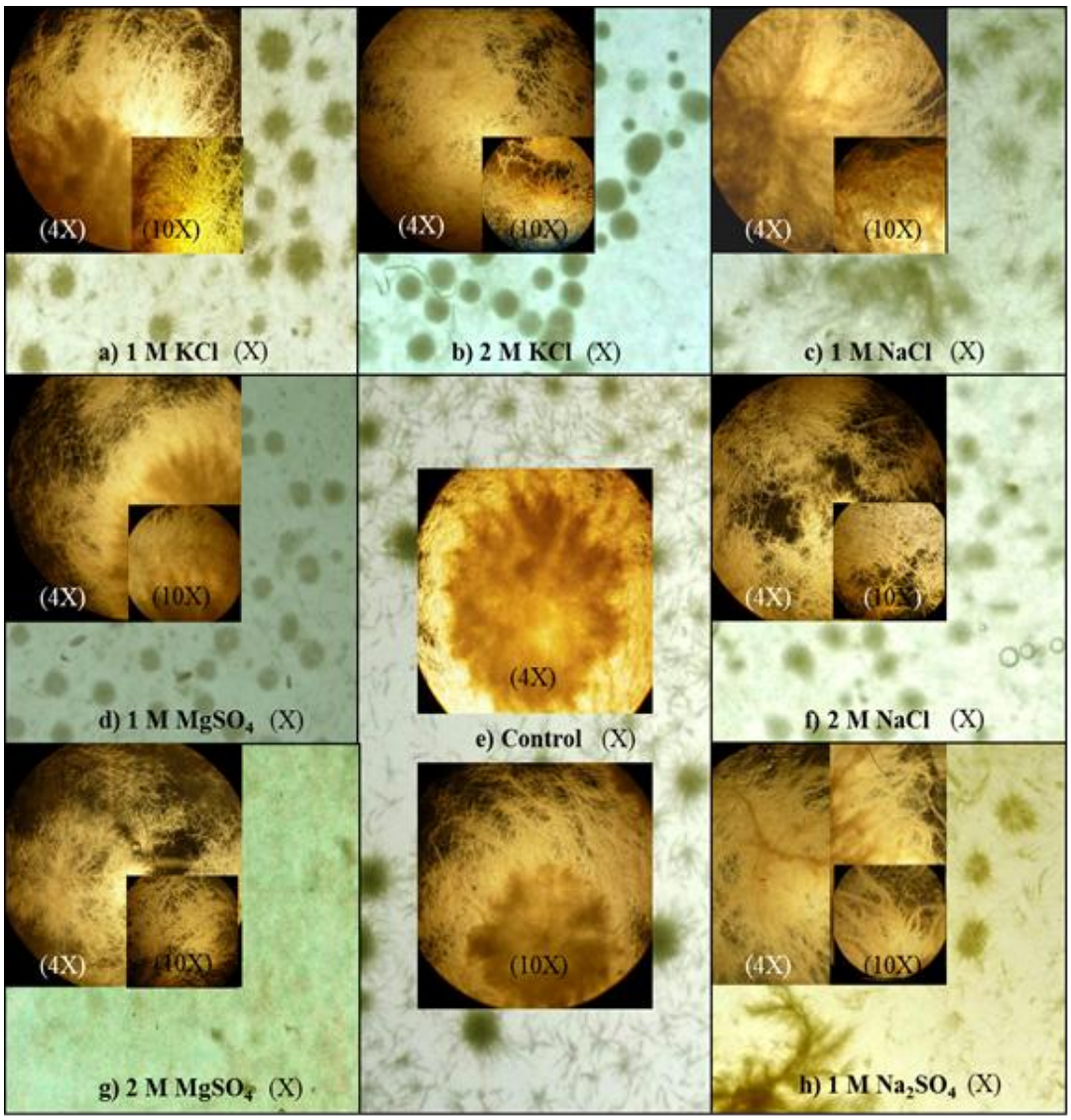

Figure 3.32 Effects of osmotic stress at 1 M and 2 M concentrations on non-adapted fungal macro (X) and micro-morphology (4X and 10X)

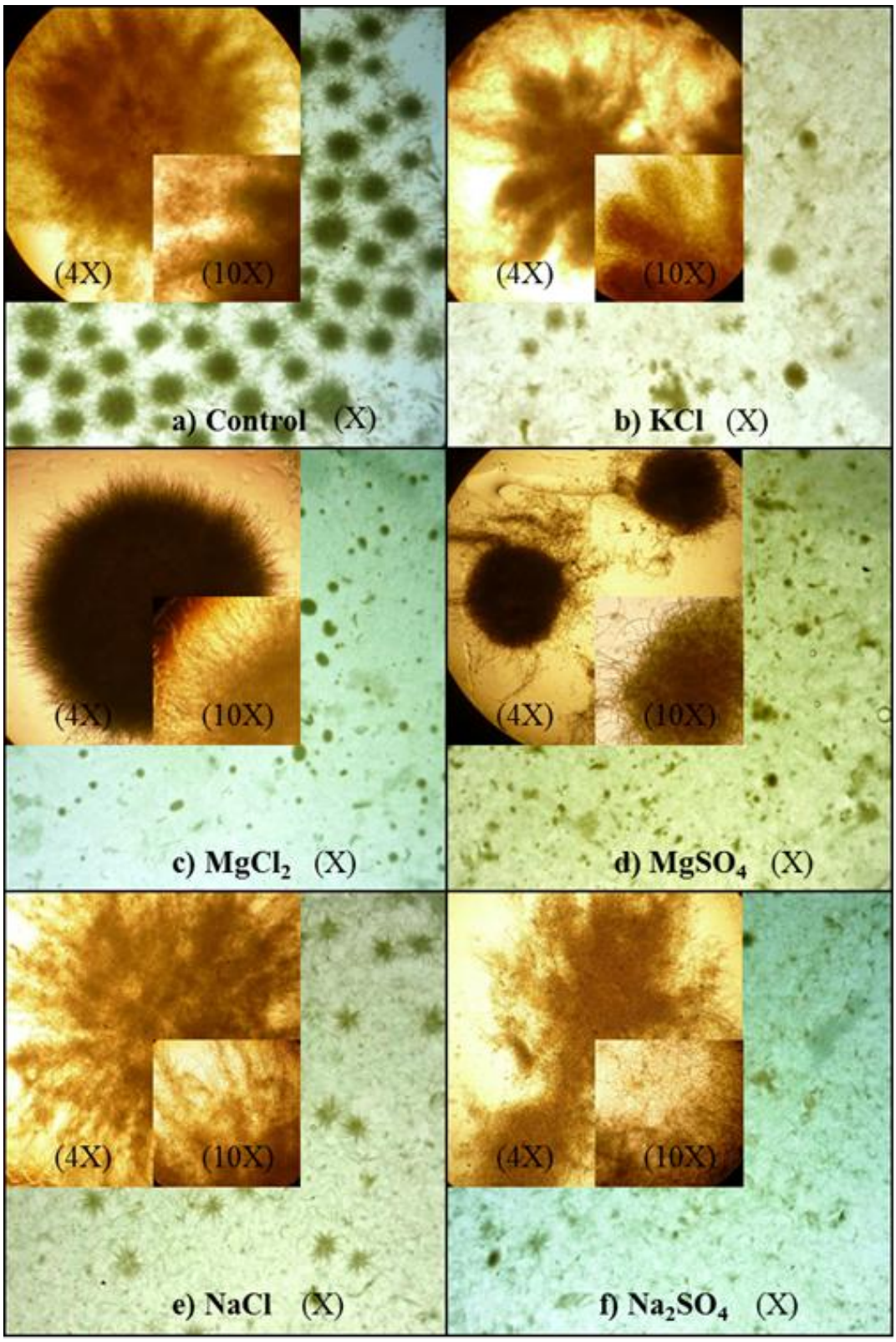

Figure 3.33 Effects of osmotic stress at 1 M concentration on salt-adapted fungal macro (X) and micro-morphology (4X and 10X)

In salt-adapted cultures, similar morphologic structures were observed with looser and more hairy clumpy pellets in KCl (Figure 3.33.b) and NaCl (Figure 3.33.e) containing cultures and clumpy mycelia in Na_2SO_4 (Figure 3.33.f) containing cultures. Unlike the non-adapted cultures, fungus could grow in the presence of 1 M $MgCl_2$ after gradual adaptation. Small-sized, compact, aggregated mycelial structures were observed in both $MgCl_2$ (Figure 3.33.c) and $MgSO_4$-containing cultures (Figure 3.33.d). Besides the clumpy growth forms, dispersed filaments were also encountered in all salt-adapted cultures extensively.

In nature, the alteration of fungal morphology could be a protective mechanism in response to osmotic stress. Filamentous fungi like *A. nidulans* and *Neurospora crassa* showed multiple apical tip formation generally near the hyphal apex under stress conditions (Markham, 1992). This phenomenon might be due to the interference with the tip extension by the adverse conditions, but increase in the number of branches helps fungus to locate relatively more favourable regions. Besides survival, fungal morphology has important effects on the rheological nature of the fermentation broth. Under high osmotic conditions, the changes in the morphology towards smaller pellet sizes and filamentous growth form might help to increase the productivity as the oxygen and nutrient transfer from the culture fluid to the inner parts of the pellet would be better in smaller pellets. On the other hand, for some bioprocesses, the pellet form is preferred over the filamentous growth due to non-viscous rheology of the broth (Zhaou *et al*., 2000). The observed enhancements in α-galactosidase production under osmotic stress conditions may be the total effects of both morphological changes and the induction of the *gpd*A promoter at transcriptional level by the osmotic signals.

As mentioned earlier in section 3.4, increased agitation rates of the cultivation had resulted in similar alterations in fungal morphology. The pellets were smaller and the fragmentation was higher in the cultures

agitated at 325 rpm compared to the control culture agitated at 155 rpm and the productivity at higher agitation rates (optimum at 276 rpm) was higher than the control culture. Beyond the optimum level of agitation, the productivity dropped probably due to shear stress on the fungus. Likewise, while the salts at 1 M mostly stimulated the productivity, exposure to 2 M of the salts caused probably extreme osmotic stress on the fungus and therefore reduced the growth and product formation drastically.

Further improvement of enzyme production can be obtained by optimization of the applied salt concentrations. More comprehensive studies on osmotic stress regulation and stress response in fungi may help to develop higher stress-tolerant strains for higher yield in industrial productions.

3.12 Transgalactosylation activity of recombinant α-galactosidase

The ability of recombinant α-galactosidase to perform transfer reaction in addition to hydrolysis was studied. α-Galactosidase from *A. fumigatus* previously shown to catalyse efficient transgalactosylation reaction with oligosaccharides, especially with β-1,4-manno-series acceptors, yielded low level of transfer ability to a variety of monosaccharide and disaccharides (Puchart and Biely, 2005). In this thesis, different monosaccharides and disaccharides were tested as acceptor in α-galactosidase mediated transfer reactions and the results were analysed by TLC, ESI-MS, and HPLC.

3.12.1 Detection of transgalactosylation products

In the presence of high acceptor concentrations (1 M), purified recombinant α-galactosidase (0.5 U/mL) catalysed the transfer of α-*D*-galactosyl residues from *p*NPαGal (0.25 M) on to monosaccharide (galactose, glucose, and mannose) and disaccharide (cellobiose, lactose, maltose, and sucrose) acceptors, as monitored by TLC (Figure 3.34). On the other hand, the

monosaccharides, xylose, arabinose, fucose, which do not possess the 6-hydroxymethyl group, the ketose, fructose, and the disaccharide, melibiose did not prove to be good acceptors for α-galactosidase-mediated transgalactosylation.

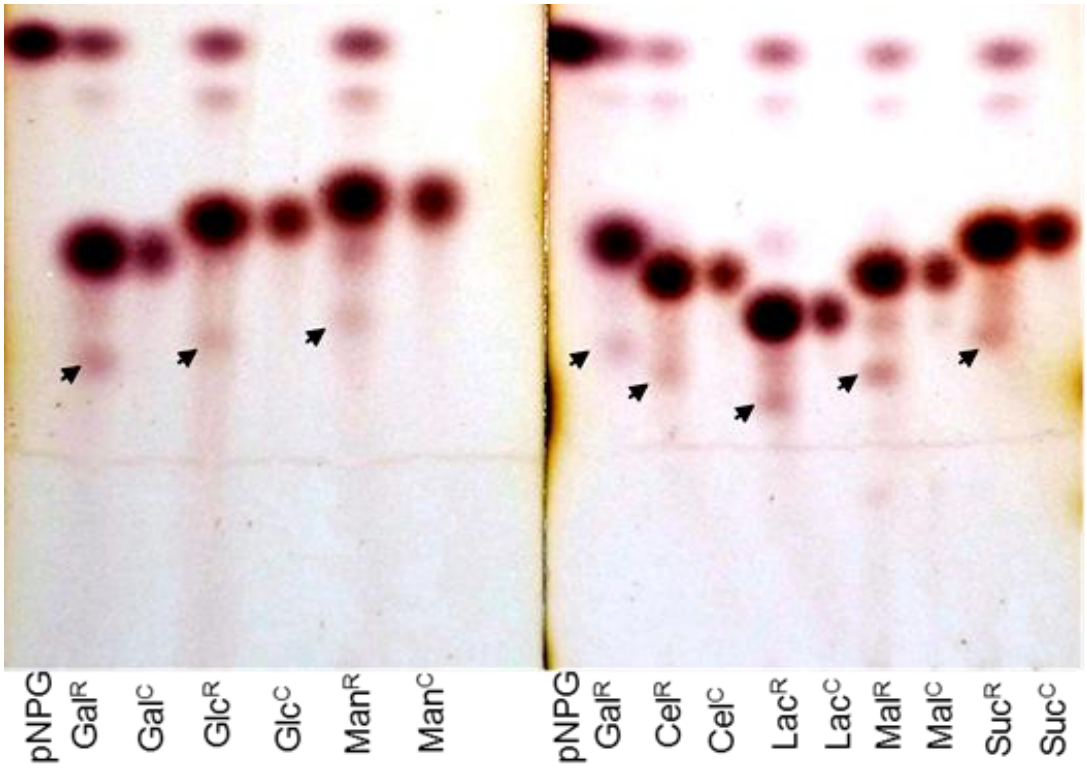

Figure 3.34 TLC analysis of 1-hour transgalactosylation reaction at 50 °C. Reaction mixtures were composed of 0.5 U/mL recombinant α-galactosidase, 0.25 M *p*NPαGal (*p*NPG), and 1 M of each acceptor sugar. R: reaction mixture; C: control acceptor sugar

Transgalactosylation reaction mixtures, obtained after an hour reaction at 50 °C, were also analysed more sensitively using electrospray ionization-time of flight mass spectrometry (ESI-TOF MS) in positive mode. ESI-MS analysis of reactions with xylose, arabinose, fucose, fructose, and melibiose did not give any positive signal corresponding to transgalactosylation products.

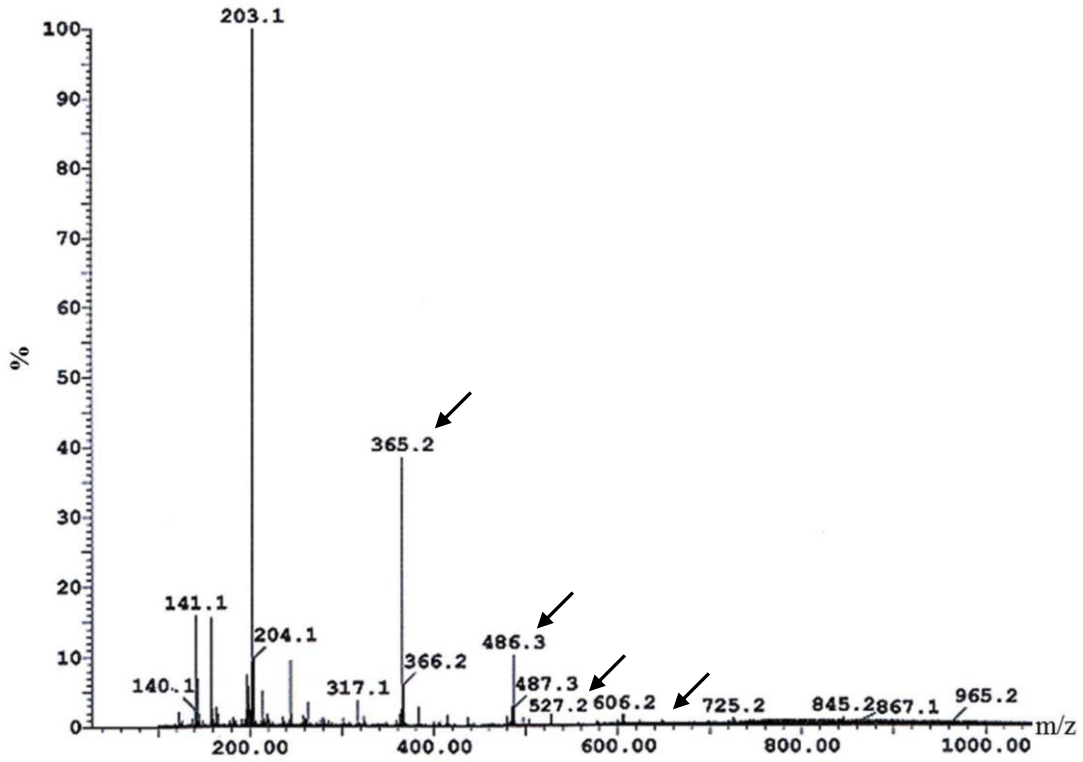

Figure 3.35 ESI-MS analysis of transgalactosylation mixture of recombinant α-galactosidase (0.5 U/mL) with galactose (1 M) as acceptor and *p*NPαGal (0.25 M) as donor at 50 °C for 1 hour

The ESI-MS showed *m*/*z* of 365, 486, 527, and 648 corresponding to the calculated values of the Na^+ adduct of α-*D*-galactobiose (Gal_2), *p*NP-α-*D*-galactobioside (*p*NPαGal_2), α-*D*-galactotriose (Gal_3) and *p*NP-α-*D*-galactotrioside (*p*NPαGal_3), respectively with the galactose ($[M+Na]^+$ at m/z 203) as acceptor (Figure 3.35). The products except Gal_2 might be in trace amount that they could be detected only by ESI-MS but not by TLC and HPLC.

The possible structures of transgalactosylation reaction products of recombinant α-galactosidase in the presence of α-*D*-galactose acceptor are schemed in Figure 3.36.

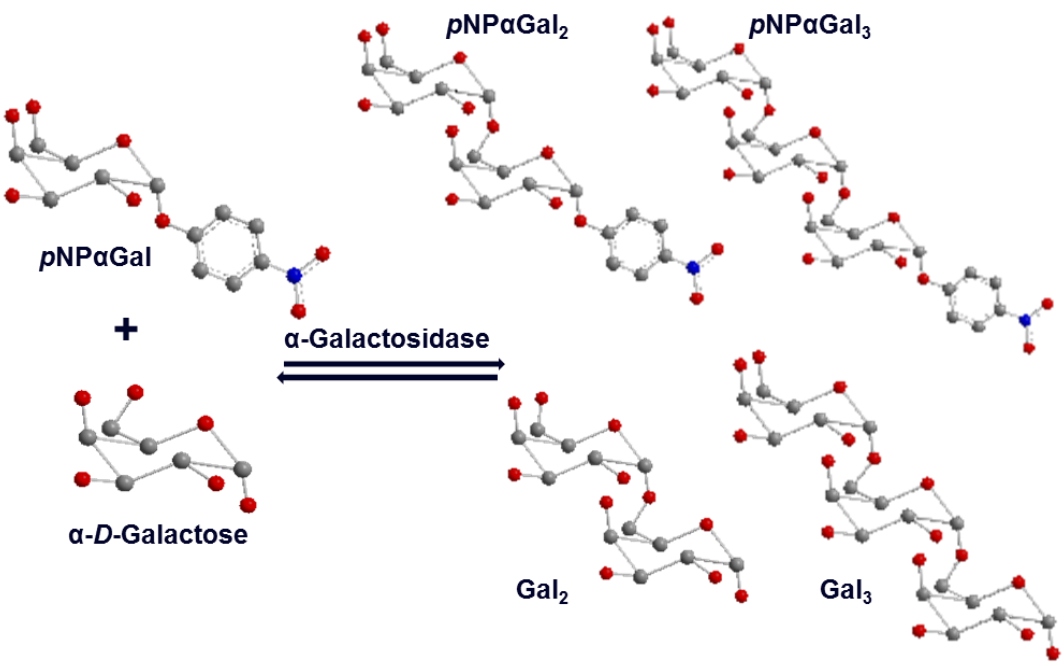

Figure 3.36 Products of transglycosylation reaction catalysed by recombinant α-galactosidase in the presence of α-*D*-galactose as acceptor. Drawn by ChemBioOffice Ultra 2010 Trial Version.

A similar ESI-MS spectrum was observed when mannose ($[M+Na]^+$ at m/z 203) was used as the acceptor molecule in transgalactosylation. The peaks of $[M+Na]^+$ at m/z 365 (α-*D*-disaccharide:GalMan and Gal_2), 486 (*p*NP-α-*D*-disaccharide), 527 (trisaccharide:Gal_3, Gal_2Man, $GalMan_2$), and 648 (*p*NP-trisaccharide) were detected (Figure 3.37).

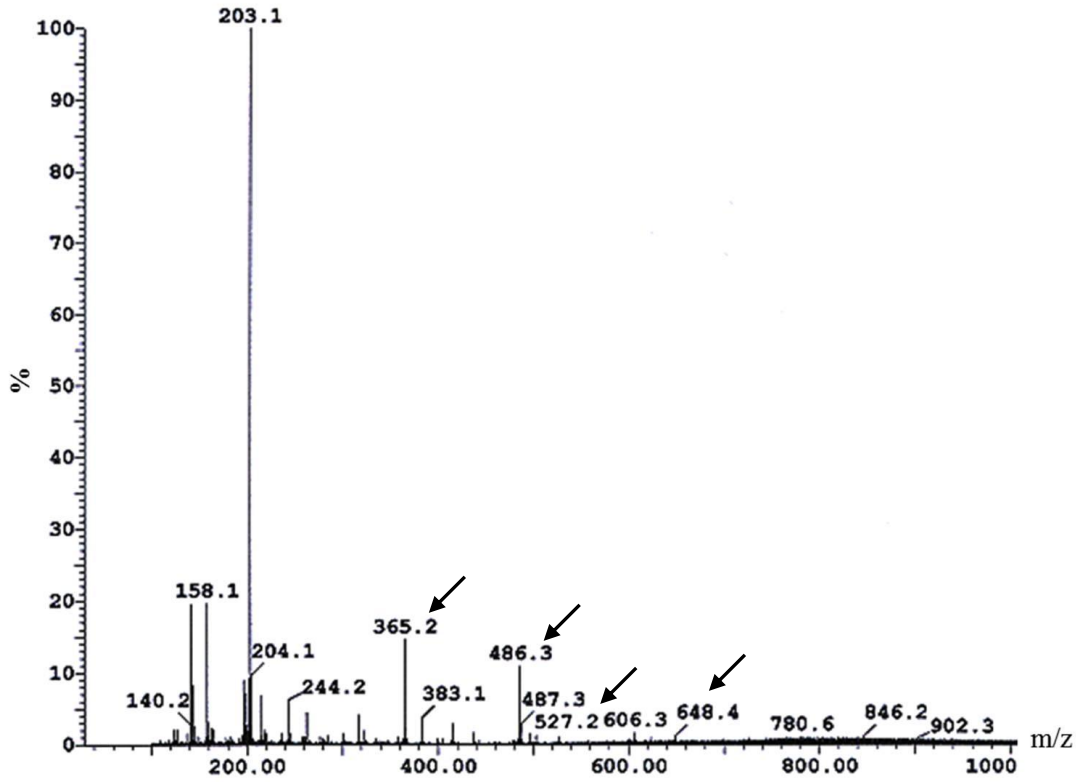

Figure 3.37 ESI-MS analysis of transgalactosylation mixture of recombinant α-galactosidase (0.5 U/mL) with mannose (1 M) as acceptor and *p*NPαGal (0.25 M) as donor at 50 °C for 1 hour

In the case of glucose acceptor ($[M+Na]^+$ at m/z 203), only the *m*/*z* of 365 corresponding to a calculated value of the Na^+ adduct of a disaccharide (GalGlc and Gal_2) was observed by ESI-MS analysis (Figure 3.38). Unlike galactose and mannose acceptors, trisaccharide or *p*NP-trisaccharide formations were not observed in glucose acceptor.

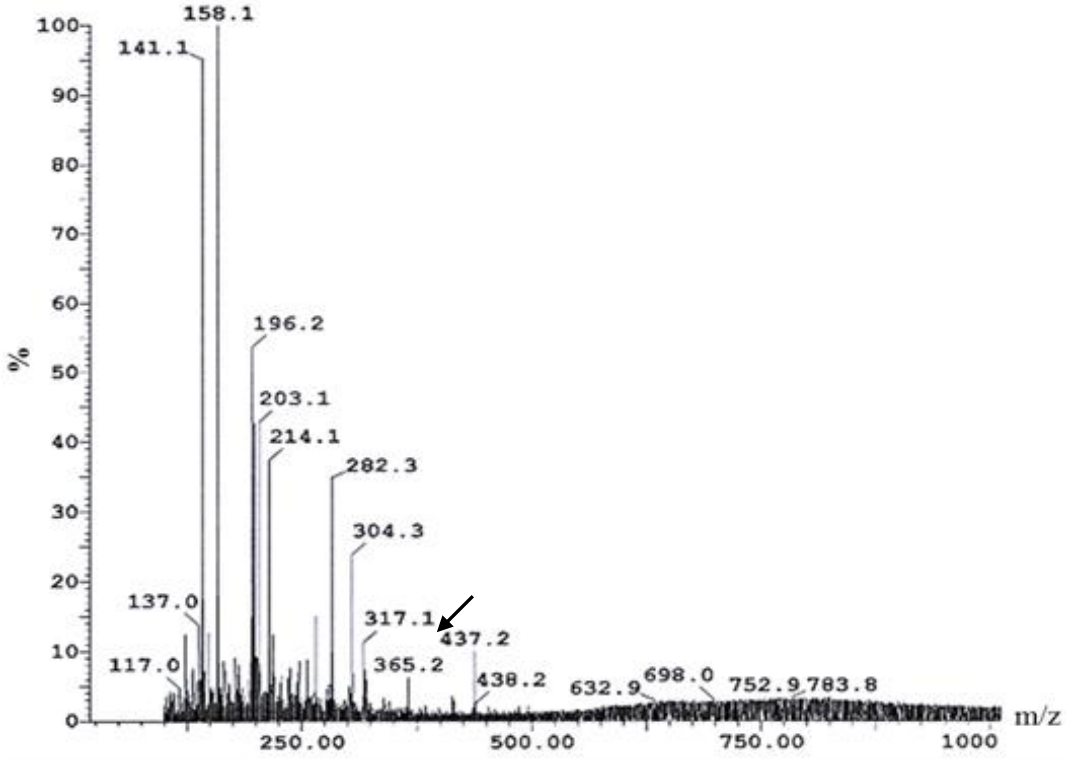

Figure 3.38 ESI-MS analysis of transgalactosylation mixture of recombinant α-galactosidase (0.5 U/mL) with glucose (1 M) as acceptor and *p*NPαGal (0.25 M) as donor at 50 °C for 1 hour

The formation of Gal_2 in the reaction mixtures containing glucose and mannose as acceptor sugars also takes place by the auto condensation reaction of galactose units liberated from *p*NPαGal hydrolysis. These disaccharides could not be differentiated by ESI-MS due to the equal molecular weights of the disaccharides. In addition, *p*NP-α-*D*-disaccharides and *p*NP-trisaccharides produced in the presence of mannose and galactose acceptors could not be differentiated by ESI-MS due to the same reason. On the other hand, the amounts of these products were negligible, as the corresponding spots could not be detected by TLC analysis as shown in Figure 3.34 (Glc^R and Man^R). Excess amounts of acceptors, glucose and mannose, obviously changed the preference of the reaction towards glucose and mannose acceptors than the galactose.

Furthermore, after 1 h reaction, α-galactosidase synthesized trisaccharides from disaccharides ([M+Na]$^+$ at m/z 365), cellobiose, lactose, maltose, and sucrose by the addition of galactose units as shown by TLC analysis (Figure 3.34) and ESI-MS analyses gave m/z signals of 527 corresponding to the calculated molecular masses of the Na$^+$ adduct of galactosyl-cellobiose (Figure 3.39), galactosyl-lactose (Figure 3.40), galactosyl-maltose (Figure 3.41), and galactosyl-sucrose (Figure 3.42).

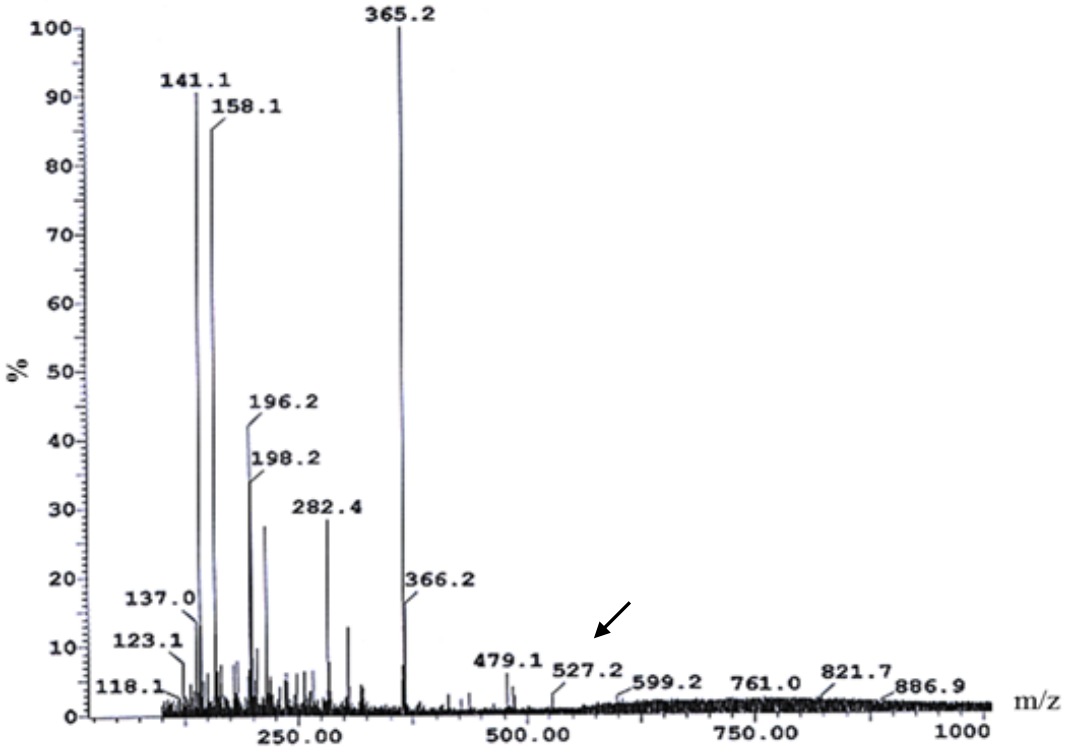

Figure 3.39 ESI-MS analysis of transgalactosylation mixture of recombinant α-galactosidase (0.5 U/mL) with cellobiose (1 M) as acceptor and *p*NPαGal (0.25 M) as donor at 50 °C for 1 hour

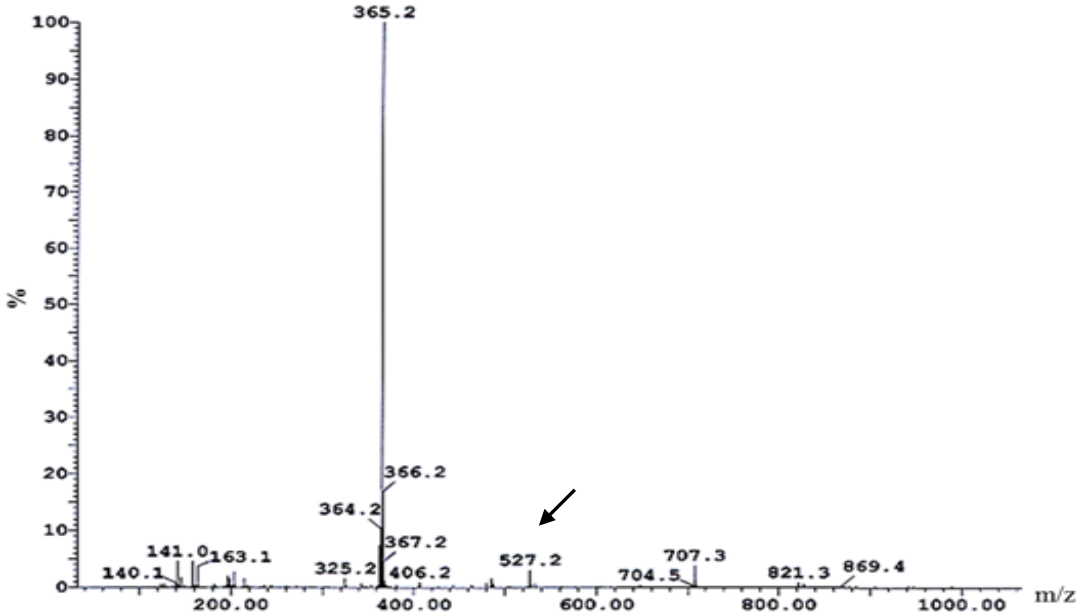

Figure 3.40 ESI-MS analysis of transgalactosylation mixture of recombinant α-galactosidase (0.5 U/mL) with lactose (1 M) as acceptor and *p*NPαGal (0.25 M) as donor at 50 °C for 1 hour

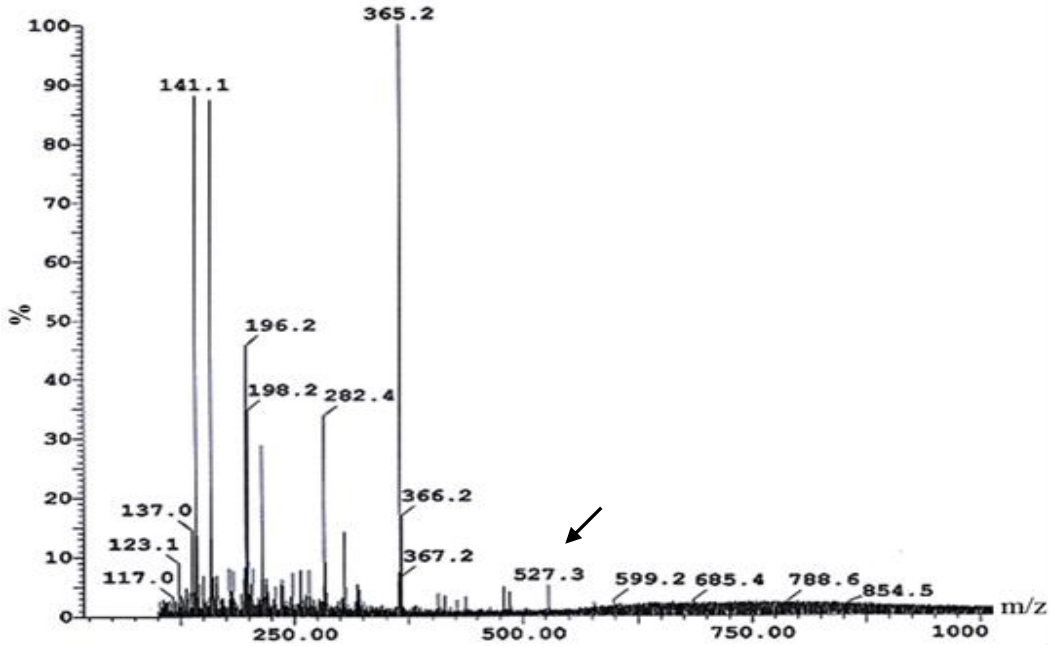

Figure 3.41 ESI-MS analysis of transgalactosylation mixture of recombinant α-galactosidase (0.5 U/mL) with maltose (1 M) as acceptor and *p*NPαGal (0.25 M) as donor at 50 °C for 1 hour

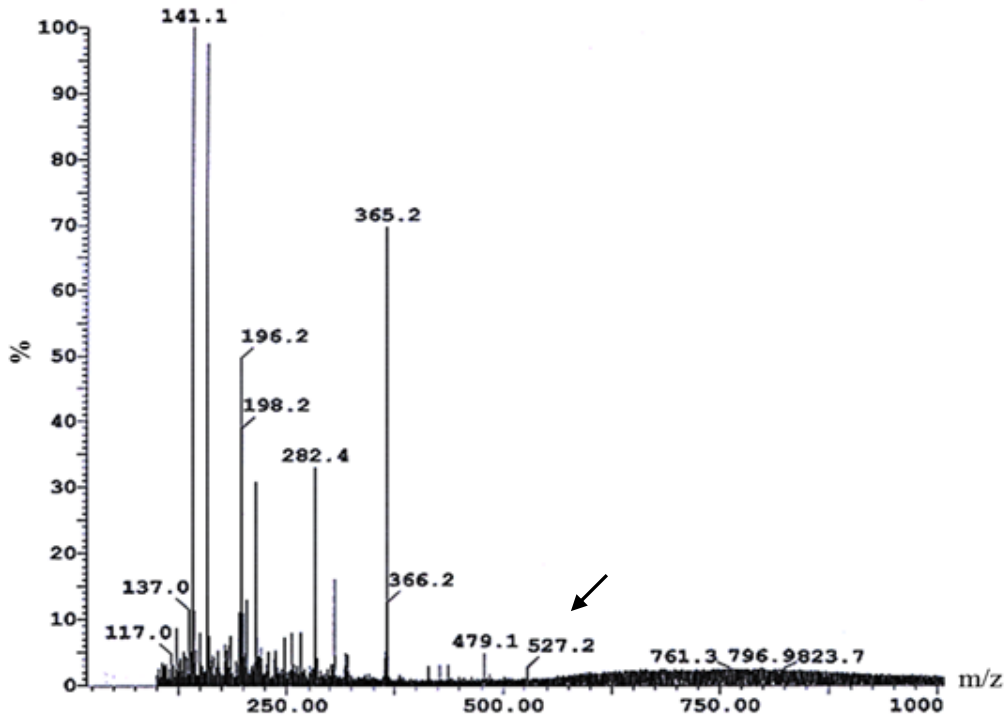

Figure 3.42 ESI-MS analysis of transgalactosylation mixture of recombinant α-galactosidase (0.5 U/mL) with sucrose (1 M) as acceptor and *p*NPαGal (0.25 M) as donor at 50 °C for 1 hour

While the stereoselectivity on synthesis is rigid for either α or β configuration in the anomeric centre, glycosidases generally lack the regioselectivity for the formation of glycosidic bond. Consequently, isolation of the desired regioisomer from the reaction mixtures is difficult. Two principal factors, the source of the enzyme and the types of substrates used, affecting the regioselectivity of glycosidases have been reported previously (Homann and Seibel, 2009; Miyasato and Ajisaka, 2004; Usui *et al*., 1996).

As known from the previous NMR analyses of the transgalactosylated products carried out by Puchart and Biely (2005), α-galactosidase specifically transgalactosylates the oligosaccharide acceptors at primary *C*-6 hydroxymethyl groups. In addition, auto condensation of *p*NPαGal with galactosyl residue was found to take place predominantly at positions *O*-6 and *O*-3.

Apart from being one of the most important groups of prebiotic oligosaccharides, galactooligosaccharides with α-*D*-galactosidic linkages, especially the various positional isomers of α-galactobiose (α-Gal_2), participate in many biological processes, some of which are listed in Table 3.7.

Table 3.7 Linkages and functions of natural α-galactosides in animals (Yamashita *et al*., 2005)

Linkage	Compound	Functions
α-1,6	Raffinose (Gal-Glc-Fru)	- Alleviation of atopic dermatitis (Matsuda *et al*., 1998) - Immunopotenting activity (Kiyonobu *et al*., 1998; Nagura *et al.,* 2002) - Prevention of allergic airway eosinophilia (Watanabe *et al*., 2004) - Sequence in glycosylphosphatidylinositol anchor of *Trypanosoma brucei* (Li *et al.,* 1999)
α-1,4	α-Gal_2	-Prevention of infection of pathogenic *E. coli* (O157 and p-fimbriated) (Ofek and Sharon, 1990; Stromberg *et al*., 1990)
α-1,3	α-Gal_2	- Reduction of transplant rejection (Chen *et al*., 1999) - Inhibitor of toxin A produced by C*lostridium difficile* (enteric pathogen) (Glaser, 1998) - Anti-infection factors against pathogenic organisms in newborn pig and bear (terminal moiety structure of milk oligosaccharides) (Urashima *et al*., 2001)
α-1,2	α-Gal_2	- Sequence in glycosylphosphatidylinositol anchor of *trypanosoma brucei* (Ferguson *et al*., 1988) - Repeating unit of *Streptococcus pneumoniae* type 15 antigen (Wang *et al*., 2002)
α-Galactosylceramide		- Specific ligand of vα14 natural killer T cells (Taniguchi *et al*., 2003)

3.12.2 Quantitative analysis of transgalactosylation products

Quantitative analysis of α-galactooligosaccharide formation was performed by HPLC and the results are given in Table 3.8 and Figures 3.43–3.49. Galactose, glucose, and mannose were found to be efficiently transgalactosylated among the monosaccharides.

After 1-hour reaction at 50 °C, galactose (Figure 3.43) and glucose (Figure 3.44) acceptors were transgalactosylated by α-galactosidase with 46% and 33.4% yields, respectively. As galactose and mannose had the same retention time on chromatogram (Figure 3.45), HPLC could not separate them. However, the yield of transgalactosylation reaction containing mannose acceptor was estimated to be lower than the yield of reaction with galactose acceptor (46%) and higher than the yield of reaction with glucose acceptor (33.4%) based on visual evaluation of TLC chromatograms (Figure 3.34). The trisaccharides detected by ESI-MS analysis of reaction mixtures with galactose (Figure 3.35) and mannose (Figure 3.37) acceptors were not detected and quantified by HPLC.

In the transgalactosylation reaction mixtures containing disaccharides as acceptor, Gal_2 formation was preferred over the trisaccharide formation and cellobiose (Figure 3.46), lactose (Figure 3.47), maltose (Figure 3.48), and sucrose (Figure 3.49), were transgalactosylated with low yields, 1.2, 2.2, 4, and 2.5%, respectively (Table 3.8).

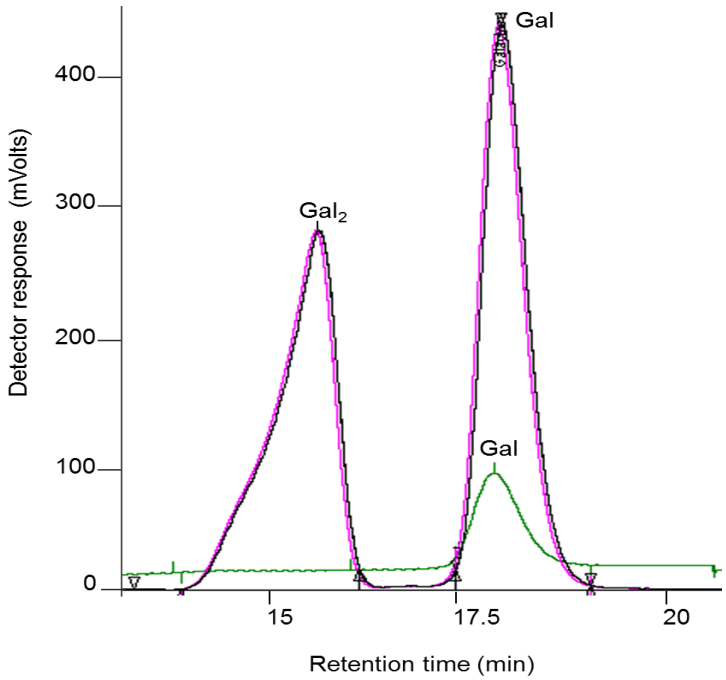

Figure 3.43 HPLC chromatogram of galactose standard against the transgalactosylation reaction mixture of recombinant α-galactosidase (0.5 U/mL) with galactose (1 M) and *p*NPαGal (0.25 M) at 50 °C for 1 hour

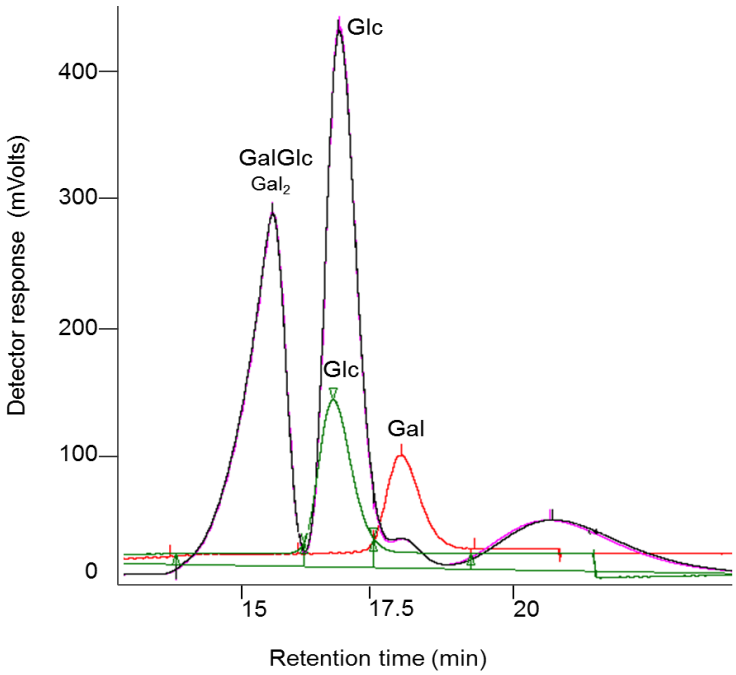

Figure 3.44 HPLC chromatogram of glucose standard against the transgalactosylation reaction mixture of recombinant α-galactosidase (0.5 U/mL) with glucose (1 M) and *p*NPαGal (0.25 M) at 50 °C for 1 hour

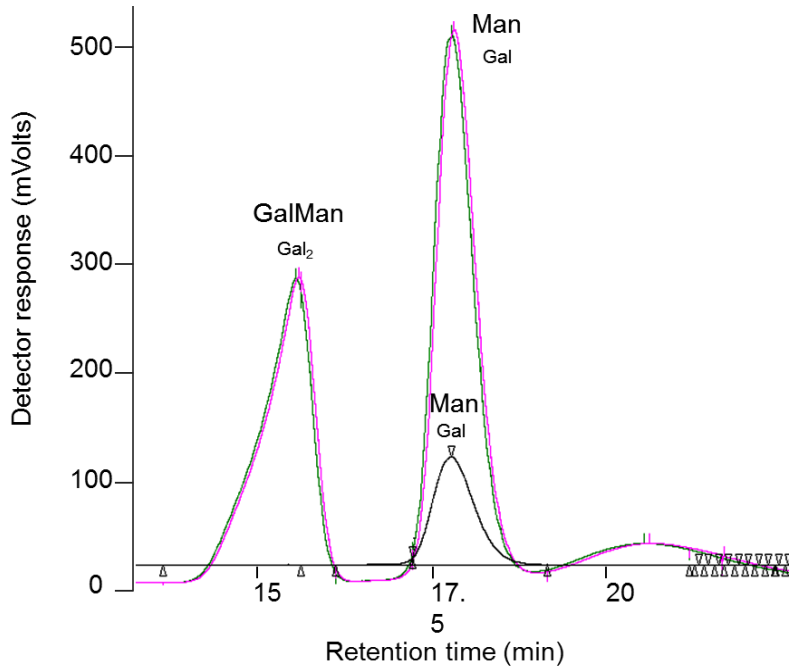

Figure 3.45 HPLC chromatogram of mannose standard against the transgalactosylation reaction mixture of recombinant α-galactosidase (0.5 U/mL) with mannose (1 M) and *p*NPαGal (0.25 M) at 50 °C for 1 hour

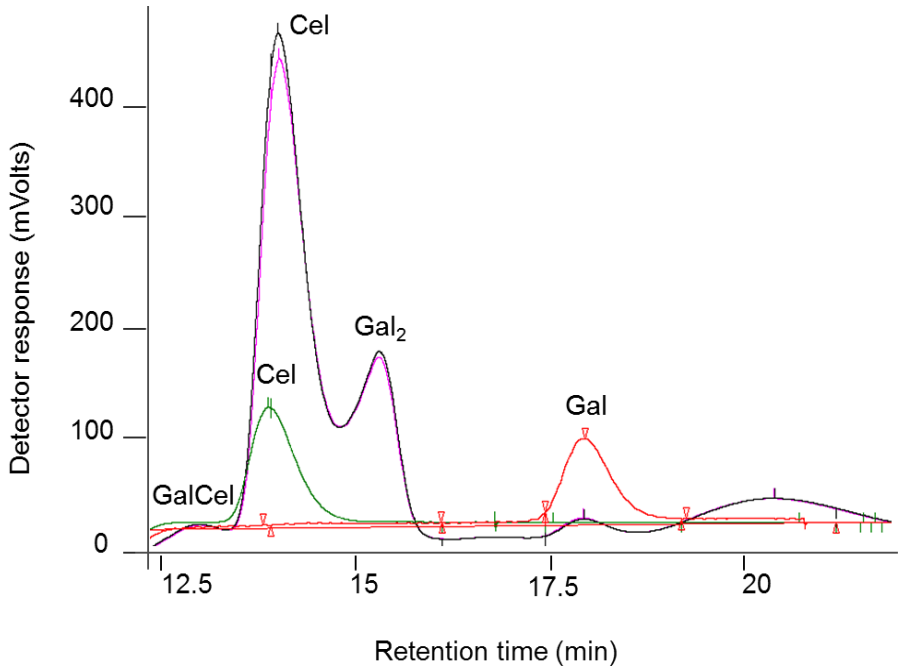

Figure 3.46 HPLC chromatogram of cellobiose standard against the transgalactosylation reaction mixture of recombinant α-galactosidase (0.5 U/mL) with cellobiose (1 M) and *p*NPαGal (0.25 M) at 50 °C for 1 hour

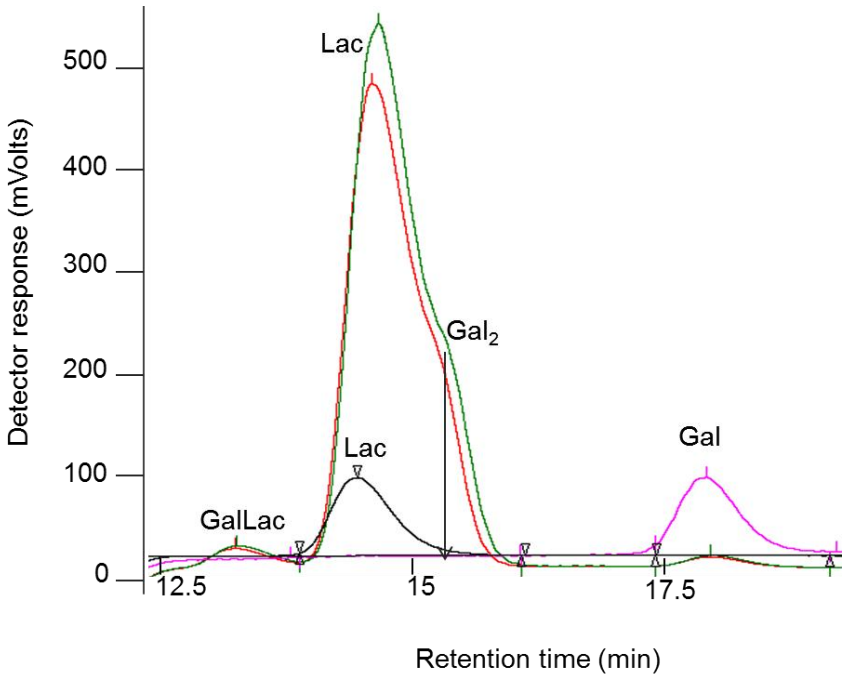

Figure 3.47 HPLC chromatogram of lactose standard against the transgalactosylation reaction mixture of recombinant α-galactosidase (0.5 U/mL) with lactose (1 M) and *p*NPαGal (0.25 M) at 50 °C for 1 hour

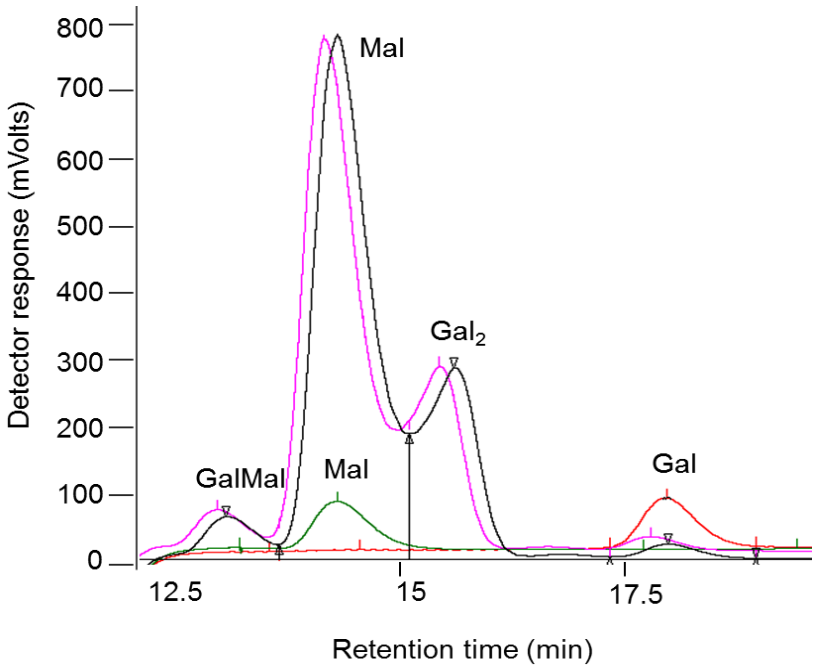

Figure 3.48 HPLC chromatogram of maltose standard against the transgalactosylation reaction mixture of recombinant α-galactosidase (0.5 U/mL) with maltose (1 M) and *p*NPαGal (0.25 M) at 50 °C for 1 hour

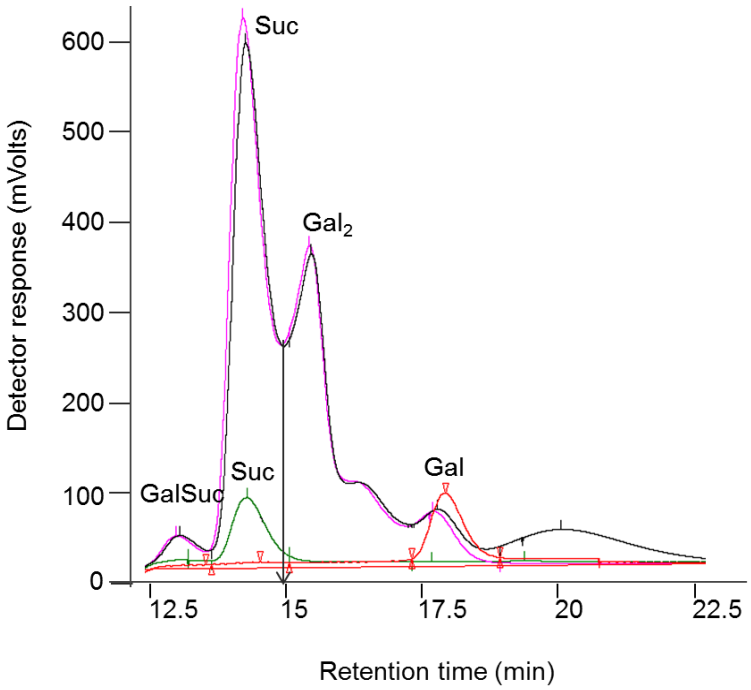

Figure 3.49 HPLC chromatogram of sucrose standard against the transgalactosylation reaction mixture of recombinant α-galactosidase (0.5 U/mL) with sucrose (1 M) and *p*NPαGal (0.25 M) at 50 °C for 1 hour

The monosaccharides, xylose, arabinose, fucose, fructose, and the disaccharide, melibiose did not serve as acceptor for α-galactosidase mediated transgalactosylation. Based on the results, it was concluded that α-galactosidase needs a C-6 hydroxyl group at the non-reducing end of the acceptor substrate for transglycosylation. In the case of melibiose, which is one of the substrate of α-galactosidase hydrolysis, water can compete with melibiose as acceptor molecule and therefore hydrolysis takes place instead of synthesis.

Table 3.8 Yields of galactosylation products analysed by HPLC after 1-hour incubation of 0.5 U/mL recombinant α-galactosidase with 0.25 M *p*NPαGal and 1 M acceptor sugar at 50 °C

Acceptors	**Transgalactosylated product (%)**
Monosaccharides	
Arabinose	n.d.
Fructose	n.d.
Fucose	n.d.
Xylose	n.d.
Galactose	46
Glucose	33.4
Mannose	33.4<x<46
Disaccharides	
Cellobiose	1.2
Lactose	2.2
Maltose	4
Melibiose	n.d.
Sucrose	2.5

n.d.: not detected

The observed yields, especially with the monosaccharides, are quite higher than those obtained by the native α-galactosidase from *A. fumigatus* IMI 385708, where the yields with the same mono- and disaccharide acceptors did not exceeded 1% (Puchart and Biely, 2005). The only exception was with cellobiose acceptor, which resulted in 3.5% transgalactosylation yield by native enzyme. In transgalactosylation reaction mixture of the previous study, Puchart and Biely (2005) used 150 mM donor and 50 mM acceptor sugar in the presence of 5 U/mL α-galactosidase. Although they increased the acceptor concentration to 4 M and prolonged the reaction course from 8

hours to 48 hours, the yields with glucose, galactose, mannose, and disaccharides sucrose, maltose, and lactose acceptors did not exceeded 1%, estimated on the basis of a visual evaluation of TLC chromatograms. On the other hand, high efficiency with β-1.4-linked manno-oligosaccharide galactosyl acceptors (Man_2–Man_6) in α-galactosidase-mediated transgalactosylation were obtained and the galactosylation yield increased up to 35% with the increased polymerization degree of acceptor. The obtained higher yield of transgalactosylation to mannooligosaccharides with higher degree of polymerization was suggested to be due to some kind of a specific recognition of galactomannan main chain (Puchart and Biely, 2005).

Based on these results, α-galactosidase has proved to be a promising, efficient, and inexpensive tool for the synthesis of new galactose-containing oligosaccharides, which participate in many biological processes in addition to its use as prebiotic food ingredient.

CHAPTER 4

CONCLUSIONS

α-Galactosidases have increasingly practical potential in food, feed, and pharmaceutical industries. In addition, *A. fumigatus* 385708 α-galactosidase bears unique transgalactosylation activity and therefore, deserves more attention. *A. fumigatus* is an opportunistic saprophytic fungus and a human pathogen. Therefore, it is not suitable for the purpose of enzyme production.

In this study, *A. fumigatus* α-galactosidase gene, *agl*B, was cloned onto an expression vector, pAN52-4 (Accession Number Z32699) and transformed into a GRAS organism, *A. sojae* ATCC11906. This system allowed high-level heterologous production under the control of strong and constitutive *gpd*A promoter without any requirement of inducing carbon sources.

Cultivation conditions for *A. sojae* expression system were optimized by the use of response surface methodology. The optimum values for the variables were 10.5% molasses (w/v), 1.3% NH_4NO_3 (w/v), and 276 rpm agitation speed. Application of the optimized values of variables yielded *c*.12 fold increase in α-galactosidase production by *A. sojae* expression system.

The use of osmotic signals for improving a heterologous enzyme production was studied in this study. Salt-adapted and non-adapted recombinant *A. sojae* Ta1 genetically engineered to produce α-galactosidase using the constitutive *gpd*A promoter was treated with five different salts at 1 M and 2 M concentrations to improve α-galactosidase production. The growth,

morphology, and heterologous protein production were strongly influenced by osmotic stress. Among the salts applied, higher than 3-fold increase in the enzyme production was achieved on 1 M NaCl by non-adapted cells. In salt-adapted cultures, highest increase with 2.5 fold was also obtained with 1 M NaCl. Addition of salt negatively affected fungal growth in both salt-adapted and non-adapted cells. Gradual adaptation promoted growth on $MgCl_2$ and Na_2SO_4. The results suggested that observed achievements in the productivity might be due to the combinatorial effects of both the use of *gpd*A promoter for the control of heterologous gene expression and the morphological changes occurred in the fungus upon exposure to high osmolarity. Exposure to salt conditions changed the morphology of the fungus from the regular pellet structure to either hairy smaller pellets or filamentous growth form, depending on the salt type and concentration

The recombinant α-galactosidase was purified 18.7 times with 56% overall yield and 64.7 U/ mg protein specific activity. The kinetic parameters, V_{max} (78 ±2 U/mg protein) and K_m (0.45 ±0.04 mM), for the hydrolysis of *p*NPαGal, optimum pH (4.5) and temperature (50−60 °C) values and the effect of different additives on α-galactosidase were determined.

Finally, purified and characterized recombinant α-galactosidase was used for transgalactosylation of various mono- and disaccharides with the donor *p*NPαGal. Significant increases in the galactosylation of acceptors were obtained by the recombinant enzyme. Among the monosaccharides tested, galactose, glucose, and mannose were found to be good acceptors, resulting in disaccharide yields between 33.4–46%. The disaccharides, cellobiose, lactose, maltose, and sucrose were also galactosylated with yield between 1.2-4%.

CHAPTER 5

RECOMMENDATIONS

The pAN52-4 expression system used in this study is rather efficient and allowed us to obtain high heterologous expression of α-galactosidase of *A. fumigatus* in *A. sojae* Ta1 without the use of any inducer. This system can also be used for the expression of different homologous or heterologous proteins of interest.

In stress treatment studies, the decrease in the mycelial growth may be prevented with optimization of the salt concentration. In addition, different stress signals such as oxidative, pH, cold, and heat stresses may be employed to increase the expression.

More detailed studies of osmotic stress regulation and response in fungi may help to develop more stress-tolerant strains for high yield industrial productions. On the other hand, $MgCl_2$ and Na_2SO_4 can be further studied in terms of their antifungal activities for future antifungal drug design.

As an attractive tool, α-galactosidase can be analysed with different acceptor and donor substrates for galactooligosaccharide synthesis and more detailed structural characterization of the transgalactosylation products can be performed.

REFERENCES

Albertyn, J., Hohmann, S., Thevelein, J. M., Prior, B.A., 1994. GPD1, which encodes glycerol-3-phosphate dehydrogenase, is essential for growth under osmotic stress in *Saccharomyces cerevisiae*, and its expression is regulated by the high-osmolarity glycerol response pathway. Molecular and Cellular Biology 14, 4135–4144.

Allen, D.G., Robinson, C.W., 1990. Measurement of rheological properties of filamentous fermentation broth. Chemical Engineering Science 45, 37–48.

Archer, D.B., 2000. Filamentous fungi as microbial cell factories for food use. Current Opinion in Biotechnology 11, 478–483.

Baik, S.H., Saito, K., Yokota, A., Asano, K., Tomita, F., 2000. Molecular cloning and high-level expression in *Escherichia coli* of fungal α-galactosidase from *Absidia corymbifera* IFO8084. Journal of Bioscience and Bioengineering 90, 168–173.

Box, G.E.P., Behnken D.W., 1960. Some new three level design for the study of quantitative variables. Technometrics 2, 455–75.

Box GEP, Hunter W.G. In: Statistics for experimenters. NY: John Wiley and Sons, 1978.

Brookman, J.L., and Denning, D.W., 2000. Molecular genetics in *Aspergillus fumigatus*. Current Opinion in Biotechnology 3, 468–474.

Burstein, C., and Kepes. A., 1971. α-Galactosidase from *Escherichia coli* K12. Biochimica *et* Biophysica ACTA 236, 52–63.

Bulpin, P.V., Gildley, M.J., Jeffcoat, R., Underwood, D.R., 1990. Development of a biotechnological process for the modification of galactomannan polymers with plant α-galactosidase. Carbohydrate Polymers 12, 155–168.

Cao, Y., Wang, Y., Luo, H., Shi, P., Meng, K., Zhou, Z., Zhang, Z., Yao, B., 2009a. Molecular cloning and expression of a novel protease-resistant GH-36 α-galactosidase from *Rhizopus* sp. F78 ACCC 30795. Journal of Microbiology and Biotechnology 19 (11), 1295–1300.

Cao, Y., Wang, Y., Meng, K., Bai, Y., Shi, P., Luo, H., Yang, P., Zhou, Z., Zhang, Z., Yao, B., 2009b. A novel protease-resistant α-galactosidase with high hydrolytic activity from *Gibberella* sp. F75: gene cloning, expression, and enzymatic characterization. Applied Microbiology and Biotechnology 83, 875–855.

Chang, P.K., 2003; Lack of interaction between AFLR and AFLJ contributes to nonaflatoxigenicity of *Aspergillus sojae*. Journal of Biotechnology 107, 245–253.

Chen, X., Andreana, P.R., Wang, P.G., 1999. Carbohydrates in transplantation. Current Opinion in Chemical Biolology 3, 650–658.

Crout, D. H.G., Vic,G., 1998. Glycosidases and glycosyl transferases in glycoside and oligosaccharide synthesis. Current Opinion in Chemical Biol. 2, 96–111.

Cruz, R., Bastistela, J.C., Wosiacki, G., 1981. Microbial α-galactosidase for soybean processing. Journal of Food Science 46, 1196–1200.

De Nadal, E., Zapater, M., Alepuz, P.M., Sumoy, L., Mas, G., Posas, F., 2004. The MAPK Hog1 recruits Rpd3 histone deacetylase to activate osmoresponsive genes. Nature 427, 370–374.

De Vries, R. P., van den Brock, H.C., Dekkers, E., Manzanares, P., de Graff, L.H., Visser, J., 1999. Differential expression of three alpha-galactosidase genes and a single beta-galactosidase gene from *Aspergillus nige*r. Applied and Environmental Microbiology 65, 2453–2460.

De Vries, R.P., Flitter, S.J., van de Vondervoort, P.J., Chaveroche, M.K., Fontaine, T., Fillinger, S., Ruijter, G.J., d'Enfert, C., Visser, J., 2003. Glycerol dehydrogenase, encoded by *gld*B is essential for osmotolerance in *Aspergillus nidulans*. Molecular Microbiology *49*, 131–141.

Denning, D.W., 1998. Invasive aspergillosis. Clinical Infectious Disease 26, 781–805.

Desnick R.J., Ioannou Y.A., Eng C.M., 2001. A-Galactosidase a deficiency: Fabry disease. In: Scriver C.R., Beaudet A.L., Sly W.S., Valle D., Kinzler K.E., Vogelstein B., editors. The metabolic and molecular bases of inherited disease, 8th ed. New York: MaGraw-Hill. 3733–3774.

Dey, P.M., and Pridham, J. B., 1972. Biochemistry of α-galactosidases. Advanced Enzymology 36, 91–130.

Dey, P.M. 1978. Biochemistry of plant galactomannans. Advanced Carbohydrate Chemistry and Biochemistry 35, 341–376.

Dias, F.V., Vincent, F., Pell, G., Prates, J.A.M., Centeno, M.S.J., Tailford, L.E., Ferreira, L.M.A., Fontes, C.M.G.A., Davies, G.J., and Gilbert. H.J., 2004. Insights into the Molecular Determinants of Substrate Specificity in Glycoside Hydrolase Family 5 Revealed by the Crystal Structure and Kinetics of *Cellvibrio mixtus* Mannosidase 5A. The Journal of Biological Chemistry 279, 25517–25526.

Duffaud, G.D., McCutchen, C.M., Leduc, P., Parker, K.N., Kelly, R.M., 1997. Purification and characterization of extremely thermostable beta-mannanase, beta-mannosidase, and alpha-galactosidase from the hyperthermophilic eubacterium *Thermotoga neapolitana* 5068. Applied and . Environmental Microbiology 63, 169–177.

Duran, R., Cary, J.W., Calvo, A.M., 2010. Role of the osmotic stress regulatory pathway in morphogenesis and secondary metabolism in filamentous fungi. Toxins 2, 367–381.

El-Abyad, M.S., Hindorf, H., Rizk, M.A., 1988. Impact of salinity stress on soil-borne fungi of sugarbeet. Plant Soil 110, 27–32.

El-Abyad, M.S., Hamissa, F.A., Gad, A.S., 1992. Treatment of beet molasses for citric acid production by a potent strain of *Aspergillus niger* van *Tieghem*. Bioresource Technology 39, 191–197.

El-Enshasy, H., Kleine, J., Rinas, U., 2006. Agitation effects on morphology and protein productive fractions of filamentous and pelleted growth forms of recombinant *Aspergillus niger*. Process Biochemistry 41, 2103–2112.

Eneyskaya, E.V., Golubev A.M., Kachurin, A.M., Savel'ev, A.N., Neustroev, K.N., 1998. Transglycosylation activity of α-D-galactosidase from *Trichoderma reesei*. An investigation of the active site. Carbohydrate Research 303, 83–91.

Eng C.M., Guffon N., Wilcox W.R., 2001. Safety and efficacy of recombinant human alpha-galactosidase replacement therapy in Fabry's disease. The New England Journal of Medicine 345, 9–16.

Ferguson, M.A.J., Homans, S.W., Dwek, R.A., Rademacher, T.W., 1988. Glycosyl-phosphatidylinositol moiety that anchors *Trypanosoma brucei* variant surface glycoprotein to the membrane. Science, 239, 753–759.

Fiedurek, J., 1998a. Effect of osmotic stress on glucose oxidase production and secretion by *Aspergillus niger*. Journal of Basic Microbiology 38, 107–112.

Fiedurek, J., 1998b. Enhancement of β-galactosidase production and secretion by high osmotic stress in *Penicillium notatum*. Microbiological research 153, 65–69.

Fillinger, S.; Chaveroche, M.K.; van Dijck, P.; de Vries, R.; Ruijter, G.; Thevelein, J., d'Enfert, C., 2001. Trehalose is required for the acquisition of tolerance to a variety of stresses in the filamentous fungus *Aspergillus nidulans*. Microbiology 147, 1851–1862.

Fridjonsson, O., Watzlawıck, H., Gehweıler, A., Rohrhırsch, T., Mattes, R., 1999. Cloning of the gene encoding a novel termostable α-galactosidase from *Thermus brokianus* ITI360. Applied and Environmental Microbiology 65, 3955–3963.

Fujimoto, Z., Kaneko, S., Momma, M., Kobayashi, H., and Mizuno, H., 2003. Crystal structure of rice α-galactosidase complexed with *D*-galactose. Journal of Biological Chemistry 278, 20313–20318.

Gilsenan, J.E.M., Atherton, G., Bartholomew, J., Giles, P.F., Attwood, T.K., Denning, D.W., Bowyer, P., 2009. Aspergillus Genomes and The Aspergillus Cloud. Nucleic Acids Research 37, D509–D514.

Glaser, V., 1998. Carbohydrate-based drugs move closer to market: drugs in clinical pipeline validate glycobiology targets. Genetic Engineering News, 18(8), 1, 12, 32.

Golubev, A.M., Nagem, R.A.P., Brandao Neto, J.R., Neustroev, K.N., Eneyskaya, E.V., Kulminskaya, A.A., Shabalin, K.A., Savel'ev, A.N., Polikarpov, I., 2004. Crystal structure of α-galactosidase from *Trichoderma reesei* and its complex with galactose: Implications for catalytic mechanism. Journal of Molecular Biology 339, 413–422.

Gote, M., Umalkar, H., Khan, I., Khire, J., 2004. Thermostable α-galactosidase from the *Bacillus stearothermophilus* (NCIM 5146) and its application in the removal of flatulence causing factors soymilk. Process Biochemistry 39, 1723–9.

Grimm, L.H., Kelly, S., Krull, R., Hempel, D.C., 2005. Morphology and productivity of filamentous fungi. Applied Microbiology and Biotechnology 69, 375–84.

Guce, A.I., 2010. Structural and mechanistic studies of alpha-galactosidase A and pharmacological chaperones. University of Massachusetts-Amherst.

Gupta, R., Jung, E. and Brunak, S., 2004. Prediction of N-glycosylation sites in human proteins. In preparation.

Haaland, P. D.,1989. Experimental design in biotechnology. New York: Dekker.

Hashimoto, H., Katayama, C., Goto, M., Okinaga, T., Kitahata, S., 1995. Transgalactosylation catalyzed by α-galactosidase from *Candida guilliermondii* H-404. Bioscience, Biotechnology, and Biochemistry 59, 619–623.

Heerikhuisen M., van den Hondel C.A., Punt P.J., van Biezen N., Albers A., Vogel K., 2001. Novel means of transformation of fungi and their use for heterologous protein production. World Patent Application WO01/09352.

Henrissat, B., 1991. A Classification of glycosyl hydrolases based on amino acid sequence similarities. Biochemical Journal 280, 309–316.

Henrissat, B., Bairoch, A., 1993. New families in the classification of glycosyl hydrolases based on amino acid sequence similarities. Biochemical Journal 293, 781–788.

Henrissat, B., Callebaut, I., Fabrega, S., Lehn, P., Mornon, J.P., and Davies, G. 1995. Conserved catalytic machinery and the prediction of a common fold for several families of glycosyl hydrolases. Proceedings of the National Academy of Sciences of the United States of America 92, 7090–7094.

Hohmann, S., 2002. Osmotic stress signaling and osmoadaptation in yeasts. Microbiology and Molecular Biology Reviews 66, 300–372.

Hohmann, S., Krantz, M., Nordlander, B., 2007. Yeast osmoregulation. Methods in Enzymology 428, 29–45.

Homann, A., Seibel, J., 2009. Towards tailor-made oligosaccharides-chemo-enzymatic approaches by enzyme and substrate engineering. Applied Microbiology and Biotechnology 83, 209–216.

Ikram-ul, H., Ali, S., Qadeer, M.A., Iqbal, J., 2004. Citric acid production by selected mutants of *Aspergillus niger* from cane molasses. Bioresource Technology 93, 125–130.

Katrolia, P., Jia, H., Yan, Q., Song, S., Jiang, Z., Xu, H., 2012. Characterization of a protease-resistant α-galactosidase from the thermophilic fungus *Rhizomucor miehei* and its application in removal of raffinose family oligosaccharides. Bioresource Technology 110, 578–86.

Kaur, P., Satyanarayana, T., 2005. Production of cell-bound phytase by *Pichia anomala* in an economical cane molasses medium: Optimization using statistical tools. Process Biochemistry 40, 3095–3102.

Kim, Y., Nandakumar, M.P., Marten, R.M., 2007. Proteome map of *Aspergillus nidulans* during osmoadaptation. Fungal Genetics and Biology 44, 886–895.

Kiyonobu, K., Ohsaki, T., Azuma, A., Osawa, G., Kanda, Y., Kamoi, K., 1998. Effect of an oligosaccharide (raffinose) on immunocytes. Shigaku (in Japanese), 85, 551–558.

Kobayashi, H., Suzuki, H., 1972. Studies on the decomposition of raffinose by alpha-galactosidase of mold. Journal of Fermentation Technology 50, 625–32.

Koshland, D.E., 1953. Stereochemistry and the mechanism of enzymatic reactions. Biological Reviews of the Cambridge Philosophical Society. 28, 416–436.

Kotwal, S.M., Gote, M.M., Sainkar, S.R., Khan, M.I., Khire, J.M., 1998. Production of α-galactosidase by thermophilic fungus Humicola sp. in solid-state fermentation and its application in soyamilk hydrolysis, Process Biochemistry 33, 337–343.

Kren, V., Thiem, J., 1997. Glycosylation employing bio-systems: from enzymes to whole cells. Chemical Society Reviews 26, 463–473.

LaemmLi, U.K., 1970. Cleavage of structural protein during the assembly of the head of bacteriophage T4. Nature 227, 680–685.

Latgé, J. P., 1999. *Aspergillus fumigatus* and aspergillosis. Clinical Microbiology Reviews 12, 310–50.

Lhomme, B., Roux, J.C., 1991. Utilization of experimental designs for optimization of *Rhizopus arrhizus* culture. Bioresource Technology 35(3), 301–312.

Li, J., Robertson, D.E., Short, J. M., Wang, P.G., 1999. Chemical and enzymatic synthesis of glycoconjugates 5: one-pot regioselective synthesis of bioactive galactobiosides using a Clonezyme™ thermophilic glycosidase library. Bioorganic and Medicinal Chemistry Letters 9, 35–38.

Liebl, W., Wagner, B., Schellhase, J., 1998. Properties of an a-galactosidase, and structure of its gene, *gal*A, within an a- and ß-galactoside utilization gene cluster of the hyperthermophilic bacterium *Thermotoga maritima*. Systematic Applied Microbiology 21, 1–11.

Liljeström, P.L., Liljeström P., 1987. Nucleotide sequence of the *melA* gene coding for α-galactosidase in *Escherichia coli* K12. Nucleic Acids Research 15, 2213–2220.

Liljeström-Suominen, P.L., Joutsjoki, V., and Korhola, M., 1988. Construction of a stable α-galactosidase-producing baker's yeast strain Applied and Environmental Microbiology 54(1), 245–249.

Limongi, P., Kjalke, M., Vind, J., Tams, J.W., Johansson, T., Welinder, K.G., 1995. Disulfide bonds and glycosylation in fungal peroxidases. European Journal of Biochemistry 227, 270–276.

Lockington, R.A., Rodbourn, L., Barne tt, S., Carter, C.J., Kelly, J.M., 2002. Regulation by carbon and nitrogen sources of a family of cellulases in *Aspergillus nidulans*. Fungal Genetics and Biology 37, 190–196.

Lotfy, W. A., 2007. The utilization of beet molasses as a novel carbon source for cephalosporin C production by *Acremonium chrysogenum*: Optimization of process parameters through statistical experimental designs. Bioresource Technology 98, 3491–3498.

Lowry, O.H., Rosebrough, N.J. Farr, A.L. and Randall, R.J., 1951. Protein measurement with the Folin-Phenol reagents. The Journal of Biological Chemistry 193, 265–275.

Maras, M., van Die, I. Contreras, R., and van den Hondel, C.A.M.J.J., 1999. Filamentous fungi as production organisms for glycoproteins of biomedical interest. Glycoconjugate Journal 16, 99–107.

Margolles-Clark, E., Tenkanen, M., Luonteri, E., and Penttila, M., 1996. Three α-galactosidase genes of *Trichoderma reesei* cloned by expression in yeast. European Journal of Biochemistry 240, 104–111.

Markham, R., 1992. Stress management: Filamentous fungi as exemplary survivors. FEMS Microbiology Letters 100, 379–386.

Martendal, E., Budziak, D., Carasek, E., 2007. Application of fractional factorial experimental and Box-Behnken designs for optimization of single-drop microextraction of 2,4,6-trichloroanisole and 2,4,6-tribromoanisole from wine samples. Journal of Chromatography A 1148 (2), 131–136.

Martinez, A., Aviles, P., Jimenez, E., Caballero, J., Gargallo-Viola, D., 2000. Activities of sordarins in experimental models of candidiasis, aspergillosis, and pneumocystosis. Antimicrobial Agents Chemotherapy 44, 3389–3394.

Mas, G., de Nadal, E., Dechant, R., Rodriguez de la Concepcion, M.L., Logie, C., Jimeno-Gonzalez, S., Chavez, S., Ammerer, G., Posas, F., 2009. Recruitment of a chromatin remodeling complex by the Hog1 MAP kinase to stress genes. EMBO Journal 28, 326–336.

Matsuda, M., Takeuchi, S., Nagura, T., 1998. Influence of raffinose for atopic dermatitis. Allergy in Practice (in Japanese), 18, 1092–1095.

Matsushima, K., Yashiro, K., Hanya, Y., Abe, K., Yabe, K., Hamasaki, T., 2001. Absence of aflatoxin biosynthesis in koji mold (*Aspergillus sojae*). Applied Microbiology and Biotechnology 55, 771–776.

McCarter, J.D., Withers, S.G., 1994. Mechanisms of enzymatic glycoside hydrolysis. Current Opinion in Structural Biology 4(6), 885–892.

Mi, S., Meng, K., Wang, Y., Bai, Y., Yuan, T., Luo, H., Yao, B., 2007. Molecular cloning and characterization of a novel α-galactosidase gene from *Penicillium* sp. F63 CGMCC 1669 and expression in *Pichia pastoris*. Enzyme and Microbial Technology 40, 1373–1380.

Miskei, M., Karanyi, Z., Pocsi, I., 2009. Annotation of stress-response proteins in the *aspergilli*. Fungal Genetics and Biology 46 (Suppl. 1), 105–120.

Miyasato, M., Ajisaka, K., 2004. Regioreselectivity in beta-galactosidase-catalyzed transglycosylation for the enzymatic assembly of D-galctosyl-D-mannose. Bioscience Biotechnology and Biochemistry 68, 2086–2090.

Murthy M.S.R.C., Swaminathan, T., Rakshit, S.K., Kosugi, Y., 2000. Statistical optimization of lipase catalyzed hydrolysis of methyloleate by response surface methodology. Bioprocess Engineering 22, 35–39.

Nagura, T., Hachimura, S., Hashiguchi, M., Ueda, Y., Kanno, T., Kikuchi, H., Sayama, K., Kaminogawa, S., 2002. Suppressive effect of dietary raffinose on T-helper 2 cell-mediated immunity. British Journal of Nutrition 88, 421–426.

Neustroev, K.N., Krylov, A. S., Abroskina, O.N., Firsov, L. M., Nasonov, V.V., and Khorlin, A.Y., 1991, Isolation and properties of α-galactosidase from Aspergillus awamori. Biochemistry in the U.S.S.R. 56, 288–296.

Nikolaou, E., Agrafioti, I., Stumpf, M., Quinn, J., Stansfield, I. and Brown, A.J.P., 2009. Phylogenetic diversity of stress signalling pathways in fungi. BMC Evolutionary Biology 9, 44.

Norbeck, J., Pahlman, A.K., Akhtar, N., Blomberg, A., Adler, L., 1996. Purification and characterization of two isoenzymes of DL-glycerol-3-phosphatase from Saccharomyces cerevisiae. Identification of the corresponding GPP1 and GPP2 genes and evidence for osmotic regulation of Gpp2p expression by the osmosensing mitogen-activated protein kinase signal transduction pathway. Journal of Biological Chemistry 271, 3875–3881.

Ofek, I., Sharon, N., 1990. Adhesins as lectins: specificity and role in infection. Current Topics in Microbiology and Immunology 151, 91–113.

Olsson, M.L., Hill, C.A., Vega, H., Liu, Q.P., Stroud, M.R., Valdinocci, J., Moon, S., Clausen, H., Kruskall, M.S., 2004. Universal red blood cells-enzymatic conversion of blood group A and B antigens. Transfusion Clinique et Biologique 11, 33–39.

Osborn, H.M.I. (Editor), 2003. Carbohydrates: Best Synthetic Methods. Academic Press pp. 389.

Panchal, T., Wodzinski, R.J., 1998. Comparison of glycosylation patterns of phytase from Aspergillus niger (A. ficuum) NRRL 3135 and recombinant phytase. Preparative Biochemistry and Biotechnology 28, 201–217.

Payne, G.A., Brown, M.P., 1998. Genetics and physiology of aflatoxin biosynthesis. Annual Review of Phytopathology 36, 329–362.

Peberdy, J.F., 1994. Protein secretion in filamentous fungi trying to understand a highly productive black box. Trends in Biotechnology 12, 50–7.

Pitt, J.I., Samson, R.A., Frisvad, J.C., 2000. List of accepted species and their synonyms in the family *Trichocomaceae*. In: Samson RA, Pitt, JI, eds. Integration of modern taxonomic methods for *Penicillium* and *Aspergillus* classification. Amsterdam, Harwood Publishers. 9–49.

Puchart, V., Vrsanska, M., Bhat, M.K., and Biely, P., 2000. Purification and characterization of α-galactosidase from a thermophilic fungus *Thermomyces lanuginosu*s. Biochimica et Biophysica Acta 1524, 27–37.

Puchart, V., Biely. P., 2005. Glycosylation of internal sugar residues of oligosaccharides catalyzed by α-galactosidase from *Aspergillus fumigatus*. Biochimica et Biophysica Acta 1726, 206–216.

Punt, P.J., van Biezen, N., Conesa, A., Albers, A., Mangnus, J., van den Hondel, C., 2002. Filamentous fungi as cell factories for heterologous protein production. Trends in Biotechnology 20(5), 200-206.

Punt, P.J., Dingemanse, M.A., Kuyvenhoven, A., Soede, R.D.M, Pouwels, P.H., van den Hondel C.A.M.J.J., 1990. Functional elements in the promoter region of the *Aspergillus nidulans gpdA* gene coding for glyceraldehyde-3-phosphate dehydrogenase. Gene 93, 101–109.

Punt, P.J., Oliver, R.P., Dingemanse, M.A., Pouweisa, P.H., van den Hondel C.A., 1987. Transformation of *Aspergillus* based on the hygromycin B resistance marker from *Eschericia coli*. Gene 56, 117−124.

Punt, P.J., Zegers, N.D., Busscher, M., Pouwels, P.H., van den Hondel, C.A.M.J. J., 1991. Intracellular and extracellular production of proteins in *Aspergillus* under the control of expression signals of the highly expressed *Aspergillus nidulans gpdA* gene. Journal of Biotechnology 17, 19−34.

Raffaello, T., Kerio, S., Asiegbu, F.O., 2012. Role of the HaHOG1 MAP kinase in response of the conifer root and but rot pathogen (*Heterobasidion annosum*) to osmotic and oxidative stress. PLoS ONE 7(2), e31186. doi:10.1371/journal.pone.0031186.

Ratto, M., Siika-aho, M., Buchert, J., Valkeajarvi, A., Viikari, L., 1993. Enzymatic hydrolysis of isolated and fibre bound galactoglucomannans from pine-wood and pine kraft pulp. Applied Microbiology and Biotechnology 40, 449–454.

Redkar, R.J., Lemke, P.A., Singh, N.K., 1996a. Isolation of differentially expressed cDNA clones from salt-adapted *Aspergillus nidulans*. Current Genetics 29, 130–135.

Redkar, R.J., Lemke, P.A. Singh, N.K., 1996b. Altered gene expression in *Aspergillus nidulans* in response to salt stress. Mycologia 88, 256–263.

Redkar, R.J., Locy, R.D., Singh, N.K., 1995. Biosynthetic pathways of glycerol accumulation under salt stress in *Aspergillus nidulans*. Experimental Mycology 19, 241–246.

Redkar, R.J., Herzog, R.W., Singh, N.K., 1998. Transcriptional activation of the *Aspergillus nidulans gpd*A promoter by osmotic signals. Applied and Environmental Microbiology 64, 2229–2231.

Rezessy-Szabó, J. M., Nguyen Q.D., Hoschke, A., Braet, C., Hajós, G., Claeyssens, M., 2007. A novel thermostable α-galactosidase from the thermophilic fungus *Thermomyces lanuginosus* CBS 395.62/b: Purification and characterization. Biochimica et Biophysica Acta. 1770, 55–62.

Sanada, C.T.N., Karp, S.G., Spier, M.R., Portella, A.C., Gouvêa, P.M., Yamaguishi, C.T., Vandenberghe, L.P.S., Pandey, A., Soccol, C.R., 2009. Utilization of soybean vinasse for α-galactosidase production. Food Research International 42, 476−483.

Schiffmann, R., Kopp J.B., Austin, H.A., 2001. Enzyme replacement therapy in Fabry disease: a randomized controlled trial. Journal of the American Medical Association 285, 2743 –2749.

Sinnott, M.L. 1990. Catalytic mechanisms of enzymatic glycosyl transfer. Chemical Reviews 90, 1171–1202.

Smith, J.M.B., 1989. Opportunistic mycoses of man and other animals. Wallingford, UK. CAB International.

Söyler, B.Ö., 2004. Cloning and characterization of industrially important alpha-galactosidase genes from the human pathogen *Aspergillus fumigatus*. METU, The Graduate School of Natural and Applied Sciences.

Spangenberg, P., Andre C., Dion, M., Rabiller, C., Mattes, R., 2000. Comperative study of new α-galactosidases in transglycosilation reactions. Carbohydrate Research 329, 65–73.

Svastits-Dücsö, L., Nguyen, Q.D., Lefler, D.D., Rezessy-Szabó, J.M., 2009. Effects of galactomannan as carbon source on production of α-galactosidase by *Thermomyces lanuginosus*: Fermentation, purification and partial characterisation. Enzyme and Microbial Technology 45, 367−371.

Stromberg, N., Marklund, B.I., Lund, B., Ilver, D., Hamers, A., Gaastra, W., Karlsson, K.A., Normark, S., 1990. Host-specificity of uropathogenic *Escherichia coli* depends on differences in binding specificity to Galα1-4Gal-containing isoreceptors. EMBO Journal 9, 2001–2010.

Takahashi, T., Chang, P. K., Matsushima, K., Yu, J., Abe, K., Bhatnagar, D., Cleveland, T. E., Koyama, Y., 2002. Nonfunctionality of *Aspergillus sojae aflR* in a strain of *Aspergillus parasiticus* with a disrupted *aflR* gene. Applied and Environmental Microbiology 68, 3737–3743.

Taniguchi, M., Harada, M., Kojo, S., Nakayama, T., Wakao, H., 2003. The regulatory role of Vα14 NKT cells in innate and acquired immune response. Annual Review of Immunology 21, 483–513.

Thomas, C.R., Paul, G.C., 1996. Applications of image analysis in cell technology. Current Opinion in Biotechnology 7, 35–45.

Urashima, T., Saito, T., Nakamura, T., Messer, M., 2001. Oligosaccharides of milk and colostrum in non-human mammals. Glycoconjugate. Journal 18, 357–371.

Usui, T., Morimoto, S., Hayakawa, Y., Kawaguchi, M., Murata, T., Matahira, Y., 1996. Regioselectivity of beta-D-galactosyl-disaccharide formation using the beta-D-galactosidase from *Bacillus circulans*. Carbohydrate Research 285, 29–39.

Wang, C.C., Lee, J.C., Luo, S.Y., Fan, H.F., Pai, C.L., Yang, W.C., Lu, L.D., Hung, S.C., 2002. Synthesis of biologically potent α-1,2-linked disaccharide derivatives via regioselective one-pot protection-glycosylation. Angewandte Chemie International 41, 2360–2362.

Wang, H., Luo, H., Li, J., Bai, Y., Huang, H., Shi, P., Fan, Y., Yao, B., 2010. An alpha-galactosidase from an acidophilic *Bispora* sp. MEY-1 strain acts synergistically with beta-mannanase. Bioresource Technology 101(21), 8376–8382.

Watanabe, H., Sonoyama, K., Watanabe, J., Yamaguchi, N., Kikuchi, H., Nagura, T., Aritsuka, T., Fukumoto, K., Kasai, T., 2004. Reduction of allergic airway eosinophilia by dietary raffinose in Brown Norway rats. British Journal of Nutrition, 92, 247–255.

Watkins, W.M., 1980. Biochemistry and genetics of the ABO, Lewis and P blood group systems. In: Harris H, Hirschhorn K, editors. Advances in human genetics. NewYork: Plenum Press; 1–136.

Watson, A.J., Fuller, L.J., Jeenes, D.J., Archer, D.B., 1999. Homologs of aflatoxin biosynthesis genes and sequence of *aflR* in *Aspergillus oryzae* and *Aspergillus sojae*. Applied and Environmental Microbiology 65, 307–310.

Xu, F., Tao, W., Cheng, L., Guo, L., 2006. Strain improvement and optimization of the media of taxol-producing fungus *Fusarium maire*. Biochemical Engineering Journal 31, 67–73.

Yalçındağ, B., 2002. Alpha-galactosidase gene cloning from *Aspergillus fumigatus*. METU The Graduate School of Natural and Applied Sciences.

Yamashita, A., Hashimoto, H., Fujita, K., Okada, M., Mori, S, Kitahata, S 2005. Reverse Reaction of *Aspergillus niger* APC-9319 α-Galactosidase in a Supersaturated Substrate Solution: Production of α-Linked Galactooligosaccharide (α-GOS). Bioscience Biotechnology and Biochemistry 69 (7), 1381–1388.

Zapater, I.G., Ullah, A.H.J., Wodzinsky, R.J., 1990, Extracellular alpha galactosidase (E.C. 3.2.1.22) from *Aspergillus ficuum* NRRL 3135 purification and characterization. Preparative Biochemistry 20, 263–296.

Zhang, J., Marcin, C., Shifflet, M.A., Salmon, P., Brix, T., Greasham, R., Buokland, B., Chartrain, M., 1996. Development of a defined medium fermentation process for physostigmine production by *Streptomyces griseofuscus*. Applied Microbiology and Biotechnology 44(5), 568−575.

Zhaou, Y., Du, J., Tsao, G.T., 2000. Mycelial pellet formation by *Rhizopus oryzae* ATCC 20344. Applied Biochemistry and Biotechnology 84–86, 779–789.

APPENDIX A

CHEMICALS, ENZYMES, AND THEIR SUPPLIERS

Chemicals/Enzymes	Supplier
β-mercaptoethanol	Merck
Agar	Invitrogen
Agarose	Sigma
Ammonium sulfate	Applichem
Ammonium chloride	Applichem
Ammonium nitrate	Applichem
Ampicillin	Mustafa Nevzat İlaç
ATP (Adenosine-5'-triphosphate)	Fermentas
Biotin	Sigma
Calcium chloride	Merck
Carboxymethyl cellulose, sodium salts	ICN Medical
Casein hydrolysate	Fluka
Chloroform	Merck
Coomassie Brilliant Blue R-250	Merck
Cupric sulfate	Sigma
Dipotassium hydrogen phosphate (K_2HPO_4)	Merck
DNA Ladders	Genemark
dNTP mix	Fermentas
EDTA	Merck
Ethanol	Merk
Ethidium bromide	Sigma
Ferrous Sulfate	Sigma

Chemicals/Enzymes	**Supplier**
Fructose	Merk
Galactose	Sigma
Glacial acetic acid	Merck
Glycerol	Merck
Glucose monohydrate	Merck
Glycine	Merck
Hydrochloric acid	Merck
IPTG	Fermentas
Isopropanol	Merck
Lysing enzymes from *Trichoderma harzianum*	Sigma
Locust bean gum	Sigma
Magnesium sulfate heptahydrate	Merck
Maltose	Merck
Mineral oil	Sigma
Nicotinamide	Sigma
p-nitrophenol	Sigma
*p*NPαGal	Sigma
PageRuler™ Unstained Protein Ladder (#SM0661)	Fermentas
PageRuler™ Prestained Protein Ladder Plus (#SM1811)	Fermentas
Pantothenic acid	Sigma
PEG-6000	Fluka
Peptone from meat pancreatically digest	Merck
Phenol:chloroform:isoamylalcohol	AppliChem
Pfx DNA polymerase	Invitrogen
Potassium Chloride	Merck
Potassium dihydrogen phosphate	Merck
Potato dextrose agar	Merck
Prestained Protein Molecular Weight Marker #SM0441	Fermentas
RNase A	Roche
Restriction enzymes	MBI Fermentas

Chemicals/Enzymes	Supplier
Riboflavin	Fluka
SDS	Merck
Silver nitrate	Merck
Sodium acetate	Merck
Sodium citrate	Merck
Sodium chloride	Merck
Sodium hydroxide	Merck
Sodium nitrate	Applichem
Sodium sulfate	Applichem
Sodium tetraborate	Sigma
Sorbitol	Sigma
Spermidine	Sigma
Sucrose	Merck
T_4 DNA ligase	Roche
Taq DNA polymerase	MBI Fermentas
Tryptone	Merck
Tris	Merck
Triton X-100	Sigma
Tryptone	Difco
Tween 20 and 80	Sigma
Uracil	Sigma
Uridine	Sigma
X-gal (bromo-chloro-indolyl-galactopyranoside)	MBI Fermentas
Yeast extract	Merck

APPENDIX B

PREPARATION OF GROWTH MEDIA, BUFFERS, AND SOLUTIONS

Agarose Gel (0. 8%)

0.8 g agarose is dissolved in 100 mL 1X TAE buffer by heating in microwave.

Ampicillin

Stock solution of 50 mg/mL ampicillin in deionized water is prepared and sterilized through 0.22 µm filter membrane. To prepare a selective medium, after the medium is cooled down to about 50 °C after autoclaving, 1 mL from the ampicillin stock solution is added to 1 L of the medium for a final concentration of 50 µg/mL. The stock solution is stored at −20 °C.

Acetate Buffer (pH 5)

Stock Solutions:
A: 0.2 M solution of sodium acetic acid
B: 0.2 M solution of sodium acetate

14.8 mL of solution A and 35.2 mL of solution B are mixed in 100 mL total volume to adjust the pH 5.

Biotin (0.2 mg/mL)

5 mg biotin is dissolved in 25 mL distilled water. The solution is sterilized by autoclave and stored at 0 °C.

Buffer P1 (Resuspension Buffer)

50 mM Tris-Cl, pH 8.0
10 mM EDTA
100 µg/mL RNase A

Buffer P2 (Lysis Buffer)

200 mM NaOH
1% SDS

Buffer P3 (Neutralization Buffer)

3.0 M potassium acetate, pH 5.5

Buffer QBT (Equilibration Buffer)

750 mM NaCl
50 mM MOPS, pH 7.0
15% isopropanol
0.15% triton X-100

Buffer QC (Wash Buffer)

1.0 M NaCl
50 mM MOPS, pH 7.0
15% isopropanol

Buffer QF (Elution Buffer)

1.25 M NaCl, 50 mM Tris-Cl, pH 8.5, 15% isopropanol

$CaCl_2$ (1 M)

5.55 g of $CaCl_2$ is dissolved in 40 mL distilled water. The volume is adjusted to 50 mL and the solution is sterilized by filtration.

Complete (Transformation) Medium

5.95 g $NaNO_3$ (70 mM)
0.52 g KCl (7 mM)
1.5 g KH_2PO_4 (11 mM)
2 mL, 1 M Mg_2SO_4 (2 mM)
25 mL, 40% glucose (1%)
5 g yeast extract (0.5%)
2 g casamino acids (0.2%)
1 mL 1000 X trace elements (1X))
1 mL 1000 X vitamin complex (1X)
[10 mM uridine and 10 mM uracil are added to the medium for *A. sojae* ATCC11906 (*pyr*G$^-$) cultivation]
20 g agar (for solid medium)

Final volume is adjusted to 1 L with distilled water. The pH is adjusted to 6.5 with KOH. Vitamin complex, $MgSO_4$ and glucose are added after autoclaving and the medium is stored at 4°C. (In solid media, the sterile medium is poured into the petri plates and the plates are stored at 4 °C after solidification).

DNA Extraction Wash Buffer

300 µL Concentrated Wash Buffer (DNA Extraction Kit - Fermentas)
5.7 mL distilled water, 6 mL 95% ethanol

DNA Extraction Binding Solution

125 mL of 6 M sodium iodide solution.

EDTA (0.5 M, pH 8.0)

186.1 g of ethylenedinitrilotetraacetic acid (EDTA) disodium salt dihydrate is added to 800 mL of distilled water. The solution is stirred vigorously on a magnetic stirrer while the pH is adjusted to 8.0 with NaOH pellets and is dispensed into aliquots and then, sterilized by autoclaving.

Glucose (25%)

2.5 g of glucose is dissolved in 8 mL distilled water. The volume is adjusted to 10 mL and the solution is sterilized by filtration.

IPTG (100 mM)

0.24 g of IPTG is dissolved in 10 mL distilled water. The solution is filter sterilized, dispensed into aliquots and stored at 4 °C.

LB (Luria-Bertani) Medium

10 g tryptone
5 g yeast extract
10 g NaCl
20 g agar (for solid medium)

The final volume is adjusted to 1 L with distilled water and the pH is adjusted to 7.0 with NaOH. When required, ampicillin (50 µg/mL) or tetracycline (35 µg/mL) is added to the medium once the medium is cooled down to 55 °C after autoclaving. The medium is stored at 4 °C. (In solid media, the sterile medium is poured into the petri plates and the plates are stored at 4 °C after solidification).

LBG (Induction Medium)

14.3 g yeast extract
2.1 g $(NH_4)_2SO_4$
3.0 g $MgSO_4.7H_2O$
0.3 g $CaCl_2.2H_2O$
0.5 g $FeSO_4.7H_2O$
10.0 g K_2HPO_4
5.0 g LBG

The final volume is adjusted to 1 L with distilled water. The medium is sterilized by autoclaving and stored at 4 °C.

Lysis buffer

40 mM Tris-HCl
10 mM EDTA
0.2 M NaCl
1.5 % SDS

$MgSO_4$ (10 mM)

2.46 g $MgSO_4.7H_2O$ is dissolved in 1 L distilled water and the solution is sterilized by autoclaving.

NaCl (5 M)

292.2 g NaCl is dissolved in 800 mL distilled water. The volume is adjusted to 1 L and the solution is sterilized by autoclaving.

NaAc (3 M)

408.3 g of $NaAC.3H_2O$ is dissolved in 800 mL of distilled water. The pH is adjusted to the desired value with glacial acetic acid and the volume is adjusted to 1 L with distilled water. The solution is dispensed into aliquots and is sterilized by autoclaving.

NaOH (10 N)

40 g of NaOH pellets is added slowly to 80 mL of distilled water. When the pellets are dissolved completely, the volume is adjusted to 1 L with distilled water. The solution is stored at room temperature.

***p*NPαGal Stock Solution (20 mM)**

60.20 mg *p*NPαGal is dissolved in 10 mL distilled water or reaction buffer. The solution is stored at −20 °C. The solution is heated to 30 °C before use.

PEG Buffer (25%, PEG-6000)

25% PEG-6000
0.01 M Tris, pH 7.5
50 mM $CaCl_2$.

Pantothenic Acid (1 mg/mL)

5 mg pantothenic acid is dissolved in 5 mL distilled water. The solution is sterilized by autoclaving and is stored at −20 °C.

Phosphate Buffer (pH 4.5)

13.6 g of monosodium phosphate monohydrate and 0.36 g of disodium phosphate, heptahydrate are dissolved in distilled water. The final volume is adjusted to 1 L.

Saline Tween

0.8% NaCl and 0.005% tween-80 [1:100 dilutions from 0.5% (v/v) tween-80 stock] were mixed. The solution is sterilized by autoclaving.

SDS (10%)

100 g of SDS is dissolved in 900 mL of distilled water. The solution is heated to 68 °C by stirring with a magnetic stirrer to assist dissolution. pH is adjusted to 7.2 by adding a few drops of concentrated HCl. The final volume is adjusted to 1 L with distilled water. The solution is stored at room temperature.

SDS-PAGE Solutions

a. Separating Gel Buffer

18.5 g tris and 0.4 g SDS were dissolved in 80 mL distilled water. The pH is adjusted to 8.9 with concentrated HCl and the final volume is adjusted to 100 mL. The buffer is filtered and is stored at 4 °C.

b. Stacking Gel Buffer

5.1 g tris and 0.4 g SDS were dissolved in 80 mL distilled water. The pH is adjusted to 6.7 with concentrated HCl and the final volume is adjusted to 100 mL. The buffer is filtered and is stored at 4 °C.

c. Ammonium Persulfate (25%)

1 g ammonium persulfate is dissolved in 4 mL distilled water.

d. 10x Running Buffer

30 g tris, 144 g glycine, and 10 g SDS were dissolved in 900 mL distilled water. The pH should be 8.3. The final volume is adjusted to 1 L. The buffer is filtered and is stored at 4 °C.

e. Sample Buffer (4X)

2 mL 20% SDS, 1 mL 1 M tris-HCl (pH 7), 1 mL glycerol, and few grains of bromophenol blue were mixed. The buffer is stored at room temperature. Before use, mercaptoethanol is added such that the final concentration is 20%.

f. Coomassie Brilliant Blue Stain (0.1−0.5 μg/track)

2.5 g Coomassie Brilliant Blue R-250 is dissolved in 450 mL methanol and 70 mL acetic acid is added. The final volume is adjusted to 1 L with distilled water. The stain is stored in dark bottle at room temperature.

g. Destaining Solution

250 mL methanol and 75 mL acetic acid are mixed. The final volume is adjusted to 1 L with distilled water. The solution is stored in dark bottle at room temperature.

h. Silver Staining

Fixer Solution: 150 mL methanol, 36 mL acetic acid, and 150 μL of 37% formaldehyde are mixed. The final volume is adjusted to 300 mL with distilled H_2O.

50% Ethanol: 500 mL ethanol and 500 mL distilled water are mixed.

Pretreatment Solution: 0.02 g sodium thiosulfate ($Na_2S_2O_3.5H_2O$) is dissolved in 100 mL distilled water. 2 mL of pretreatment solution is separated for further use in developing solution preparation.

Silver Nitrate Solution: 0.2 g of silver nitrate is dissolved in 100 mL distilled water and 75 µL of 37% formaldehyde is added.

Developing Solution: 2.25 g of potassium carbonate, 2 mL of previously separated pre-treatment solution, and 75 µL of 37% formaldehyde are mixed. The final volume is adjusted to 100 mL with distilled water.

Stop Solution: 50 mL methanol and 12 mL acetic acid are mixed. The final volume is adjusted to 100 mL with distilled water.

Sodium Tetraborate (1 M)

201.3 g sodium tetraborate ($Na_2B_4O_7$) is dissolved in 1 L distilled water.

Stabilized Minimal Medium Agar

5.95 g $NaNO_3$ (70 mM)
0.52 g KCl (7 mM)
1.5 g KH_2PO_4 (11 mM)
2 mL, 1 M Mg_2SO_4 (2 mM)
25 mL, 40% glucose (1%)
1 mL 1000X trace element solution (1X)
1 mL 1000X vitamin complex (1X)
325.2 g Sucrose (0.95 M)

Final volume is adjusted to 1 L with distilled water. The pH is adjusted to 6.5. 1.2% agar is added. In the case of top agar 0.6% agar is used. Vitamin complex, Mg_2SO_4, and glucose are added after autoclaving.

STC Solution

1.33 M sorbitol, 0.01 M Tris pH 7.5, and 50 mM $CaCl_2$

TAE Buffer (50X)

242 g of tris base is dissolved in 600 mL distilled water. The pH is adjusted to 8.0 with approximately 57 mL glacial acetic acid. Then 100 mL 0.5 M EDTA (pH 8.0) is added and the final volume is adjusted to 1 L with distilled water.

TC Buffer

50 mM $CaCl_2$ and 10 mM tris/HCl, pH 7.5.

TE Buffer

10 mM tris-HCl, pH 8.0 and 1 mM EDTA, pH 8.0.

Tris-HCl Buffer (1 M)

121.1 g tris base is dissolved in 800 mL of distilled water. The pH is adjusted to the desired value with concentrated HCl. The final volume is adjusted to 1 L with distilled water. The buffer is sterilized by autoclaving.

Trace Element Solution (1000X)

76 mM $ZnSO_4$
178 mM H3BO3
25 mM $MnCl_2$
18 mM $FeSO_4$
7.1 mM $CoCl_2$
6.4 mM $CuSO_4$
6.2 mM Na_2MoO_4
174 mM EDTA

Trace elements are dissolved in 80 mL distilled water and the final volume is adjusted to 100 mL. The solution is autoclaved and stored at 4 °C.

TTE Buffer

10 mM Tris-HCl, pH 8.5
10 mM EDTA, pH 8.0
4 mM spermidine
10 mM β-mercaptoethanol
0.5 M sucrose
36 mM KCl
0.25% Triton X-100

Vitamin Complex (1000X)

100 mg/L thiamin
100 mg/L riboflavin
100 mg/L nicotinamide
50 mg/L pyridoxine
10 mg/L pantothenic acid
0.2 mg/L biotin

The final volume is adjusted to 1 L with distilled water. The complex is filter sterilized and stored at 4 °C

YpSs Medium

4 g/L yeast extract
1 g/L K_2HPO_4
0.5 g/L $MgSO_4.7H_2O$
15 g/L soluble starch (20 g/L glucose in modified YpSs broth)
(10 mM uridine and 10 mM uracil are added to the medium for *A. sojae* ATCC11906 (*pyr*G$^-$) cultivation).
20 g/L agar (for solid medium)

The final volume is adjusted to 1 L with distilled water. Glucose is added to the autoclaved modified medium and the medium is stored at 4 °C.

APPENDIX C

PLASMIDS

C.1 pUC 19 Cloning Vector

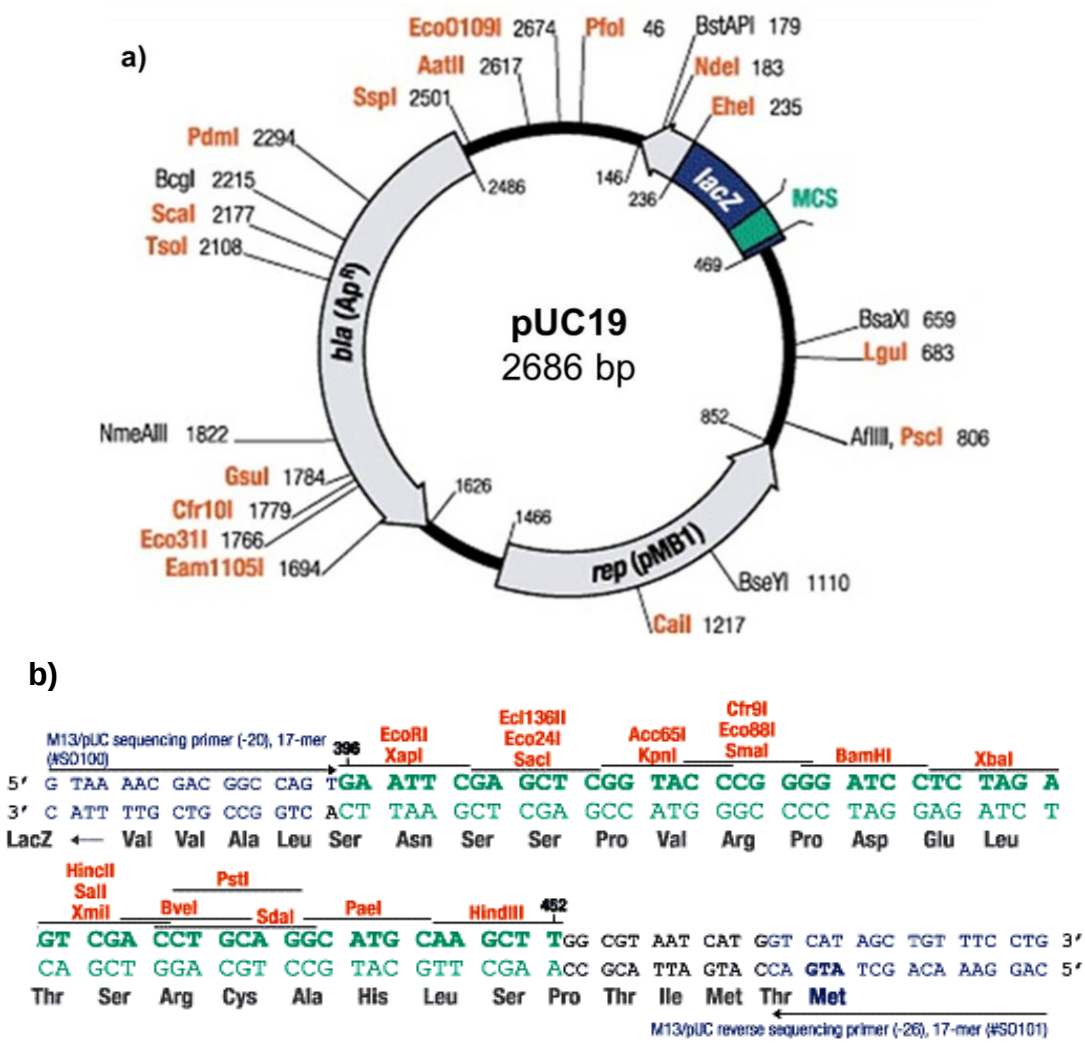

Figure C.1. Cloning vector pUC19; (a) map and (b) multiple cloning site (http://www.fermentas.com)

C.2 pAN52-4 Expression Vector

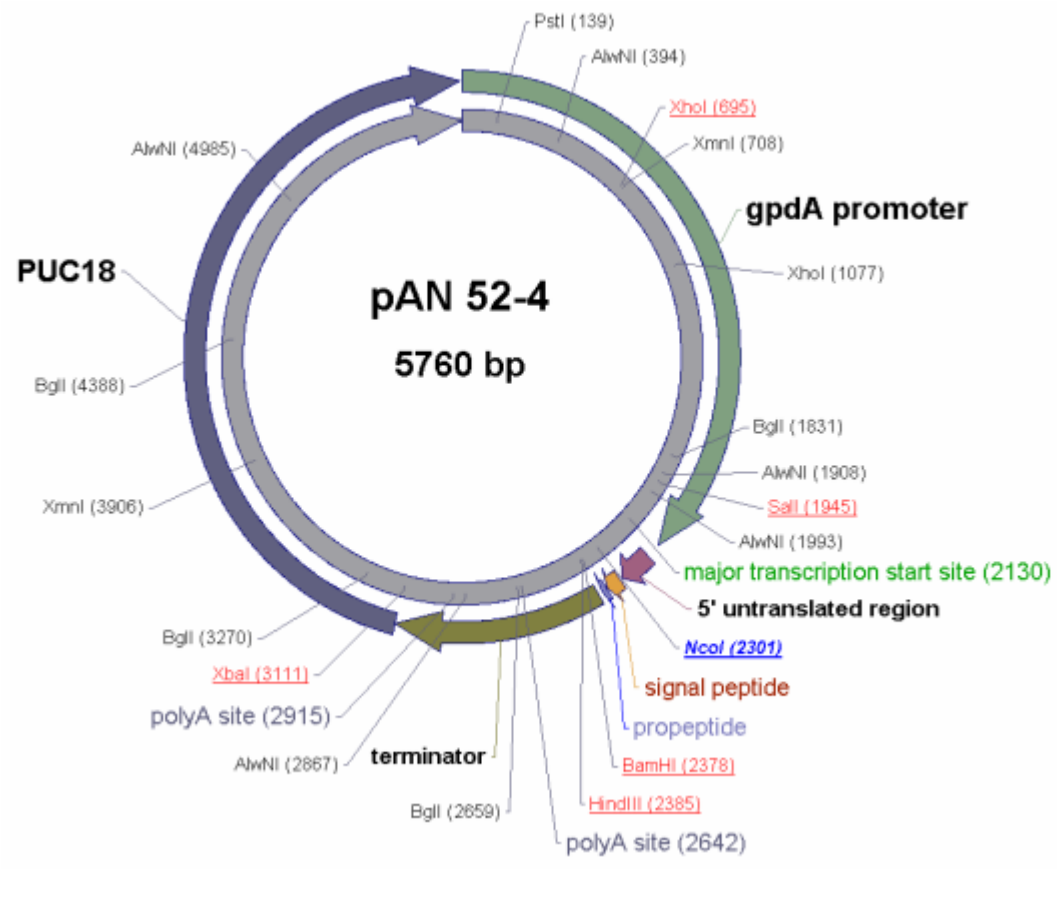

Figure C.2 Map of expression vector pAN52-4 (Acc. No: Z32699). Enzymes with unique restriction sites are shown in red.

APPENDIX D

MARKERS

D.1 DNA MOLECULAR SIZE MARKERS

D.1.1 Lambda DNA/EcoRI + HindIII Marker

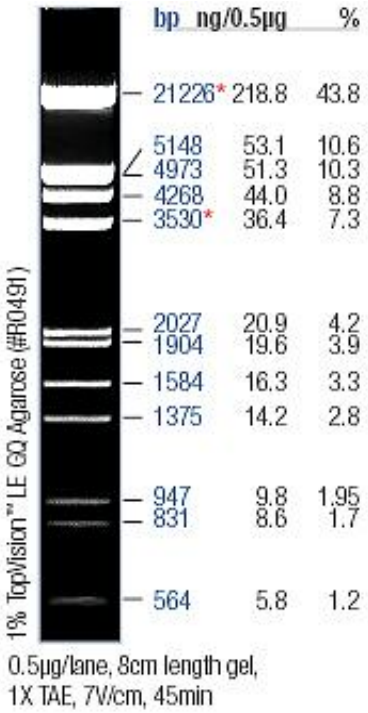

Figure D.1 Lambda DNA/EcoRI + HindIII Marker (www.fermentas.com)

D.2 PROTEIN MOLECULAR WEIGHT MARKERS

D.2.1 PageRuler™ Unstained Protein Ladder

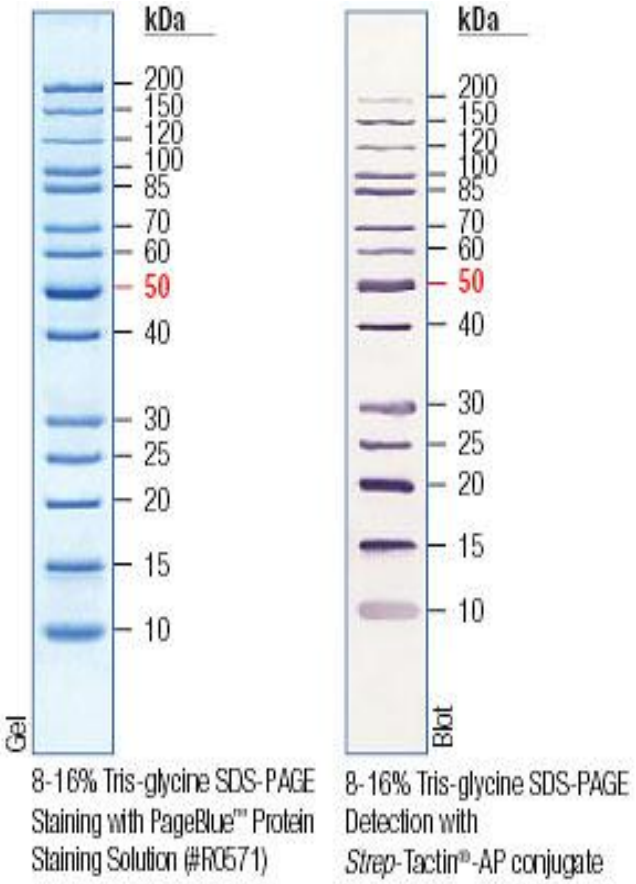

Figure D.2 PageRuler™ unstained protein ladder (www.fermentas.com)

D.2.2 PageRuler™ Prestained Protein Ladder Plus

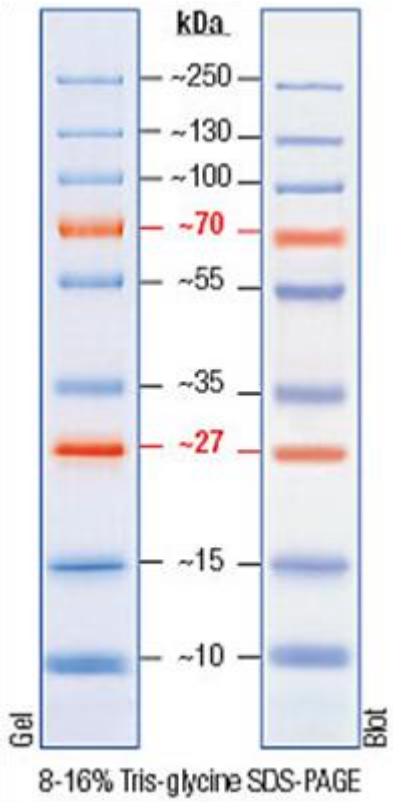

Figure D.3 PageRuler™ Plus prestained protein ladder (www.fermentas.com)

APPENDIX E

SEQUENCES OF THE PRIMERS

Table E.1 Sequences of the primers used for PCR

Name	Sense / Antisense	Sequence of Primer (5′ to 3′)
pB1	Sense	GTATGCAGCCA AGCTTCTCGTCAGACCGGGCAA HindIII cut site
pB2	Antisense	TTCGCGGTACA AGCTTCTAGCACGCTCTCCCAA HindIII cut site
pA1	Sense	CTAGGCCTCCCTGCA GACCAG PstI cut site
pA2	Antisense	CCAACCAA AGCTTTTCATTCC PstI cut site
pV1	Sense	AGGGTTTTCCCAGTCACGAC

*Restriction enzyme cut sites are underlined.

Table E.2 Primers for sequence analysis of pANaglB

Name	Sense / Antisense	Sequence of Primer (5′ to 3′)
F1	Sense	CCACTTCATCGCAGCTTG
R1	Antisense	GGTCCGGGATGATTCGCT
F2	Sense	GAGCTGCCTCATCCAGCT
R2	Antisense	GTCGGGGACGCAGTATGT
F3	Sense	GTCTGATCTCGGCAAGCG
R3	Antisense	TTTCATTGGCGATGGCGG
F4	Sense	GACTGGGGATATCACGCG
R4	Antisense	GGGGTCAAACGTCCAGTC
F5	Sense	GGACCACCTCGCTATCCT
R5	Antisense	GGAGCTGACATCGACACC

APPENDIX F

NUCLEOTIDE AND AMINO ACID SEQUENCE

F.1 Nucleotide sequence of *agl*B cloned into *A. sojae*

GenBank: FJ843023.1

1	ATGACGACGT	TTTTCTCTCT	GACCACTGCA	GCTGCAGTGT
41	TAACCCTCGC	CCGAGGGAGC	AATGCTTTAG	TCAGACCGGG
81	CAATGTGGTA	AGCTGCTTGT	CTCTTCCAAC	ATCTGTATGA
121	GCAGGTCTAA	AACTCGACAG	GGAAAACTAC	CCGCTCTAGG
161	CTGGAACACG	TGGAATGCGT	TCGGCTGCGA	CATTGATGCG
201	ACCAAGATCA	TGACTGCCGC	GAACGAGGTC	GTCAATCTGG
241	GTCTGAAGGA	TCTAGGATAT	GAGTATATCA	ATAGTGAGCT
281	GCCTCATCCA	GCTTCTAGGA	TGTACGTTTG	TTGACGTGAG
321	CAGTCGATGA	TTGCTGGTCT	GTCAAAAGCG	GACGAGACGC
361	GAGCACGCAG	CGAATCATCC	CGGACCCTGA	CAAGTTCCCT
401	GATGGTATCT	CTGGCGTAGC	GGACCAGATA	CATGATCTGG
441	GGCTGAAAAT	TGGAATCTAT	AGCAGTGAGT	CACTGCCGAT
481	GGATAGATAC	AGACGACCAA	GGCGCTGACA	CATGAAGGTG
521	CCGGGCTCAC	GACCTGCGCC	GGGTACCCTG	CCAGTCTGGG
561	ATACGAAGAC	ATCGATGCTC	AGACGTTCGC	GGAATGGGGC
601	ATAGATTGTA	TGTTGTGTGT	TCCCAAGTCT	GATCTCGGCA
641	AGCGACTCGG	CTAACTAACC	CTCAATCAGA	CCTGAAGTAC
681	GACAACTGCG	GCGTCCCCTC	AAACTGGACA	GACACGTACA
721	CATACTGCGT	CCCCGACCCG	GGCAGTAAAG	CCACAAACGG
761	GACCTGTCCC	GATAACAAGA	ATCCCGCGCC	GGCGGGTTAT
781	GACTGGCGCA	CGTCGTTGAC	AGCGGAGCGG	TACAGGCGGA
841	TGCGCGATGC	GTTGGTCAGC	GTCGACCGCA	CAATCCTGTA
881	CTCGCTATGT	GAATGGGGCC	AAGCGAATGT	GAACGACTGG

921	GGCAACGAGA	CAGGCAATTC	CTGGCGAACG	ACTGGGGATA
961	TCACGCGTAA	GATCCAACCT	TGACCTTCAC	GCGTGCCTGT
1001	GCCTAGTAAC	TAACCGATAC	CACCAGCATC	CTGGCCTCGT
1041	ATCGCCGCCA	TCGCCAATGA	AAACTCCTTC	CTGATGAACC
1081	ATGTTGATTT	CTGGGGTTAT	CCGGACCCGG	ACATGCTGGA
1121	GGTCGGCAAC	GGCAATCTCA	CACTAGCAGA	GAACCGAGCG
1161	CACTTTGCGC	TCTGGGCGGC	AATGAAGTCG	CCCTTGATCA
1201	TTGGGACTGC	TGTACGTTTG	TCTCTGTAAT	CGGACTCATC
1241	AGGGCAGTGG	ACATGTATTG	ACGTGGTTGA	CAGCTCGACT
1281	CCATTAGCCA	GGACCACCTC	GCTATCCTCT	CTAACAAGAT
1321	TCTCCTAAAG	TTCCACCAGG	ACCCGGTGAT	CGGCCGTCCT
1361	GCGCAGCCAT	ACAAATGGGG	GTACAATCCT	GACTGGACGT
1401	TTGACCCCGC	TCATCCCGCA	GAGTACTGGT	CCGGCGCATC
1441	GTCAGTGCTG	GGTGGCACGC	TGGTGCTGAT	GCTGAATTCG
1481	GAAGATACGA	CGCAGAGGCG	AACGGCTGTG	TGGAAGGAGG
1521	TCCCTGAGCT	GAAAGATGTG	CTCGGTAGAC	AGGGAAAACG
1561	GCGCATTGGA	TTTCGTGTGA	CGGATGTGTG	GACCGGGAAG
1601	GATCTGGGTT	GCGTGAGAGA	TCATTACAGT	GTGGAATTAG
1641	AGAGTCATGA	TGTGGCCGCG	TTAGTTGTTG	GGAGAGCGTG
1681	G			

F.2 Amino acid sequence of α-galactosidase cloned İnto *A. sojae*

Protein ID: ACO72591.1

MTTFFSLTTAAAVLTLARGSNALVRPGNVGKLPALGWNTWNAFGCDIDAT
KIMTAANEVVNLGLKDLGYEYINIDDCWSVKSGRDASTQRIIPDPDKFPDGI
SGVADQIHDLGLKIGIYSSAGLTTCAGYPASLGYEDIDAQTFAEWGIDYLKY
DNCGVPSNWTDTYTYCVPDPGSKATNGTCPDNKNPAPAGYDWRTSLTA
ERYRRMRDALVSVDRTILYSLCEWGQANVNDWGNETGNSWRTTGDITPS
WPRIAAIANENSFLMNHVDFWGYPDPDMLEVGNGNLTLAENRAHFALWA
AMKSPLIIGTALDSISQDHLAILSNKILLKFHQDPVIGRPAQPYKWGYNPDW
TFDPAHPAEYWSGASSVLGGTLVLMLNSEDTTQRRTAVWKEVPELKDVL
GRQGKRRIGFRVTDVWTGKDLGCVRDHYSVELESHDVAALVVGRAC

F.3 Amino acid sequence of α-galactosidase of *A. fumigatus* Af293

Protein ID: XP_748129.1

MSRSKTRQGKLPALGWNTWNAFGCDIDATKIMTAANEVVNLGLKDLGYE
YINIDDCWSVKSGRDASTQRIIPDPDKFPDGISGVADQIHDLGLKIGIYSSA
GLTTCAGYPASLGYEDIDAQTFAEWGIDYLKYDNCGVPSNWTDTYTYCVP
DPGSKATNGTCPDNKNPAPAGYDWRTSLTAERYRRMRDALVSVDRTILY
SLCEWGQANVNDWGNETGNSWRTTGDITPSWPRIAAIANENSFLMNHVD
FWGYPDPDMLEVGNGNLTLAENRAHFALWAAMKSPLIIGTALDSISQDHL
AILSNKILLKFHQDPVIGRPAQPYKWGYNPDWTFDPAHPAEYWSGASSVL
GGTLVLMLNSEDTTQRRTAVWKEVPELKDVLGRQGKRRIGFRVTDVWTG
KDLGCVRDHYSVELESHDVAALVVGRAC

F.4 Sequence alignments of protein ACO72591.1 vs. XP_748129.1

Program: Clustal 2.1 Multible Sequence Alignment

Score = 867 bits (2240)

Method: Compositional matrix adjust.

Identities = 418/418 (100%)

Positives = 418/418 (100%)

Gaps = 0/418 (0%)

```
XP_74748129  ---------------MSRSK---TRQG---KLPALGWNTWNAFGCDIDATKIMTAANEVV 39
ACO72591.1   MTTFFSLTTAAAVLTLARGSNALVRPGNVGKLPALGWNTWNAFGCDIDATKIMTAANEVV 60
                              ::*..   .* *   ******************************

XP_74748129  NLGLKDLGYEYINIDDCWSVKSGRDASTQRIIPDPDKFPDGISGVADQIHDLGLKIGIYS 99
ACO72591.1   NLGLKDLGYEYINIDDCWSVKSGRDASTQRIIPDPDKFPDGISGVADQIHDLGLKIGIYS 120
             ************************************************************

XP_74748129  SAGLTTCAGYPASLGYEDIDAQTFAEWGIDYLKYDNCGVPSNWTDTYTYCVPDPGSKATN 159
ACO72591.1   SAGLTTCAGYPASLGYEDIDAQTFAEWGIDYLKYDNCGVPSNWTDTYTYCVPDPGSKATN 180
             ************************************************************

XP_74748129  GTCPDNKNPAPAGYDWRTSLTAERYRRMRDALVSVDRTILYSLCEWGQANVNDWGNETGN 219
ACO72591.1   GTCPDNKNPAPAGYDWRTSLTAERYRRMRDALVSVDRTILYSLCEWGQANVNDWGNETGN 240
             ************************************************************

XP_74748129. SWRTTGDITPSWPRIAAIANENSFLMNHVDFWGYPDPDMLEVGNGNLTLAENRAHFALWA 279
ACO72591.1   SWRTTGDITPSWPRIAAIANENSFLMNHVDFWGYPDPDMLEVGNGNLTLAENRAHFALWA 300
             ************************************************************

XP_74748129. AMKSPLIIGTALDSISQDHLAILSNKILLKFHQDPVIGRPAQPYKWGYNPDWTFDPAHPA 339
ACO72591.1   AMKSPLIIGTALDSISQDHLAILSNKILLKFHQDPVIGRPAQPYKWGYNPDWTFDPAHPA 360
             ************************************************************

XP_74748129. EYWSGASSVLGGTLVLMLNSEDTTQRRTAVWKEVPELKDVLGRQGKRRIGFRVTDVWTGK 399
ACO72591.1   EYWSGASSVLGGTLVLMLNSEDTTQRRTAVWKEVPELKDVLGRQGKRRIGFRVTDVWTGK 420
             ************************************************************

XP_74748129. DLGCVRDHYSVELESHDVAALVVGRAC 426
ACO72591.1   DLGCVRDHYSVELESHDVAALVVGRAC 447
             ***************************
```

APPENDIX G

p-NITROPHENOL STANDARD CURVE

A series of *p*-nitrophenol dilutions is prepared according to those given in table (tubes 1-8). The stock *p*-nitrophenol (*p*-NP) was 10 mM, the sodium phosphate buffer, pH 4.5 was 100 mM, and the sodium tetraborate was 200 mM.

Table G.1 Preparation of *p*-nitrophenol standard curve

Tube no	*p*-NP (µmol/mL)	*p*-NP (µL)	H_2O (µL)	Buffer (µL)	Sodium tetraborate (mL)	OD_{410} 2x Dilution
1	0	0	500	500	3.5	0
2	0.0223	10	490	500	3.5	0.32
3	0.0445	20	480	500	3.5	0.39
4	0.0667	30	470	500	3.5	0.51
5	0.0889	40	460	500	3.5	0.81
6	0.1112	50	450	500	3.5	0.95
7	0.1667	75	425	500	3.5	1.39
8	0.223	100	400	500	3.5	1.82

The absorbance of the prepared tubes was measured at 410 nm.

Table G.2 Measurements of *p*-nitrophenol absorbance

Tube No	*p*-nitrophenol (µmol/mL)	absorbance (410 nm) 2x Dilution
1	0	0
2	0.0223	0.32
3	0.0445	0.39
4	0.0667	0.512
5	0.0889	0.81
6	0.1112	0.95
7	0.1667	1.39
8	0.223	1.819

The standard curve is prepared by plotting the absorbance at 410 nm against µmoles of *p*-nitrophenol.

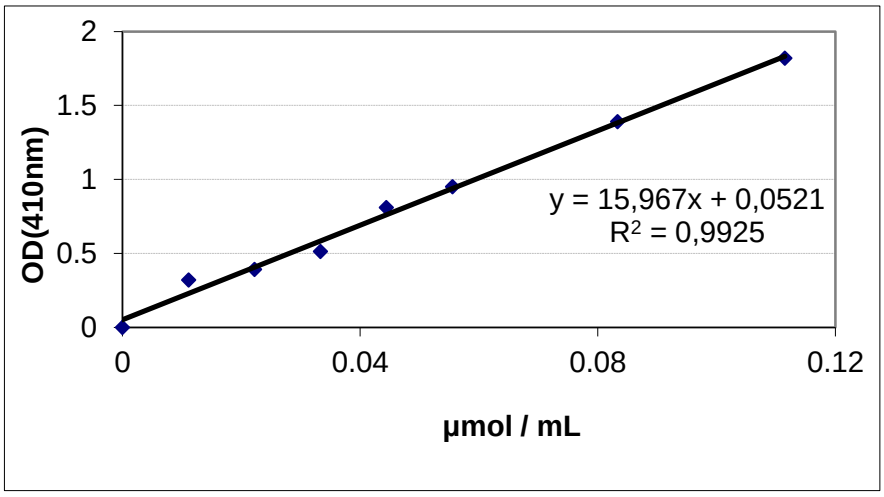

Figure G.1 Standard curve of *p*-nitrophenol. The equation y=15.967x + 0.0521 and the R^2= 0.9925 were obtained.

This standard curve was used for the enzyme activity measurements.

APPENDIX H

COLUMN CHARACTERISTICS

H.1 CHARACTERISTICS of HiPrep™ 16/10 Q XL COLUMN

• Matrix	6% highly cross-linked spherical agarose
• Mean particle size	90 µm
• Bed volume- height	20 mL - 100 mm
• i.d.	16 mm
• Column composition	Polypropylene
• Recommended flow rate	2–10 mL/min, (30–300 cm/h)
• Maximum flow rate	10 mL/min, (300 cm/h)
• Maximum pressure over the packed bed during operation	0.15 MPa, 1.5 bar, 22 psi
• HiPrep column hardware pressure limit	0.5 MPa, 5 bar, 73 psi
• Storage	4 to 30 °C in 20% ethanol
• Type of exchanger	strong anion
• Charged group	$-N^{+}(CH_3)_3$
• pH working range	
- Short term	2–14
- Working and Long term	2–12
• Total ionic capacity	0.18–0.26 (mmol Cl^{-}/mL medium)
• Dynamic binding capacity (mg/mL medium)	
BSA (M_r 67 000)	> 130

H.2 CHARACTERISTICS of HiPrep™ 26/10 DESALTING COLUMN

• Matrix	Sephadex G-25 Fine, cross-linked dextran
• Bed volume	53 mL
• Bed dimensions, i.d × h	2.6 × 10 cm
• Void volume	15 mL
• Recommended sample volume	≤ 15 mL
• Sample dilution	1.2–3 fold
• Exclusion limit	M_r 5 000, globular proteins
• Mean particle size	90 µm
• Recommended flow rate	9–31 mL/min
• Maximum flow rate	40 mL/min
• Maximum pressure over the packed bed	0.15 MPa, 1.5 bar
• Maximum pressure over column hardware	0.5 MPa, 5 bar
• Chemical stability	All commonly used buffers
• pH stability	2–13 (short and long term)
• Avoid	Oxidizing agents
• Storage	20% ethanol

APPENDIX I

LOWRY PROTEIN DETERMINATION

SOLUTIONS

Solution A: 2% Na_2CO_3 in 0.1 N NaOH

Solution B: 1% NaK Tartrate in H_2O

Solution C: 0.5% $CuSO_4.5\ H_2O$ in H_2O

Solution D: 48 mL of solution A, 1 mL of solution B, and 1 mL of solution C

Solution E (Phenol Reagent): 1 part Folin-Phenol [2N]:1 part water

BSA Standard: 1 mg BSA in 1 mL of water

PROCEDURE

1. Eleven sets of three 16 x 150 mm test tubes were set up in a rack.
2. 0, 10, 20, 30, 40, 50, 60, 70, 80, 90, 100 µL of BSA was added to these tubes.
3. 2 mL of solution D was added to each test tube.
4. Tubes were incubated at room temperature for 10 minutes.
5. 0.2 mL of dilute folin-phenol solution was added to each tube.
6. Each tube was vortexed immediately.
7. Tubes were incubated at room temperature for 30 minutes.
8. Absorbance of each sample was determined at 600 nm.
9. Absorbance was plotted against the mg protein to obtain standard curve.
10. Triplicate assays for all determinations and the unknowns were set up.

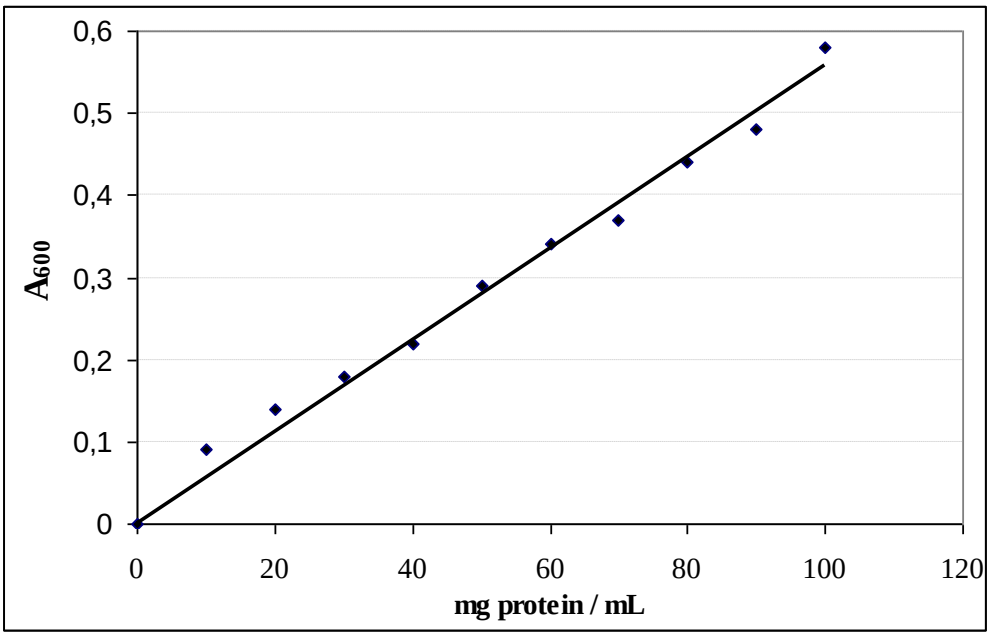

Figure I.1 BSA standard curve used in Lowry Method for the determination of total protein concentration after the purification of recombinant α-galactosidase

For each protein determination, a new BSA standard curve was plotted and the protein concentrations of the samples were calculated according to that BSA standard curve.

CURRICULUM VITAE

Surname, Name:	Gürkök, Sümeyra
Nationality:	Turkish
Date of Birth:	06.01.1981
Place of Birth:	Ankara
Marital Status:	Single
Telephone:	+90 312 2105791
Fax:	+903122102767
e-mail:	sumeyra@metu.edu.tr, sumeyrag@gmail.com
Address:	METU, Food Engineering Department, Office: AZ-24, Lab: Genetics Laboratory AZ-19 06800, Ankara, TURKEY

EDUCATION

2003−Present:	Middle East Technical University, Ankara/Turkey PhD in Department of Biotechnology
2002−2003:	Middle East Technical University, Ankara/Turkey English Preparatory Program
1998−2002:	Ankara University, Ankara/Turkey BSc in Department of Biology (Branch of Molecular Biology and Biotechnology)
1994−1997:	Rauf Denktaş High School, Ankara

PROFESSIONAL EXPERIENCES

2009−2010 (1 year) Visiting Scientist, Manchester Interdisciplinary Biocentre, The University of Manchester, UK

2002 to 2011 Research Assistant, Department of Biotechnology, METU, TURKEY

- Teaching Assistant in Department of Biology
  - Course Bio352 General and Molecular Genetics Lab.
- Teaching Assistant in Department of Biotechnology
  - Course Btec503 Fundamentals of Biotechnology
- Teaching Assistant in Department of Food Engineering
  - Course FDE305 Food Microbiology Lab.
  - Course FDE310 Food Materials Lab.

2001 (2 months) Summer Practice, Ankara Numune Hastanesi (Hospital), TURKEY

- Microbiology
- Biochemistry
- Serology

CONFERENCES AND SYMPOSIUMS

International Symposium on Biotechnology: Developments and Trends September 27−29, 2009, Middle East Technical University. Ankara-Turkey

3rd Congress of European Microbiologists (FEMS 2009) on the theme, "Microbes and Man - interdependence and future challenges" June 28−July 2, 2009 Gothenburg-Sweden.

International Enzyme Engineering Symposium (IEES) October 1−5, 2008 Kusadasi- Turkey.

XII. International Congress of Bacteriology and Applied Microbiology International Union of Microbial Society (IUMS) August 5−9, 2008, Istanbul-Turkey.

XII. International Congress of Mycology August 5−9, 2008, Istanbul-Turkey

X. Turkish Food Congress May 21−23, 2008, Erzurum-Turkey.

Turkish Ar-Ge Conference, April 28−29, 2008, Ankara-Turkey .

XV. Biotechnology Conference, October 28−31, 2007, Antalya- Turkey.

3rd European Federation of Biotechnology Conference on Physiology of Yeasts and Filamentous Fungi (PYFF3), June 13−16, 2007, Helsinki-Finland.

International Symposium of Microbial Stress and Adaptation, April 12−14, 2007, Marburg, Germany.

XIV. Biotechnology Conference, August 31−September 2, 2005, Eskisehir-Turkey.

PUBLICATIONS AND GRANTS

Gurkok, S., Cekmecelioglu, D., Ogel, Z.B., 2011. Optimization of culture conditions for *Aspergillus sojae* expressing an *Aspergillus fumigatus* α-galactosidase. Bioresource Technology 102, 4925–4929.

Gurkok, S., Soyler, B., Biely, P., Ogel, Z.B., 2010. Cloning and heterologous expression of the extracellular alpha-galactosidase from *Aspergillus fumigatus* in *Aspergillus sojae* under the control of *gpd*A promoter. Journal Molecular Catalysis B: Enzymatic 64, 146–149.

Gürkök S., Özdemir B., Biely P., Ögel Z. B., 2009. Cloning, expression, purification and characterization of *Aspergillus fumigatus* α-galactosidase and optimization of the culture conditions. International Symposium on Biotechnology: Developments and Trends, Ankara-Turkey (Poster presentation).

Gurkok S., Soyler B., Ogel B.Z., 2009. Optimization of culture conditions for heterologous expression of alpha-galactosidase from *Aspergillus fumigatus* in *Aspergillus sojae*. 3rd Congress of European Microbiologists (FEMS 2009) on the theme, "Microbes and Man-interdependence and future challenges", ***Gothenburg-Sweden*** (Poster presentation).

Gurkok S., Ozdemir B., Ögel Z.B., 2008. Heterologous expression of alpha-galactosidase from *Aspergillus fumigatus* in *Aspergillus sojae*, the influence of osmotic stress and optimization of culture conditions. International Enzyme Engineering Symposium (IEES), Kusadasi- Turkey (Oral Presentation).

Gurkok S., Ozdemir B., Ögel Z.B., 2008. Heterologous expression of alpha-galactosidase from *Aspergillus fumigatus* in *Aspergillus sojae*, the influence of osmotic stress and optimization of culture conditions. XII. International Congress of Mycology, Istanbul-Turkey (Poster Presentation).

Gurkok S., Ozdemir B., Ögel Z.B., 2008. *Aspergillus fumigatus* alfa-galaktosidaz enziminin *Aspergillus sojae'*de heterolog ifadesi ve osmotik stresin etkisi. X. Turkish Food Conference, Erzurum-Turkey (Oral presentation).

Gurkok S., Ozturk B., Ögel Z.B., 2008. Gizli Kahramanlar, Enzimler. Turkish Ar-Ge Conference, Ankara-Turkey (Poster Presentation).

Gurkok S., Ozdemir B., Ögel Z.B., 2007. *Aspergillus fumigatus* alfa-galaktosidaz enziminin *Aspergillus sojae'*de heterolog ifadesi ve osmotik stresin etkisi. XV. Biotechnology Conference, Antalya- Turkey (Poster presentation).

Gurkok S., Ozdemir B., Ögel Z.B., 2007. Production of alpha-galactosidase from *Aspergillus fumigatus* in *Aspergillus sojae* under the control of the *gpd*A promoter and the influence of osmotic stress. 3rd European Federation of Biotechnology Conference on Physiology of Yeasts and Filamentous Fungi (PYFF3), Helsinki-Finland (Poster presentation).

Gurkok S., Ozdemir B., Amarsaikhan N., Ögel Z.B., 2007. A life under stress: The effect of osmotic and phenolic stress on the growth, enzyme production and adaptation in Aspergillus species. International symposium of Microbial stress and adaptation, Marburg-Germany (Poster presentation).

Grants of State Planning Organization of Turkey; ''Heterologous expression of alpha-galactosidase from *Aspergillus fumigatus* in *Aspergillus sojae* and the influence of the osmotic stress" (2004- 2010, continuing), $22,000.

LANGUAGE

Turkish: Native language
English: Fluently spoken and written

RESEARCH INTEREST

Biotechnology, industrial microbiology, fungal genetics, enzyme production in fungi, statistical optimization of production, enzyme purification and characterization, glycoscience.

HOBBIES

Traveling, driving, shopping, dancing, cinema, music, sports.